

The virtual element method

Lourenço Beirão da Veiga

Dipartimento di Matematica e Applicazioni, Università di Milano–Bicocca, Italy
and IMATI-CNR, Pavia, Italy
E-mail: lourenco.beirao@unimib.it

Franco Brezzi

IUSS, Istituto Universitario di Studi Superiori, Pavia, Italy
and IMATI-CNR, Pavia, Italy
E-mail: brezzi@imati.cnr.it

L. Donatella Marini

Dipartimento di Matematica, Università di Pavia, Italy,
and IMATI-CNR, Pavia, Italy
E-mail: marini@imati.cnr.it

Alessandro Russo

Dipartimento di Matematica e Applicazioni, Università di Milano–Bicocca, Italy
and IMATI-CNR, Pavia, Italy
E-mail: alessandro.russo@unimib.it

The present review paper has several objectives. Its primary aim is to give an idea of the general features of virtual element methods (VEMs), which were introduced about a decade ago in the field of numerical methods for partial differential equations, in order to allow decompositions of the computational domain into polygons or polyhedra of a very general shape.

Nonetheless, the paper is also addressed to readers who have already heard (and possibly read) about VEMs and are interested in gaining more precise information, in particular concerning their application in specific subfields such as C^1 -approximations of plate bending problems or approximations to problems in solid and fluid mechanics.

2020 Mathematics Subject Classification: 65N30

CONTENTS

1	Introduction	124
2	Preliminaries	126
3	H^1 -conforming approximations	130
4	H^1 -nonconforming approximations	144
5	H^2 -conforming approximations	149
6	$H(\text{div})$, $H(\text{rot})$ and $H(\text{curl})$ -conforming approximations	154
7	The elasticity problem	173
8	The Stokes and Navier–Stokes problems	182
	References	195

1. Introduction

The virtual element method (VEM) was introduced in [Beirão da Veiga *et al.* \(2013b\)](#) and [Beirão da Veiga, Brezzi, Marini and Russo \(2014\)](#) as an alternative way of looking at mimetic finite differences for the approximation of (systems of) partial differential equations. The unknowns of the discretized problem, originally *nodal values*, in the VEM formulation instead became *functions* or, if convenient, *vector-valued functions*, characterized by a set of *degrees of freedom* that included *nodal values* or *moments* on edges or inside the element (referring to a two-dimensional problem). In mimetic finite differences these values were used *as if they were related to a polynomial function*, and the corresponding polynomial functions were used in the construction of the final discrete formulation. All this was done on polygons or polyhedra of a very general shape, thus allowing the treatment of very general decompositions. The basic idea of virtual elements was *to associate with every suitable subset of degrees of freedom a corresponding function*, and then write the discretized problem in terms of the corresponding functions, their values, their averages, and so on. Obviously, one could not expect to associate a *polynomial function* with every subset of degrees of freedom. Hence the new (virtual element) strategy was as follows: with every *set of degrees of freedom* we associate a function that is not necessarily a polynomial but rather a smooth function, a solution of a PDE problem inside the element. These functions are generally not computable (one would not dream of solving several PDE problems inside each element of the decomposition!) but one would compute their *projections onto polynomial spaces* out of the degrees of freedom, and then use them in formulating the discretized problem. With time, the *internal PDE problems* shifted from a simple Laplacian to more complex operators or systems of PDEs, connected to (but generally not coincident with) the system of PDEs to be solved on the whole domain. Of course, all these element-by-element PDE systems (with polynomial data) are *never* solved explicitly, but in the code one uses suitable projections of their solutions onto polynomial spaces.

The final outcome of this approach is a Galerkin method having the same structure as the finite element method. Furthermore, the two methods (VEM and FEM) are perfectly compatible and can coexist on the same mesh. Moreover, somewhat unexpectedly, some of the new techniques and ideas developed for polygonal elements also proved to have some interest for elements of classical shapes such as triangles or quadrilaterals, as shown in [Brezzi and Marini \(2021\)](#).

In summary, the ‘general structure’ of a VEM discretization amounts to:

- (i) generating a decomposition of the computational domain in polygons or polyhedra;
- (ii) defining, inside each polygon or polyhedron, a finite-dimensional space of functions, typically solutions of PDE problems with polynomial data (e.g. a polynomial trace on each edge and a polynomial Laplacian);
- (iii) defining a suitable set of degrees of freedom;
- (iv) specifying suitable polynomials, explicitly computable from the degrees of freedom, obtained by *projecting each of the above functions onto polynomial spaces.*

The above approach applies to an enormous variety of different PDE models, such as heat diffusion, elasticity, plate bending, fluid flows and magnetic fields.

In the past decade, since the publication of the first paper in 2013, virtual elements have seen an enormous growth of interest in the applied mathematics and engineering communities, thanks to their great flexibility, which makes them applicable to many different types of problem. The number of applications and variants is such that it would be difficult, if not prohibitive, to provide an exhaustive list. Here we have decided to mention only a few of them, chosen as samples among those that, to the best of our knowledge, appear to be particularly attractive in terms of the number of papers or the variety of groups of researchers. For each subject we will cite a couple of the most recent publications, and we refer to the references therein; more references are provided within each section of the present paper.

For topology optimization, important contributions were made by Paulino and his group ([Gain, Paulino, Duarte and Menezes 2015](#), [Chi, Pereira, Menezes and Paulino 2020](#)). Significant contributions to contact problems were made by Wriggers, Reddy and their groups ([Wriggers, Rust and Reddy 2016](#), [Cihan, Hudobivnik, Korelc and Wriggers 2022](#)). For geophysical applications, and in particular for discrete fracture networks, Berrone and his group ([Benedetto *et al.* 2016](#), [Berrone and Raeli 2022](#)) are worth mentioning. For the Helmholtz problem we refer to Perugia and collaborators ([Mascotto, Perugia and Pichler 2019](#)).

A key ingredient in all VEM applications is the integration on general polygons and polyhedra; we refer to [Chin, Lasserre and Sukumar \(2015\)](#) and [Chin and Sukumar \(2021\)](#) for a detailed study of polytopal quadrature formulas.

For more methodology-oriented papers we mention Brenner, Guan and Sung (2017) and Chen and Huang (2018) for results on *a priori* estimates, Mora, Rivera and Rodriguez (2017) and Gardini, Manzini and Vacca (2019) for eigenvalue problems, Beirão da Veiga, Chernov, Mascotto and Russo (2016e) and Chernov, Marcati and Mascotto (2021) for hp formulations, and Cangiani, Georgoulis, Pryer and Sutton (2017) and Beirão da Veiga, Manzini and Mascotto (2019a) for *a posteriori* error analysis.

One ‘hot topic’ concerns the treatment of curved edges and faces, for which there are some results – albeit still not completely satisfactory – in Bertoluzza, Pennacchio and Prada (2019), Beirão da Veiga, Russo and Vacca (2019c), Beirão da Veiga, Brezzi, Marini and Russo (2020) and Dassi, Fumagalli, Scotti and Vacca (2022).

An update on the VEM literature could be obtained via an unconventional yet very effective approach, consisting in looking (e.g. in Google Scholar) at the most recent papers citing the original paper of Beirão da Veiga *et al.* (2013b).

In the present paper, following to some extent the evolution and growth of the method and its applications, we will discuss the basic ideas, starting from the simplest Poisson problem, and then give an overview of more general problems, namely plate bending, elasticity and fluid flow equations.

An outline of the whole presentation is as follows. After setting the notation in Section 2, along with some assumptions that will be used throughout the paper, in Section 3 we describe, for a simple Poisson problem, the basic approach to constructing C^0 -conforming approximations, in two and three dimensions. Section 4 is devoted to the C^0 -nonconforming approximation of the same model problem, while Section 5 deals with C^1 -conforming approximations, taking a plate bending problem as a reference problem. Section 6 is dedicated to the discretization of the spaces $H(\text{div})$, $H(\text{rot})$ and $H(\text{curl})$. Two- and three-dimensional face and edge virtual elements are illustrated in detail, and are shown to form exact sequences. The last two sections deal with specific problems: linear and nonlinear elasticity in Section 7 and Stokes and Navier–Stokes in Section 8. Suitable discrete spaces are presented and discussed, together with convergence results.

2. Preliminaries

In this section we will define some common notation and introduce general assumptions that will be used throughout the paper. Other definitions and assumptions will be introduced as needed.

2.1. Computational domain and mesh

We let $\Omega \subset \mathbb{R}^d$, $d = 2$ or $d = 3$ denote the computational domain of the differential problem under study. We assume that Ω can be decomposed into polygons (in two dimensions) or polyhedra (in three dimensions). A generic polygon will be denoted by E and a generic polyhedron by P . We will use the general notation K to

indicate a polygon or a polyhedron. The letter e will denote an edge (of a polygon or a polyhedron) and f a face (of a polyhedron).

The number of edges and vertices of a polygon or a polyhedron K will be denoted by $N_e(K)$ and $N_V(K)$ respectively; the '(K)' will be omitted when no confusion can arise. Obviously, for a polygon $N_e = N_V$. Similarly, $N_f(P)$ will indicate the number of faces of a polyhedron P .

The outward normal to K will be denoted by \mathbf{n}_K , sometimes with the superscript f or e to indicate that \mathbf{n}_K belongs to the face f or the edge e respectively. When no confusion can arise, we will simply use the letter \mathbf{n} . Similarly, in three dimensions \mathbf{n}_f will denote the outward normal to the face f lying in the plane of f, and \mathbf{n}_e^e will be that related to edge e. Tangent unit vectors will be denoted by \mathbf{t} ; in particular, for an edge e, \mathbf{t}_e will be a unit vector parallel to e.

The diameter of an element K will be denoted by h_K ; a family of decompositions of Ω will be denoted by $\{\mathcal{T}_h\}_h$, with $h = \max\{h_K, K \in \mathcal{T}_h\}$ being a measure of the size of the decomposition \mathcal{T}_h . On $\{\mathcal{T}_h\}_h$ we make the following assumption.

Assumption 2.1 (mesh regularity). There exists a positive constant ϱ such that for any $K \in \{\mathcal{T}_h\}_h$:

- K is star-shaped with respect to a ball B_K of radius $\geq \varrho h_K$,
- (in three dimensions only) every face f of K is star-shaped with respect to a disk B_f of radius $\geq \varrho h_K$,
- any edge e of K has length $\geq \varrho h_K$.

We remark that the hypotheses above, although not too restrictive in many practical cases, could possibly be relaxed further, combining the present analysis with the studies in [Beirão da Veiga, Lovadina and Russo \(2017b\)](#), [Brenner et al. \(2017\)](#), [Brenner and Sung \(2018\)](#) and [Cao and Chen \(2018\)](#).

2.2. Polynomials

Given an integer $s \geq 0$ and a domain $\mathcal{O} \subset \mathbb{R}^d$ ($d = 1, 2, 3$), $\mathbb{P}_s(\mathcal{O})$ will denote the space of polynomials of degree $\leq s$ restricted to \mathcal{O} ; as usual, $\mathbb{P}_{-1} = \{0\}$. When no confusion is likely to occur, we will often use simply \mathbb{P}_s instead of $\mathbb{P}_s(\mathcal{O})$. With a common abuse of language, we will often say ‘polynomial of degree s ’ when we actually mean ‘polynomial of degree $\leq s$ ’. If $\mathcal{O} = \mathbb{R}^d$ ($d = 1, 2, 3$), its dimension $\pi_{s,d}$ is given by

$$\pi_{s,1} = s + 1, \quad \pi_{s,2} = \frac{(s+1)(s+2)}{2}, \quad \pi_{s,3} = \frac{(s+1)(s+2)(s+3)}{6}.$$

When no confusion can occur, we will use the simpler notation π_k . For $s \geq 1$ we define

$$\mathbb{P}_s^0(\mathcal{O}) := \left\{ q_s \in \mathbb{P}_s(\mathcal{O}): \int_{\mathcal{O}} q_s \, d\mathcal{O} = 0 \right\} \quad (2.1)$$

and

$$\mathbb{P}_s^{\text{hom}}(\mathcal{O}) := \{\text{homogeneous polynomials of degree } s \text{ in the variables } (x_i - \bar{x}_i)\},$$

where \bar{x}_i are the coordinates of the barycentre of \mathcal{O} . Next, for any non-negative integers $m \leq n$, we let $\mathbb{P}_{n/m}$ denote any subspace (fixed once and for all) of \mathbb{P}_n such that

$$\mathbb{P}_n = \mathbb{P}_m \oplus \mathbb{P}_{n/m}. \quad (2.2)$$

A common choice for $\mathbb{P}_{n/m}$ will be

$$\mathbb{P}_{n/m} = \mathbb{P}_{m+1}^{\text{hom}} \oplus \cdots \oplus \mathbb{P}_n^{\text{hom}}. \quad (2.3)$$

2.3. Differential operators

Following the standard notation, the symbols ∇ and Δ denote the gradient and the Laplacian for scalar functions, while div and curl are the divergence and the curl of a vector function. We recall that in two dimensions, the curl operator has two incarnations (as ∇ and div) given by

$$\text{rot}(v_1, v_2) := \partial_x v_2 - \partial_y v_1, \quad \text{rot}(\varphi) := (\partial_y \varphi, -\partial_x \varphi).$$

We will sometimes use the notation **grad** instead of ∇ . Finally, for a vector $v = (v_1, v_2)$ we let v^\perp indicate the vector $v^\perp = (v_2, -v_1)$.

For a face f of a polyhedron P , the tangential differential operators will be denoted by the subscript 2 , as in div_2 , rot_2 , rot_2 , grad_2 , Δ_2 and so on.

2.4. Functional spaces

Throughout the paper we will follow the common notation for Sobolev spaces, scalar products, norms and seminorms (see Adams 1975). For m integer ≥ 0 we define

$$H^m(\mathcal{O}) := \{v: D^\alpha v \in L^2(\mathcal{O}) \text{ for all } |\alpha| \leq m\},$$

where

$$D^\alpha v = \frac{\partial^{|\alpha|} v}{\partial x_1^{\alpha_1} \cdots \partial x_n^{\alpha_n}}, \quad |\alpha| = \alpha_1 + \cdots + \alpha_n.$$

With $(v, w)_{0,\mathcal{O}}$ (sometimes just $(v, w)_0$) and $\|v\|_{0,\mathcal{O}}$ (sometimes just $\|v\|_0$) we will denote the $L^2(\mathcal{O})$ scalar product and norm, whereas $|v|_{m,\mathcal{O}}$ (sometimes just $|v|_m$) and $\|v\|_{m,\mathcal{O}}$ (sometimes just $\|v\|_m$) will denote, respectively, the H^m seminorm and norm. In particular, we shall use $H^1(\mathcal{O})$ ($\mathcal{O} \subset \mathbb{R}^d$, $d = 2, 3$), $H^2(\mathcal{O})$ ($\mathcal{O} \subset \mathbb{R}^2$).

Moreover, we will also need the following.

- For $\mathcal{O} \subset \mathbb{R}^2$:

$$\left. \begin{aligned} H(\text{div}, \mathcal{O}) &:= \{\mathbf{v} \in [L^2(\mathcal{O})]^2 : \text{div } \mathbf{v} \in L^2(\mathcal{O})\}, \\ H(\text{rot}, \mathcal{O}) &:= \{\mathbf{v} \in [L^2(\mathcal{O})]^2 : \text{rot } \mathbf{v} \in L^2(\mathcal{O})\}. \\ \bullet \text{ For } \mathcal{O} \subset \mathbb{R}^3: \\ H(\text{div}, \mathcal{O}) &:= \{\mathbf{v} \in [L^2(\mathcal{O})]^3 : \text{div } \mathbf{v} \in L^2(\mathcal{O})\}, \\ H(\text{curl}, \mathcal{O}) &:= \{\mathbf{v} \in [L^2(\mathcal{O})]^3 : \text{curl } \mathbf{v} \in [L^2(\mathcal{O})]^3\}. \end{aligned} \right\} \quad (2.4)$$

2.5. Projections onto polynomial spaces

- L^2 -projection. On \mathcal{O} we let $\Pi_s^{0,\mathcal{O}}$ (or simply Π_s^0 when no confusion can occur) denote the $L^2(\mathcal{O})$ -orthogonal projection operator onto $\mathbb{P}_s(\mathcal{O})$, defined, as usual, for every $\varphi \in L^2(\mathcal{O})$, by

$$\int_{\mathcal{O}} (\Pi_s^{0,\mathcal{O}} \varphi) p_s \, d\mathcal{O} = \int_{\mathcal{O}} \varphi p_s \, d\mathcal{O} \quad \text{for all } p_s \in \mathbb{P}_s(\mathcal{O}), \quad (2.5)$$

with obvious extension for vector functions $\Pi_s^{0,\mathcal{O}} : [L^2(\mathcal{O})]^d \rightarrow [\mathbb{P}_n(\mathcal{O})]^d$ and tensor functions $\Pi_s^{0,\mathcal{O}} : [L^2(\mathcal{O})]^{d \times d} \rightarrow [\mathbb{P}_s(\mathcal{O})]^{d \times d}$.

- H_0^1 -projection: the $\Pi_s^{\nabla,\mathcal{O}}$ operator. For every $\varphi \in H^1(\mathcal{O})$ we let $\Pi_s^{\nabla,\mathcal{O}} \varphi$ (or simply $\Pi_s^\nabla \varphi$ when no confusion can occur) denote its projection onto the space $\mathbb{P}_s(\mathcal{O})$ with respect to the scalar product of $H^1(\mathcal{O})$, defined as the solution, in $\mathbb{P}_s(\mathcal{O})$, of

$$\left. \begin{aligned} \int_{\mathcal{O}} \nabla(\Pi_s^{\nabla,\mathcal{O}} \varphi) \cdot \nabla q_s \, d\mathcal{O} &= \int_{\mathcal{O}} \nabla \varphi \cdot \nabla q_s \, d\mathcal{O} \quad \text{for all } q_s \in \mathbb{P}_s(\mathcal{O}), \\ \int_{\partial\mathcal{O}} \Pi_s^{\nabla,\mathcal{O}} \varphi \, ds &= \int_{\partial\mathcal{O}} \varphi \, ds. \end{aligned} \right\} \quad (2.6)$$

Moreover, given a function $\psi \in L^2(\mathcal{O})$ and an integer $s \geq 0$, we recall that the *moments of order $\leq s$ of ψ on \mathcal{O}* are defined as

$$\int_{\mathcal{O}} \psi q_s \, d\mathcal{O} \quad \text{for } q_s \in \mathbb{P}_s(\mathcal{O}).$$

Hence *assigning the moments of ψ up to the order s on \mathcal{O}* will amount to assigning a number of conditions equal to the dimension of $\mathbb{P}_s(\mathcal{O})$. Typically this will be used when these moments are considered as *degrees of freedom*.

Remark 2.2. A quantity (depending on a function living in a discrete space with given degrees of freedom) is said to be *computable* if it can be determined directly from information provided by the degrees of freedom. This would often require

us to compute integrals of polynomials on polygonal and polyhedral domains (see e.g. (2.5) and (2.6)). Among the various quadrature techniques we refer to [Chin et al. \(2015\)](#) and [Chin and Sukumar \(2021\)](#), for example.

3. H^1 -conforming approximations

In this section we will describe the original virtual element method (VEM), as first introduced in [Beirão da Veiga et al. \(2013b\)](#). To fix ideas, we shall consider the following model problem:

$$-\Delta u = f \text{ in } \Omega, \quad u = 0 \text{ on } \Gamma_D, \quad \frac{\partial u}{\partial n} = g \text{ on } \Gamma_N, \quad (3.1)$$

where $\Omega \subset \mathbb{R}^2$ is a polygonal domain, with boundary $\partial\Omega = \Gamma_D \cup \Gamma_N$ ($\Gamma_D \neq \emptyset$, $\Gamma_D \cap \Gamma_N = \emptyset$). The data f, g are given functions with $f \in L^2(\Omega)$, and g , say, in $L^2(\Gamma_N)$. Setting

$$\begin{aligned} H_{0,\Gamma_D}^1(\Omega) &:= \{v \in H^1(\Omega) : v = 0 \text{ on } \Gamma_D\}, \\ a(u, v) &:= \int_{\Omega} \nabla u \cdot \nabla v \, dx, \\ \ell(v) &:= (f, v)_{0,\Omega} + (g, v)_{0,\Gamma_N} = \int_{\Omega} f v \, dx + \int_{\Gamma_N} g v \, ds, \end{aligned} \quad (3.2)$$

the variational formulation of (3.1) is:

$$\text{Find } u \in V := H_{0,\Gamma_D}^1(\Omega) \text{ such that } a(u, v) = \ell(v) \text{ for all } v \in V. \quad (3.3)$$

Problem (3.3) has a unique solution thanks to the Lax–Milgram lemma. In particular, $a(\cdot, \cdot)$ is a symmetric bilinear form, continuous and elliptic, that is,

$$\text{There exists } M > 0 \text{ such that } a(v, w) \leq M \|v\|_{1,\Omega} \|w\|_{1,\Omega} \text{ for all } v, w \in V, \quad (3.4)$$

$$\text{There exists } \alpha > 0 \text{ such that } a(v, v) \geq \alpha \|v\|_{1,\Omega}^2 \text{ for all } v \in V, \quad (3.5)$$

and $\ell(\cdot)$ is a linear bounded functional, that is,

$$\text{There exists } C > 0 \text{ such that } |\ell(v)| \leq C (\|f\|_{0,\Omega} + \|g\|_{0,\Gamma_N}) \|v\|_{1,\Omega} \text{ for all } v \in V. \quad (3.6)$$

The virtual element method, like all Galerkin methods, uses all the classical ingredients needed for approximating variational formulations: a decomposition \mathcal{T}_h of Ω into polygons E , and then an associated finite-dimensional space $V_h \subset V$, a bilinear form $a_h(\cdot, \cdot)$ and a linear functional $\ell_h(\cdot)$. Then the discrete problem reads:

$$\text{Find } u_h \in V_h \text{ such that } a_h(u_h, v_h) = \ell_h(v_h) \text{ for all } v_h \in V_h, \quad (3.7)$$

and we have to define V_h , $a_h(\cdot, \cdot)$, and $\ell_h(\cdot)$ in such a way that problem (3.7) has a unique solution and optimal error estimates hold. This will be done in the next subsections, following the original approach of [Beirão da Veiga et al. \(2013b\)](#).

3.1. An abstract convergence result

Let us recall the assumptions needed to prove the abstract convergence theorem. For every polygon $E \in \mathcal{T}_h$ of diameter h_E we let $V_{h|E}$, $a_h^E(\cdot, \cdot)$ and $a^E(\cdot, \cdot)$, respectively, denote the restriction to E of V_h , $a_h(\cdot, \cdot)$ and $a(\cdot, \cdot)$, so that

$$\begin{aligned} a(v, w) &= \sum_{E \in \mathcal{T}_h} a^E(v, w) \quad \text{for all } v, w \in V, \\ a_h(v_h, w_h) &= \sum_{E \in \mathcal{T}_h} a_h^E(v_h, w_h) \quad \text{for all } v_h, w_h \in V_h. \end{aligned} \tag{3.8}$$

On the bilinear form $a_h^E(\cdot, \cdot)$ we make the following assumption.

Assumption 3.1. There exists an integer $k \geq 1$ (which will be the order of accuracy) such that for all h and for all E in \mathcal{T}_h , we have $\mathbb{P}_k(E) \subset V_{h|E}$ and

- *k-consistency*: for all $p_k \in \mathbb{P}_k(E)$ and for all $v_h \in V_{h|E}$,

$$a_h^E(p_k, v_h) = a^E(p_k, v_h); \tag{3.9}$$

- *stability*: there exist two positive constants α_* and α^* , independent of h and of E , such that, for all $v_h \in V_{h|E}$,

$$\alpha_* a^E(v_h, v_h) \leq a_h^E(v_h, v_h) \leq \alpha^* a^E(v_h, v_h). \tag{3.10}$$

We notice that the symmetry of a_h^E , property (3.10) and the definition of a^E easily imply the continuity of a_h^E with

$$\begin{aligned} a_h^E(u_h, v_h) &\leq (a_h^E(u_h, u_h))^{1/2} (a_h^E(v_h, v_h))^{1/2} \\ &\leq \alpha^* (a^E(u_h, u_h))^{1/2} (a^E(v_h, v_h))^{1/2} \\ &\leq \alpha^* \|u_h\|_{1,E} \|v_h\|_{1,E} \quad \text{for all } u_h, v_h \in V_{h|E}. \end{aligned} \tag{3.11}$$

Theorem 3.2. Under Assumption 3.1 the discrete problem (3.7) has a unique solution u_h . Moreover, for every approximation $u_I \in V_h$ of u , and for every approximation u_π of u that is piecewise in \mathbb{P}_k , we have

$$|u - u_h|_{1,\Omega} \leq C(|u - u_I|_{1,\Omega} + |u - u_\pi|_{1,\mathcal{T}_h} + \mathfrak{F}_h), \tag{3.12}$$

where C is a constant depending only on α_* and α^* , $|\cdot|_{1,\mathcal{T}_h}$ is the broken H^1 -norm and, for any h , \mathfrak{F}_h is the smallest constant such that

$$\ell(v_h) - \ell_h(v_h) \leq \mathfrak{F}_h |v_h|_{1,\Omega} \quad \text{for all } v_h \in V_h. \tag{3.13}$$

Proof. Existence and uniqueness of the solution of (3.7) are a consequence of (3.10) and (3.5). Next, setting $\delta_h := u_h - u_I$, we have

$$\begin{aligned} \alpha_* |\delta_h|_1^2 &= \alpha_* a(\delta_h, \delta_h) \leq a_h(\delta_h, \delta_h) \\ &= a_h(u_h, \delta_h) - a_h(u_I, \delta_h) \quad (\text{use (3.7) and (3.8)}) \end{aligned}$$

$$\begin{aligned}
&= \ell_h(\delta_h) - \sum_E a_h^E(u_I, \delta_h) \quad (\text{use } \pm u_\pi) \\
&= \ell_h(\delta_h) - \sum_E (a_h^E(u_I - u_\pi, \delta_h) + a_h^E(u_\pi, \delta_h)) \quad (\text{use (3.9)}) \\
&= \ell_h(\delta_h) - \sum_E (a_h^E(u_I - u_\pi, \delta_h) + a^E(u_\pi, \delta_h)) \quad (\text{add } \pm u) \\
&= \ell_h(\delta_h) - \sum_E (a_h^E(u_I - u_\pi, \delta_h) + a^E(u_\pi - u, \delta_h)) - a(u, \delta_h) \quad (\text{use (3.7)}) \\
&= \ell_h(\delta_h) - \sum_E (a_h^E(u_I - u_\pi, \delta_h) + a^E(u_\pi - u, \delta_h)) - \ell(\delta_h) \\
&= \ell_h(\delta_h) - \ell(\delta_h) - \sum_E (a_h^E(u_I - u_\pi, \delta_h) + a^E(u_\pi - u, \delta_h)).
\end{aligned}$$

Now use (3.13), (3.11) and the continuity of each a^E to obtain

$$|\delta_h|_{1,\Omega}^2 \leq C(\mathfrak{F}_h + |u_I - u_\pi|_{1,\mathcal{T}_h} + |u - u_\pi|_{1,\mathcal{T}_h}) |\delta_h|_{1,\Omega} \quad (3.14)$$

for some constant C depending only on α_* and α^* . Then the result follows easily by the triangle inequality. \square

3.2. The local discrete spaces

We first recall the definition of the discrete spaces from Beirão da Veiga *et al.* (2013b). Let E be a generic polygon in \mathcal{T}_h . For k integer, $k \geq 1$, we define the local space $V_{h|E}$ as

$$V_k(E) := \{v \in C^0(\overline{E}): v|_e \in \mathbb{P}_k(e) \text{ for any edge } e \subset \partial E, \Delta v \in \mathbb{P}_{k-2}(E)\}. \quad (3.15)$$

Letting N_e denote the number of edges of E , the dimension of $V_k(E)$ is given by

$$\dim V_k(E) = kN_e + k(k-1)/2.$$

We notice that the space (3.15) contains the space $\mathbb{P}_k(E)$ but is not reduced to it, unless E is a triangle and $k = 1$, as can be seen by a simple dimensional count.

The degrees of freedom for $v_h \in V_k(E)$ are given by

- (D₁) the values of v_h at the vertices,
 - (D₂) for $k \geq 2$, the moments $\int_e v_h p_{k-2} ds$, for $p_{k-2} \in \mathbb{P}_{k-2}(e)$ and any e ,
 - (D₃) for $k \geq 2$, the moments $\int_E v_h p_{k-2} dE$, for $p_{k-2} \in \mathbb{P}_{k-2}(E)$.
- (3.16)

Clearly, instead of the moments (D₂) one could use the values at $k-1$ distinct points on each edge, more in the spirit of finite elements:

- (D'₂) the value of v_h at $k-1$ distinct points on each edge e .

We observe that it is convenient to scale the degrees of freedom so that they all have the same order of magnitude. The reason for this will become clear in the next subsection; here, however, we do not enter into the details of this issue, and we refer to [Beirão da Veiga et al. \(2014\)](#) for a more detailed discussion.

Remark 3.3. The classical definition of ‘degree of freedom’ for a generic local finite element space $V_k(K)$ (as given for instance in [Ciarlet 1978](#)) says that a degree of freedom is a linear functional $L: V_k(K) \rightarrow \mathbb{R}$, and a (finite) set $\{L_i\}$ of degrees of freedom is *unisolvant* if the set of linear equations $L_i(v) = b_i$ has a unique solution for any choice of the b'_i . Given a set of unisolvant degrees of freedom in $V_k(K)$, we can immediately define the corresponding dual basis $\{\varphi_i\}$ for $V_k(K)$ by requiring $L_i(\varphi_j) = \delta_{ij}$.

Here and in the rest of the paper, we will associate with a polynomial space a set of degrees of freedom, in the sense that statements like (D_3) in (3.16) will mean that *in practice* we have to choose a basis $\{m_i\}$ for $\mathbb{P}_{k-2}(K)$ and then define the degrees of freedom

$$L_i(v_h) := \int_K v_h m_i \, dK, \quad v_h \in V_k(K). \quad (3.17)$$

These bases are typically chosen as shifted and scaled monomials (see e.g. [Beirão da Veiga et al. 2014](#), [Dassi and Vacca 2020](#)) or, for a better condition number behaviour, in particular for high values of k , as suitable orthonormal polynomials ([Chernov et al. 2021](#), [Beirão da Veiga et al. 2016e](#)).

Lemma 3.4. The degrees of freedom (3.16) are unisolvant for $V_k(E)$.

Proof. Since the number of degrees of freedom equals the dimension of $V_k(E)$, it is enough to show that a function v_h having all the degrees of freedom vanishing is identically zero. Since v_h is a polynomial of degree k on each edge, $(D_1) = 0$ and $(D_2) = 0$ imply that $v_h \equiv 0$ on ∂E . This together with $(D_3) = 0$ gives

$$\int_E |\nabla v_h|^2 \, dE = - \int_E v_h \Delta v_h \, dE + \int_{\partial E} v_h \frac{\partial v_h}{\partial n} \, ds = 0$$

since $\Delta v_h \in \mathbb{P}_{k-2}$. Hence $\nabla v_h \equiv 0$, i.e. $v_h = \text{const.} = 0$ (since $v_h = 0$ on the boundary Γ_D). \square

3.3. Construction of a computable discrete bilinear form

From definition (3.15) we see that the functions of $V_k(E)$ are known on the boundary of ∂E but not inside, unless we are willing to solve a PDE on each element E , something that we do not want to do, not even in an approximate way. Then, in order to approximate $a^E(\cdot, \cdot)$, we use a projection onto $\mathbb{P}_k(E)$. We consider the operator Π_k^∇ defined in (2.6), for which we have the following lemma.

Lemma 3.5. The operator Π_k^∇ is computed from the degrees of freedom (3.16).

Proof. The left-hand side of (2.6) is a product of polynomials, and it is obviously computable. Integrating the right-hand side by parts, we have

$$\int_E \nabla v_h \cdot \nabla q_k \, dE = - \int_E v_h \Delta q_k \, dE + \int_{\partial E} v_h \frac{\partial q_k}{\partial n} \, ds, \quad (3.18)$$

and the two integrals are both computed from the degrees of freedom (3.16). \square

Then a discrete bilinear form can be constructed, in each element E and for $v_h, w_h \in V_k(E)$, as

$$a_h^E(v_h, w_h) := a^E(\Pi_k^\nabla v_h, \Pi_k^\nabla w_h) + \mathcal{S}^E((I - \Pi_k^\nabla)v_h, (I - \Pi_k^\nabla)w_h), \quad (3.19)$$

where \mathcal{S}^E is any symmetric bilinear form to be chosen in such a way that it scales like $a^E(\cdot, \cdot)$ and is positive on the kernel of Π_k^∇ , that is, there exist two positive constants c_1, c_2 such that

$$c_1 a^E(v_h, v_h) \leq \mathcal{S}^E(v_h, v_h) \leq c_2 a^E(v_h, v_h) \text{ for all } v_h \text{ such that } \Pi_k^\nabla v_h = 0. \quad (3.20)$$

There are various recipes for \mathcal{S}^E , the most commonly used being the so-called ‘dofi-dofi’:

$$\mathcal{S}^E(v_h, w_h) := \sum_{i=1}^{\#dofs} \text{dof}_i(v_h) \text{dof}_i(w_h), \quad (3.21)$$

where dof_i is the i th degree of freedom. As we have already anticipated, for condition (3.20) to be satisfied, the degrees of freedom (3.16) must be properly scaled. Other choices can be convenient, for example,

$$\mathcal{S}^E(v_h, w_h) := h_E^{-1} \int_{\partial E} v_h w_h \, ds, \quad (3.22)$$

where h_E is still the diameter of the element E , or

$$\mathcal{S}^E(v_h, w_h) := h_E \int_{\partial E} \frac{\partial v_h}{\partial t} \frac{\partial w_h}{\partial t} \, ds, \quad (3.23)$$

where $\partial/\partial t$ denotes the *tangential derivative*.

Lemma 3.6. The discrete bilinear form (3.19) is k -consistent and stable.

Proof. To prove consistency we observe that $\Pi_k^\nabla p_k \equiv p_k$ since Π_k^∇ is a projection. Hence

$$\mathcal{S}^E((I - \Pi_k^\nabla)v_h, (I - \Pi_k^\nabla)p_k) \equiv 0 \quad \text{for all } v_h \in V_k(E), p_k \in \mathbb{P}_k.$$

Then, using the definition (2.6) of Π_k^∇ , we immediately have

$$a_h^E(v_h, p_k) = a^E(\Pi_k^\nabla v_h, p_k) = a^E(v_h, p_k). \quad (3.24)$$

To prove stability we use (3.20) and the definition (2.6) of Π_k^∇ to obtain

$$\begin{aligned} a_h^E(v_h, v_h) &\geq a^E(\Pi_k^\nabla v_h, \Pi_k^\nabla v_h) + c_1 a^E(v_h - \Pi_k^\nabla v_h, v_h - \Pi_k^\nabla v_h) \\ &= a^E(v_h, \Pi_k^\nabla v_h) + c_1 a^E(v_h - \Pi_k^\nabla v_h, v_h) \\ &\geq \min\{1, c_1\} (a^E(v_h, \Pi_k^\nabla v_h) + a^E(v_h - \Pi_k^\nabla v_h, v_h)) = \alpha_* a^E(v_h, v_h). \end{aligned}$$

Similarly,

$$\begin{aligned} a_h^E(v_h, v_h) &\leq a^E(\Pi_k^\nabla v_h, \Pi_k^\nabla v_h) + c_2 a^E(v_h - \Pi_k^\nabla v_h, v_h - \Pi_k^\nabla v_h) \\ &= a^E(v_h, \Pi_k^\nabla v_h) + c_2 a^E(v_h - \Pi_k^\nabla v_h, v_h) \\ &\leq \max\{1, c_2\} (a^E(v_h, \Pi_k^\nabla v_h) + a^E(v_h - \Pi_k^\nabla v_h, v_h)) = \alpha^* a^E(v_h, v_h). \end{aligned}$$

□

As a consequence of Lemma 3.6 we see that the abstract estimate (3.12) holds.

3.4. Construction of a computable right-hand side

We begin by recalling the original approximation of the right-hand side, as introduced in Beirão da Veiga *et al.* (2013b). In Section 3.7 we will present an alternative approach.

For the first integral in $\ell(v_h)$ (see (3.2)) we can define an approximation f_h of f directly computable from the degrees of freedom (D_1) – (D_3) as follows. Letting $\{V_i\}$ denote the N_V vertices of E , and recalling that Π_s^0 is the L^2 -projection onto \mathbb{P}_s , we set

$$(f_h, v_h)_{0,E} = \begin{cases} \text{for } k = 1 & \int_E (\Pi_0^0 f) \bar{v}_h \, dE \quad \text{with } \bar{v}_h = \frac{\sum_i v_h(V_i)}{N_V}, \\ \text{for } k \geq 2 & \int_E (\Pi_{k-2}^0 f) v_h \, dE. \end{cases} \quad (3.25)$$

The case $k = 1$ needs special treatment, since in this case we do not have internal moments among the degrees of freedom to be used as for $k \geq 2$.

With the choice (3.25), optimal error estimates are guaranteed. For $k = 1$, adding and subtracting $f\bar{v}_h$, and using the definition of the L^2 -projection and standard approximation estimates, we have

$$\begin{aligned} (f, v_h)_{0,E} - (f_h, v_h)_{0,E} &= \int_E (fv_h - f\bar{v}_h + f\bar{v}_h - \Pi_0^0 f \bar{v}_h) \, dE \\ &= \int_E (fv_h - f\bar{v}_h) \, dE \leq Ch_E \|f\|_{0,E} |v_h|_{1,E}. \end{aligned} \quad (3.26)$$

For $k \geq 2$, again using the definition of L^2 -projection and standard approximation properties, we have

$$\begin{aligned} (f, v_h)_{0,E} - (f_h, v_h)_{0,E} &= \int_E (fv_h - \Pi_{k-2}^0 f v_h) \, dE \\ &= \int_E (f - \Pi_{k-2}^0 f) (v_h - \Pi_{k-2}^0 v_h) \, dE \\ &\leq Ch_E^{k-1} \|f\|_{k-1,E} h_E |v_h|_{1,E} \\ &\leq Ch_E^k \|f\|_{k-1,E} |v_h|_{1,E}. \end{aligned} \quad (3.27)$$

The boundary integral poses no problems, since our functions are polynomials on each edge in Γ_N , and we might assume that we can compute the integrals to any chosen accuracy.

3.5. The global problem: error estimates

The global space V_h is obviously defined as a patchwork of the spaces (3.15):

$$V_h := \{v_h \in H_{0,\Gamma_D}^1(\Omega) : v_h|_E \in V_k(E) \text{ for all } E \in \mathcal{T}_h\}. \quad (3.28)$$

The degrees of freedom in V_h are the natural extension of those defined in (3.16). The global bilinear form and right-hand side are defined, as in the FEM, by summing over the elements of \mathcal{T}_h :

$$\begin{aligned} a_h(v_h, w_h) &:= \sum_{E \in \mathcal{T}_h} a_h^E(v_h, w_h), \\ \ell_h(v_h) &:= \sum_{E \in \mathcal{T}_h} (f_h, v_h)_{0,E} + \sum_{e \subset \Gamma_N} (g, v_h)_{0,e}, \end{aligned} \quad (3.29)$$

with $a_h^E(v_h, w_h)$ defined in (3.19) and $(f_h, v_h)_{0,E}$ in (3.25). The discrete problem is then:

$$\text{Find } u_h \in V_h \text{ such that } a_h(u_h, v_h) = \ell_h(v_h) \text{ for all } v_h \in V_h. \quad (3.30)$$

With these choices the assumptions of Theorem 3.2 are satisfied, so that (3.12) holds. In terms of order of convergence, the expected optimal order k holds, and we have the following theorem.

Theorem 3.7. Let u be the solution of (3.3), and let u_h be the solution of (3.30). Under Assumption 2.1 on the mesh, we obtain

$$|u - u_h|_{1,\Omega} \leq Ch^k |u|_{k+1,\Omega}. \quad (3.31)$$

Proof. From (3.26)–(3.27) we have

$$\ell(v_h) - \ell_h(v_h) = \sum_{E \in \mathcal{T}_h} (f - f_h, v_h)_{0,E} \leq C h^k \|f\|_{k-1,\Omega} \|v_h\|_{1,\Omega} \quad \text{for all } v_h \in V_h. \quad (3.32)$$

For every element E , let $u_\pi \in \mathbb{P}_k(E)$ be defined as the L^2 -projection of u onto $\mathbb{P}_k(E)$:

$$u_\pi \in \mathbb{P}_k(E): \int_E (u - u_\pi) p_k \, dE = 0 \quad \text{for all } E \in \mathcal{T}_h, p_k \in \mathbb{P}_k(E). \quad (3.33)$$

Standard approximation properties (see [Brenner and Scott 2008](#)) give

$$\|u - u_\pi\|_{1,\mathcal{T}_h} \leq C h^k |u|_{k+1,\Omega}. \quad (3.34)$$

Now let $u_I \in V_h$ be the interpolant of u , defined locally through the degrees of freedom [\(3.16\)](#):

$u_I = u$ at the vertices,

$$\text{for } k \geq 2, \int_e (u - u_I) p_{k-2} \, de = 0, \text{ for } p_{k-2} \in \mathbb{P}_{k-2}(e) \text{ and any edge } e, \quad (3.35)$$

$$\text{for } k \geq 2, \int_E (u - u_I) p_{k-2} \, dE = 0, \text{ for } p_{k-2} \in \mathbb{P}_{k-2}(E).$$

The following interpolation estimate has been proved (see [Mora, Rivera and Rodríguez 2015](#), [Brenner et al. 2017](#), [Chen and Huang 2018](#)):

$$\|u - u_I\|_{1,\Omega} \leq Ch^k |u|_{k+1,\Omega}. \quad (3.36)$$

Combining [\(3.32\)](#), [\(3.34\)](#) and [\(3.36\)](#), we obtain the result from [\(3.12\)](#). \square

3.6. Enhanced and serendipity virtual elements

A comparison with finite elements, in terms of number of degrees of freedom and for a given degree k , shows that the boundary degrees of freedom are exactly the same as expected, on both triangles and quadrilaterals, since they have to guarantee the global continuity. Looking at [\(3.16\)](#), we see that the number of internal degrees of freedom for a VEM is at least the dimension of \mathbb{P}_{k-2} , for any polygon. Instead, the number of internal degrees of freedom for a FEM is equal to the dimension of \mathbb{P}_{k-3} on triangles and to that of \mathbb{Q}_{k-3} on quads, where we recall that \mathbb{Q}_s denotes the polynomials of degree s separately in each variable. Hence, on triangles a VEM uses $k - 1$ degrees of freedom more than a FEM, while on quads a FEM uses $(k - 1)(k - 2)/2$ degrees of freedom more than a VEM (see Figures [3.1](#) and [3.2](#)). The ideal situation would be to have the minimum number of necessary degrees of freedom, and hence it is desirable to eliminate as many internal degrees of freedom as possible. In this respect, a triangular FEM is already optimal, and a quadrilateral FEM has been optimized via the serendipity procedure (see e.g. [Arnold and Awanou 2011](#)). Following [Ahmad et al. \(2013\)](#) and [Beirão da Veiga, Brezzi, Marini and Russo \(2016c\)](#), in order to eliminate as many internal degrees of freedom as possible, and at the same time allow the computation of all the moments of order $\leq k$, we first define the local space

$$\tilde{V}_k(E) := \{v_h \in C^0(\overline{E}): v_h|_e \in \mathbb{P}_k(e) \text{ for } e \subset \partial E, \Delta v_h \in \mathbb{P}_k(E)\}, \quad (3.37)$$

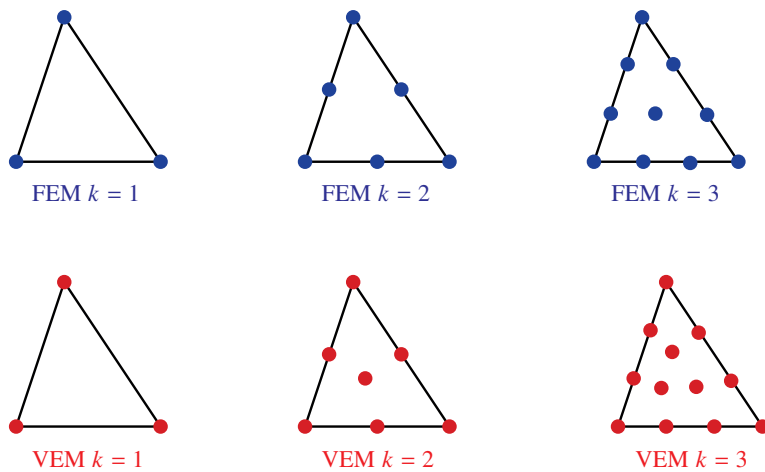


Figure 3.1. Triangles: degrees of freedom for FEM and original VEM.

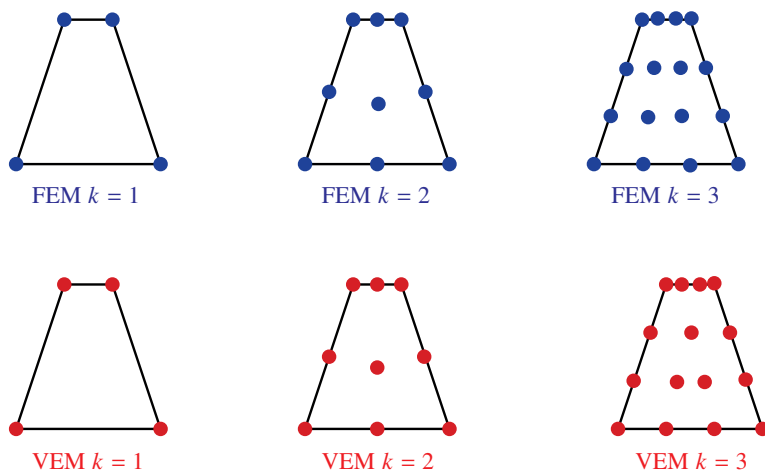


Figure 3.2. Quads: degrees of freedom for FEM and original VEM.

with the degrees of freedom

$$(D_1) - (D_2) \text{ (the same as in (3.16)) plus} \\ \text{the moments of order up to } k : \int_E v_h p_k dE \quad \text{for all } p_k \in \mathbb{P}_k(E). \quad (3.38)$$

Clearly the space (3.37) is bigger than (3.15), apparently in contradiction to our first aim, but now, thanks to the additional degrees of freedom in (3.38), the L^2 -orthogonal projection onto \mathbb{P}_k is directly available from the internal degrees of freedom. Then we begin by locally defining a projection operator

$\Pi_k : H^1(E) \rightarrow \mathbb{P}_k(E)$ as follows:

$$\Pi_k v \in \mathbb{P}_k(E) : \int_{\partial E} (\Pi_k v - v) q_k \, ds = 0 \quad \text{for all } q_k \in \mathbb{P}_k(E). \quad (3.39)$$

Clearly system (3.39) has a unique solution unless $\mathbb{P}_k(E)$ contains polynomials that are identically zero on the boundary, i.e. unless $\mathbb{P}_k(E)$ contains bubbles. This happens for $k \geq 3$ on triangles (b_3 = product of the equations of the three edges) and for $k \geq 4$ on ‘true’ quads (b_4 = product of the equations of the four edges). In these cases we need to add internal conditions, namely

$$\begin{aligned} & \underbrace{\int_E (\Pi_k v - v) q_s \, dE = 0 \text{ for all } q_s \in \mathbb{P}_{k-3}}_{\text{on triangles}} \\ \text{or } & \underbrace{\int_E (\Pi_k v - v) q_s \, dE = 0 \text{ for all } q_s \in \mathbb{P}_{k-4},}_{\text{on quads}} \end{aligned} \quad (3.40)$$

and then solve the system (3.39)–(3.40) in the least-squares sense. Once the polynomial $\Pi_k v$ has been computed, we define the new space by ‘copying’ its moments. Namely, setting N to be the maximum degree of internal moments used to define Π_k (and clearly $N = -1$ in the absence of internal moments), we introduce the new space

$$V_k^S(E) = \left\{ v_h \in \widetilde{V}_k(E) : \int_E (v_h - \Pi_k v_h) p_s \, dE = 0 \text{ for all } p_s \in \mathbb{P}_s^{\text{hom}}, N < s \leq k \right\}. \quad (3.41)$$

The degrees of freedom in (3.41) will be

$$\begin{aligned} & (D_1)–(D_2) \text{ (the same as in (3.16)) plus} \\ & \text{the moments } \int_E v_h p \, dE \quad \text{for all } p \in \mathbb{P}_N(E). \end{aligned}$$

Figure 3.3 shows that on triangles, a serendipity VEM (S-VEM) has the same number of degrees of freedom as a FEM (and in fact the two spaces coincide), while Figure 3.4 compares the degrees of freedom of serendipity VEMs and FEMs (see Arnold and Awanou 2011). The number is again the same, although serendipity FEMs are known to suffer from element distortion (see Arnold, Bozzo and Falk 2002) while VEMs do not, as shown in Beirão da Veiga *et al.* (2016c).

Remark 3.8. From the above discussion one might think that the number of internal moments necessary to define Π_k depends on k and on the number of edges: three for a triangle and four for a quad. This is true for *real* triangles and *real* quads. With the VEM approach the same geometrical entity (say, a triangle),

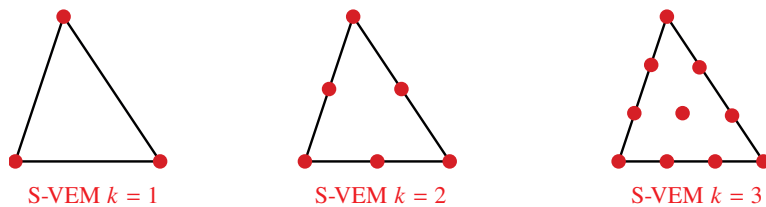


Figure 3.3. Triangles: degrees of freedom for serendipity VEM.

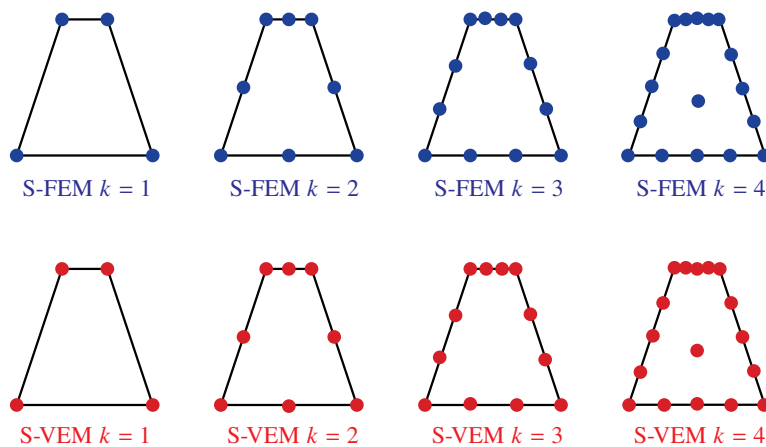


Figure 3.4. Quads: degrees of freedom for serendipity FEM and VEM.

might be considered as a polygon, a quad, or a pentagon or a hexagon, according to the number of points on its boundary that we consider as vertices (and then considering the portion of the boundary between two consecutive vertices as an edge). See Figure 3.5.

In the VEM terminology \tilde{Q} is a quad while \tilde{P} is a pentagon, but the set of bubbles is the same, equal to that on triangles: $B_k = b_3 p_{k-3}$. What really counts is not the number of edges but rather the number η of straight lines needed to cover the boundary (here $\eta = 3$ in both cases). Hence the internal conditions necessary to compute Π_k , to be added to (3.39), are

$$\int_E (\Pi_k v - v) q_s \, dE = 0 \quad \text{for all } q_s \in \mathbb{P}_{k-\eta}(E).$$

Remark 3.9. One might argue that static condensation could be a simpler procedure to reduce the number of internal degrees of freedom. This is true in two-dimensional problems, but it is no longer the case for three-dimensional problems, where the reduction of degrees of freedom on faces is important. Static condensation on faces might turn into a nightmare, while the serendipity approach works very well.

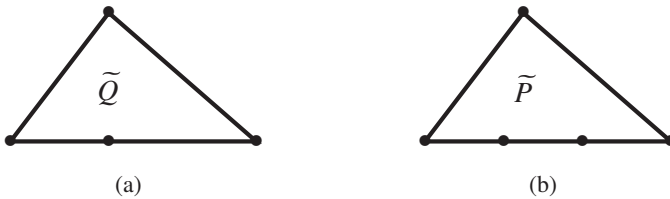


Figure 3.5. Fake triangles: (a) a quad, (b) a pentagon.

A typical variant of this procedure can be identified in the original *enhancement trick* as designed first in Ahmad *et al.* (2013). We again consider the space (3.37), with the degrees of freedom (3.38). Then, using only the boundary degrees of freedom and the moments up to $k - 2$, we construct the $\Pi_k^{\nabla,E}$ operator as in (2.6), and use it (mimicking (3.41) with $\Pi_k^{\nabla,E}$ instead of Π_k) to define the moments of v_h of order $k - 1$ and k . Thus the new space is

$$V_k^{\text{enh}}(E) := \left\{ v_h \in \tilde{V}_k(E) : \int_E (v_h - \Pi_k^{\nabla} v_h) p_s \, dE = 0 \text{ for all } p_s \in \mathbb{P}_s^{\text{hom}}, s = k-1, k \right\}. \quad (3.42)$$

Remark 3.10. We observe that both the serendipity and enhancement approaches allow us to compute the L^2 -projection onto \mathbb{P}_k . This can be used to compute an approximation of the right-hand side that is simpler than the original one described in (3.25). Setting $f_h := \Pi_{k-1}^0 f$, we have

$$\begin{aligned} (f - f_h, v_h)_{0,E} &= \int_E (f - \Pi_{k-1}^0 f) v_h \, dE = \int_E (f - \Pi_{k-1}^0 f) (v_h - \Pi_0^0 v_h) \, dE \\ &\leq Ch_E^{k-1} \|f\|_{k-1,E} h_E |v_h|_{1,E} \leq Ch_E^k \|f\|_{k-1,E} |v_h|_{1,E}. \end{aligned} \quad (3.43)$$

3.7. L^2 -projection of the gradient, and variable coefficients

From the degrees of freedom (3.16) we can compute, for any $v_h \in V_k(E)$, the L^2 -projection of ∇v_h onto $[\mathbb{P}_{k-1}(E)]^2$, defined as

$$\int_E \Pi_{k-1}^0 \nabla v_h \cdot \mathbf{q}_{k-1} \, dE = \int_E \nabla v_h \cdot \mathbf{q}_{k-1} \, dE \quad \text{for all } \mathbf{q}_{k-1} \in [\mathbb{P}_{k-1}(E)]^2. \quad (3.44)$$

In fact the left-hand side is an integral of polynomials, and the right-hand side, after integration by parts, becomes

$$\int_E \nabla v_h \cdot \mathbf{q}_{k-1} \, dE = - \int_E v_h \operatorname{div} \mathbf{q}_{k-1} \, dE + \int_{\partial E} v_h \mathbf{q}_{k-1} \cdot \mathbf{n} \, ds,$$

and both integrals on the right-hand side are computable.

As pointed out in Beirão da Veiga, Brezzi, Marini and Russo (2016d), and experimentally verified, in the presence of variable coefficients the Π_k^{∇} operator produces a loss of order of convergence for $k \geq 3$. For this reason the consistency

part of the discrete bilinear form needs to be changed. More precisely, if the problem to be approximated is $-\operatorname{div}(\kappa(x)\nabla u) = f$, we choose

$$a_h^E(v_h, w_h) = \int_E \kappa(x) \Pi_{k-1}^0 \nabla v_h \cdot \Pi_{k-1}^0 \nabla w_h \, dE + \mathcal{S}^E((I - \Pi_k^\nabla)v_h, (I - \Pi_k^\nabla)w_h)$$

instead of (3.19). It can be easily seen that the two forms coincide for $k = 1$ but not for $k \geq 2$. In the presence of variable coefficients the consistency property (3.9) cannot hold, but the consistency error can be controlled in terms of the right powers of h . In fact, from the properties of the L^2 -projection we have, for any $v_h \in V_k(E)$ and $p_k \in \mathbb{P}_k(E)$,

$$\begin{aligned} a_h^E(v_h, p_k) - a^E(v_h, p_k) &= \int_E \kappa(x) (\Pi_{k-1}^0 \nabla v_h - \nabla v_h) \cdot \nabla p_k \, dE \\ &= \int_E (\Pi_{k-1}^0 \nabla v_h - \nabla v_h) \cdot (\kappa(x) \nabla p_k - \Pi_{k-1}^0 \kappa(x) \nabla p_k) \, dE \\ &\leq Ch_E^k |\kappa \nabla p_k|_{k,E} |v_h|_{1,E}. \end{aligned}$$

This result will be used in the abstract convergence Theorem 3.2 with $p_k = u_\pi$. Consequently

$$a_h^E(v_h, u_\pi) - a^E(v_h, u_\pi) \leq Ch_E^k |\kappa \nabla u_\pi|_{k,E} |v_h|_{1,E} \leq C_\kappa h_E^k \|\nabla u\|_{k,E} |v_h|_{1,E}.$$

Hence, as shown in Beirão da Veiga *et al.* (2016d), the optimal estimate (3.31) holds true.

3.8. Extension to three dimensions

As a model problem, we now take the natural extension of problem (3.1) to three dimensions.

The first attempt that comes to mind, given a polyhedron P and an integer $k \geq 1$, is to extend what we did in the two-dimensional case. Let \mathcal{T}_h be a decomposition of Ω into polyhedra P . To begin with, we define the local spaces

$$\begin{aligned} V_k(P) := \{v_h \in C^0(\bar{P}): v_h|_e \in \mathbb{P}_k(e) \text{ for any edge } e \subset \partial P, \\ \Delta_2 v_h|_f \in \mathbb{P}_{k-2}(f) \text{ for any face } f \subset \partial P, \Delta_3 v_h \in \mathbb{P}_{k-2}(P)\}, \end{aligned} \quad (3.45)$$

with the degrees of freedom

- (D₁) the values of v_h at the vertices,
 - (D₂) for $k \geq 2$, the moments $\int_e v_h p_{k-2} \, ds$, for $p_{k-2} \in \mathbb{P}_{k-2}(e)$ and any e ,
 - (D₃) for $k \geq 2$, the moments $\int_f v_h p_{k-2} \, df$, for $p_{k-2} \in \mathbb{P}_{k-2}(f)$ and any f ,
 - (D₄) for $k \geq 2$, the moments $\int_P v_h p_{k-2} \, dP$, for $p_{k-2} \in \mathbb{P}_{k-2}(P)$.
- (3.46)

Then, following the two-dimensional path, for each $P \in \mathcal{T}_h$ and for each virtual element function v_h , we can define its $H_0^1(P)$ -projection $\Pi_k^{\nabla, P} v_h$ as in (2.6), that is, as the unique solution (up to a constant that can be easily fixed) in $\mathbb{P}_k(P)$ of

$$\int_P \nabla(\Pi_k^{\nabla, P} v_h) \cdot \nabla p_k \, dP = \int_P \nabla v_h \cdot \nabla p_k \, dP \quad \text{for } p_k \in \mathbb{P}_k(P). \quad (3.47)$$

Unfortunately, when we attempt to *compute* the right-hand side of (3.47) using the degrees of freedom (3.46), we have

$$\int_P \nabla v_h \cdot \nabla p_k \, dP = \int_{\partial P} v_h \frac{\partial p_k}{\partial n} \, dS - \int_P v_h \Delta p_k \, dP. \quad (3.48)$$

Now, the second term on the right-hand side of (3.48) does not cause any trouble: for p_k in \mathbb{P}_k we see that $\Delta p_k \in \mathbb{P}_{k-2}$ and the term can be computed using the degrees of freedom (D_4) in (3.46). But for the first term on the right-hand side of (3.48), we would need to know the moments of v_h on each face up to order $k-1$ (the degree of $\partial p_k / \partial n$), while in (3.46) we have the moments only up to $k-2$. The way out, as presented first in Ahmad *et al.* (2013), is as follows:

$$\begin{aligned} &\text{split } \frac{\partial p_k}{\partial n} \text{ into } \frac{\partial p_k}{\partial n} = p_{k-2} + p_{k-1}^{\text{hom}}, \quad p_{k-2} \in \mathbb{P}_{k-2}, \quad p_{k-1}^{\text{hom}} \in \mathbb{P}_{k-1}^{\text{hom}}, \\ &\text{and replace } \int_f v_h \frac{\partial p_k}{\partial n} \, df \text{ with } \int_f v p_{k-2} \, df + \int_f (\Pi_k^{\nabla, f} v_h) p_{k-1}^{\text{hom}} \, df. \end{aligned} \quad (3.49)$$

In (3.49), $\Pi_k^{\nabla, f} v_h$ is the two-dimensional projection of v_h , as defined in (2.6), whose computation, in turn, on each face f requires the moments of v_h on f only up to order $k-2$. One might regard this as a typical use of the approach described in Section 3.6, the so-called *enhancement trick*, which allows us to have all the moments up to order k , and consequently the L^2 -projection onto \mathbb{P}_k . More precisely, the *enhancement trick* is as follows.

- For each face f we consider the space $\tilde{V}_k(f)$ defined in (3.37), with the degrees of freedom (3.38).
- In $\tilde{V}_k(f)$ we can construct the operator $\Pi_k^{\nabla, f}$, for which only the moments of degree up to $k-2$ are needed, and use its moments of degree $k-1$ and k to define the enhanced space $V_k^{\text{enh}}(f)$ on each face as in (3.42).
- Finally, the enhanced space on the polyhedron P is given by

$$V_k^{\text{enh}}(P) := \{v_h \in C^0(\bar{P}): v_h|_f \in V_k^{\text{enh}}(f) \text{ for any face } f, \Delta_3 v_h \in \mathbb{P}_{k-2}(P)\}. \quad (3.50)$$

Once the operator $\Pi_k^{\nabla, P}$ has been computed, the local bilinear form can be defined, for each $P \in \mathcal{T}_h$ and for each $v_h, w_h \in V_k^{\text{enh}}(P)$, exactly as in (3.19):

$$a_h^P(v_h, w_h) := a^P(\Pi_k^{\nabla, P} v_h, \Pi_k^{\nabla, P} w_h) + S^P((I - \Pi_k^{\nabla, P}) v_h, (I - \Pi_k^{\nabla, P}) w_h). \quad (3.51)$$

Let us turn to the right-hand side. The first term in $\ell(v_h)$ (see (3.2)) is treated exactly as in (3.25), just by replacing the polygon E with the polyhedron P . Instead the treatment of the boundary term needs some care, since now the functions in $V_k^{\text{enh}}(P)$ are not known on the faces. Thanks to the *enhancement trick* we know their projections onto polynomials, in particular of degree $k - 1$, on each face. Hence

$$\int_f g v_h \, df \text{ can be replaced by } \int_f g \Pi_{k-1}^0 v_h \, df, \text{ for any face } f \subset \Gamma_N. \quad (3.52)$$

Here too, as in the two-dimensional case, we assume that the integrals to the right of (3.52) can be computed exactly. Then, adding and subtracting $\Pi_{k-1}^0 g$, and using the properties of the L^2 -projection and classical estimates, we obtain

$$\begin{aligned} & \int_f g v_h \, df - \int_f g \Pi_{k-1}^0 v_h \, df \\ &= \int_f (g - \Pi_{k-1}^0 g) v_h \, df + \int_f ((\Pi_{k-1}^0 g) v_h - g \Pi_{k-1}^0 v_h) \, df \\ &= \int_f (g - \Pi_{k-1}^0 g) (v_h - \Pi_{k-1}^0 v_h) \, df + 0 \\ &\leq C h^{k-1/2} |g|_{k-1/2,f} h^{1/2} |v_h|_{1/2,f} \leq C h^k |g|_{k-1/2,f} \|v_h\|_{1,P}. \end{aligned} \quad (3.53)$$

Finally, the global quantities are defined by collecting the local ones:

$$\begin{aligned} V_h &:= \{v_h \in H_{0,\Gamma_D}^1(\Omega) : v_h|_P \in V_k^{\text{enh}}(P) \text{ for all } P \in \mathcal{T}_h\}, \\ a_h(v_h, w_h) &:= \sum_{P \in \mathcal{T}_h} a_h^P(v_h, w_h) \quad \text{for all } v_h, w_h \in V_h, \\ \ell_h(v_h) &:= \sum_{P \in \mathcal{T}_h} (f_h, v_h)_{0,P} + \sum_{f \subset \Gamma_N} (g, \Pi_{k-1}^0 v_h)_{0,f} \quad \text{for all } v_h \in V_h. \end{aligned} \quad (3.54)$$

4. H^1 -nonconforming approximations

Nonconforming approximations for H^1 were first introduced and analysed by [Ayuso de Dios, Lipnikov and Manzini \(2016\)](#). In this section we will recall their approach, always applied to the continuous model problem (3.1), with some modifications in the treatment of the right-hand side. As for nonconforming finite element approximations, the discrete spaces that we are going to introduce are not subspaces of $H^1(\Omega)$, as they are made up of functions which are only weakly continuous at the inter-element boundaries. Therefore we need some preliminary notation. Let \mathcal{T}_h be a decomposition of Ω into polygons E , and let

$$H^1(\mathcal{T}_h) := \prod_{E \in \mathcal{T}_h} H^1(E).$$

Let \mathcal{E}_h be the set of edges of \mathcal{T}_h , \mathcal{E}_h^o the set of internal edges and \mathcal{E}_h^∂ the set of boundary edges. For a function $v \in H^1(\mathcal{T}_h)$ (or a vector $\mathbf{v} \in [H^1(\mathcal{T}_h)]^2$) we define

its averages and jumps on the edges as (see e.g. Arnold, Brezzi, Cockburn and Marini 2001)

$$\begin{aligned}\{v\}|_e &:= \frac{v^+ + v^-}{2} && \text{on } e \in \mathcal{E}_h^o, & \{v\}|_e &:= v && \text{on } e \in \mathcal{E}_h^\partial, \\ [[v]]|_e &:= v^+ \mathbf{n}^+ + v^- \mathbf{n}^- && \text{on } e \in \mathcal{E}_h^o, & [[v]]|_e &:= v \mathbf{n} && \text{on } e \in \mathcal{E}_h^\partial,\end{aligned}\quad (4.1)$$

where v^\pm is the restriction of v to the elements E^\pm having the edge e in common, and \mathbf{n}^\pm is the outward unit normal to E^\pm . For an edge on the boundary, \mathbf{n} is the outward unit normal to $\partial\Omega$. With these definitions the following useful formula holds for v and w in $H^1(\mathcal{T}_h)$ (see Arnold *et al.* 2001):

$$\sum_{E \in \mathcal{T}_h} \int_{\partial E} \frac{\partial w}{\partial n} v \, ds = \sum_{e \in \mathcal{E}_h^o} \int_e [[\nabla w]] \cdot \{v\} \, de + \sum_{e \in \mathcal{E}_h} \int_e [[v]] \cdot \{\nabla w\} \, de. \quad (4.2)$$

Let u be the solution of (3.1). By integrating by parts and applying (4.2), taking into account that $[[\nabla u]]|_e = 0$ on $e \in \mathcal{E}_h^o$, we deduce, for all $v \in H^1(\mathcal{T}_h)$,

$$\begin{aligned}a(u, v) &= \sum_{E \in \mathcal{T}_h} a^E(u, v) = \sum_{E \in \mathcal{T}_h} \left(\int_E -\Delta u v \, dE + \int_{\partial E} \frac{\partial u}{\partial n} v \, ds \right) \\ &= (f, v)_{0, \Omega} + \sum_e \int_e [[v]] \cdot \{\nabla u\} \, de \\ &= (f, v)_{0, \Omega} + \sum_{e \subset \Gamma_N} \int_e g v \, de + \sum_{e \notin \Gamma_N} \int_e [[v]] \cdot \{\nabla u\} \, de \\ &= \ell(v) + \sum_{e \notin \Gamma_N} \int_e [[v]] \cdot \{\nabla u\} \, de.\end{aligned}\quad (4.3)$$

The term

$$\mathcal{N}_h(u, v) := \sum_{e \notin \Gamma_N} \int_e [[v]] \cdot \{\nabla u\} \, de \quad (4.4)$$

is a measure of the nonconformity and needs to be estimated. To this end, we anticipate that the discrete VEM spaces that we are going to build, made up of functions weakly continuous at the inter-elements, will be subspaces of

$$H^{1,nc}(\mathcal{T}_h) := \left\{ v \in H^1(\mathcal{T}_h) : \int_e [[v]] \cdot \mathbf{n} p_{k-1} \, ds = 0 \text{ for } e \notin \Gamma_N, p_{k-1} \in \mathbb{P}_{k-1}(e) \right\}.$$

We can now prove the following lemma.

Lemma 4.1. Let u be the solution of problem (3.1). There exists a constant C independent of h such that the following estimate holds:

$$\mathcal{N}_h(u, v_h) \leq C h^k \|u\|_{k+1, \Omega} \|v_h\|_{1, \mathcal{T}_h} \quad \text{for all } v_h \in H^{1,nc}(\mathcal{T}_h). \quad (4.5)$$

Proof. We briefly sketch the proof, which is the same as for nonconforming finite elements. Using the properties of the L^2 -projection and the definition of $H^{1,\text{nc}}(\mathcal{T}_h)$, we have

$$\begin{aligned}\mathcal{N}_h(u, v_h) &:= \sum_{e \notin \Gamma_N} \int_e \{\nabla u\} \cdot [[v_h]] \, de \\ &= \sum_{e \notin \Gamma_N} \int_e (\{\nabla u\} - \{\Pi_{k-1}^0 \nabla u\}) \cdot [[v_h]] \, de \\ &= \sum_{e \notin \Gamma_N} \int_e (\{\nabla u\} - \{\Pi_{k-1}^0 \nabla u\}) \cdot ([[[v_h]] - \Pi_0^{0,e}([[v_h]]]) \, de \\ &\leq \sum_{e \notin \Gamma_N} \|\{\nabla u\} - \{\Pi_{k-1}^0 \nabla u\}\|_{0,e} \cdot \|[[v_h]] - \Pi_0^{0,e}([[v_h]])\|_{0,e}\end{aligned}$$

where $\{\Pi_{k-1}^0 \nabla u\}$ on an edge e is obtained by taking the average of $\Pi_{k-1}^{0,E^\pm} \nabla u$, where E^\pm are the two elements having e as common edge.

Then the trace inequality and standard approximation properties give the result. \square

We are now ready to introduce the nonconforming approximation of (3.1).

4.1. The local discrete spaces and bilinear forms

Again let E be a generic polygon in \mathcal{T}_h , and let \mathbf{n} be, as usual, the unit outward normal to each edge. For $k \geq 1$ we define

$$V_k^{\text{nc}}(E) := \left\{ v_h \in C^0(\overline{E}) : \frac{\partial v_h}{\partial n} \Big|_e \in \mathbb{P}_{k-1}(e) \text{ for any } e \subset \partial E, \Delta v_h \in \mathbb{P}_{k-2}(E) \right\}, \quad (4.6)$$

with the degrees of freedom given by

$$\begin{aligned}(D_1) \quad &\text{the moments } \int_e v_h p_{k-1} \, de, \text{ for } p_{k-1} \in \mathbb{P}_{k-1}(e) \text{ and any } e, \\ (D_2) \quad &\text{for } k \geq 2, \text{ the moments } \int_E v_h p_{k-2} \, dE, \text{ for } p_{k-2} \in \mathbb{P}_{k-2}(E).\end{aligned} \quad (4.7)$$

We emphasize that from definition (4.6) it is clear that $\mathbb{P}_k(E) \subset V_k^{\text{nc}}(E)$.

Lemma 4.2. The degrees of freedom (4.7) are unisolvant for $V_k^{\text{nc}}(E)$.

Proof. Since the number of degrees of freedom equals the dimension of $V_k^{\text{nc}}(E)$, it is enough to show that a function v_h having all the degrees of freedom vanishing is identically zero. Then let $v_h \in V_k^{\text{nc}}(E)$ such that

$$\begin{aligned}\int_e v_h p_{k-1} \, de &= 0 \quad \text{for } p_{k-1} \in \mathbb{P}_{k-1}(e) \text{ and any edge } e, \\ \int_E v_h p_{k-2} \, dE &= 0 \quad \text{for } p_{k-2} \in \mathbb{P}_{k-2}(E).\end{aligned}$$

Since $\Delta v_h \in \mathbb{P}_{k-2}(E)$, and $\partial v_h / \partial n|_e \in \mathbb{P}_{k-1}(e)$ for any edge e , integration by parts gives

$$\int_E |\nabla v_h|^2 dE = - \int_E v_h \Delta v_h dE + \int_{\partial E} v_h \frac{\partial v_h}{\partial n} ds = 0.$$

Hence $v_h = \text{const.}$, which together with $(D_1) = 0$ implies $v_h \equiv 0$. \square

Remark 4.3. The space (4.6) was the original space defined in Ayuso de Dios *et al.* (2016). Here we will instead use an enhanced space that significantly simplifies the treatment of the right-hand side. Without repeating the details of the *enhancement trick*, which would be exactly the same as what we did in the previous section, we define the space

$$\tilde{V}_k^{\text{nc}}(E) := \left\{ v_h \in C^0(\bar{E}) : \frac{\partial v_h}{\partial n}|_e \in \mathbb{P}_{k-1}(e) \text{ for any } e \subset \partial E, \Delta v_h \in \mathbb{P}_k(E) \right\}, \quad (4.8)$$

with the degrees of freedom (4.7) plus the moments of order $k-1$ and k . After computing the Π_k^∇ operator as in (2.6) using only the degrees of freedom (4.7), we define the enhanced space as

$$\begin{aligned} & V_k^{\text{nc,enh}}(E) \\ &:= \left\{ v_h \in \tilde{V}_k^{\text{nc}}(E) : \int_E (v_h - \Pi_k^\nabla v_h) p_s dE = 0 \text{ for all } p_s \in \mathbb{P}_s^{\text{hom}}, s = k-1, k \right\}. \end{aligned} \quad (4.9)$$

Once the local spaces $V_k^{\text{nc,enh}}(E)$ have been defined, we follow the same path as in the previous section in order to write the discrete problem. The local bilinear forms are constructed as in (3.19)–(3.21):

$$a_h^E(v_h, w_h) := a^E(\Pi_k^\nabla v_h, \Pi_k^\nabla w_h) + S^E((I - \Pi_k^\nabla)v_h, (I - \Pi_k^\nabla)w_h).$$

k -consistency and stability hold with the same arguments as in Lemma 3.6.

4.2. Construction of a computable right-hand side

Thanks to the enhancement procedure of Remark 4.3, the approximation of the volume term on the right-hand side simplifies significantly with respect to the original one, and goes exactly as in (3.43) of Remark 3.10. Thus, with $f_h = \Pi_{k-1}^0 f$,

$$(f, v_h)_{0,E} - (f_h, v_h)_{0,E} \leq Ch_E^k \|f\|_{k,E} |v_h|_{1,E}. \quad (4.10)$$

For the term on the Neumann boundary, letting $\Pi_{k-1}^0 g$ denote the L^2 -projection of g onto $\mathbb{P}_{k-1}(e)$ for each edge $e \subset \Gamma_N$, and setting

$$g_h|_e = \Pi_{k-1}^0 g \quad \text{for any } e \subset \Gamma_N, \quad (4.11)$$

we obtain

$$\begin{aligned} \int_e g v_h \, de - \int_e g_h v_h \, de &= \int_e (g - \Pi_{k-1}^0 g) (v_h - \Pi_{k-1}^0 v_h) \, de \\ &\leq C h^{k-1/2} |g|_{k-1/2,e} h^{1/2} |v_h|_{1/2,e} \\ &\leq C h^k |g|_{k-1/2,e} \|v_h\|_{1,E}. \end{aligned} \quad (4.12)$$

4.3. The global problem: error estimates

The global space is defined as a patchwork of the spaces (4.6), with the addition of a weak continuity condition at the inter-elements:

$$\begin{aligned} V_h^{\text{nc}} := \Big\{ v_h \in H^1(\mathcal{T}_h) : v_h|_E \in V_k^{\text{nc},\text{enh}}(E) \text{ for all } E \in \mathcal{T}_h, \text{ and} \\ \int_e [[v_h]] \cdot \mathbf{n} p_{k-1} \, de = 0 \text{ for any } e \notin \Gamma_N, p_{k-1} \in \mathbb{P}_{k-1}(e) \Big\}. \end{aligned} \quad (4.13)$$

The global bilinear form and right-hand side are defined, as usual, by summing over the elements of \mathcal{T}_h ,

$$\begin{aligned} a_h(v_h, w_h) &:= \sum_{E \in \mathcal{T}_h} a_h^E(v_h, w_h), \\ \ell_h(v_h) &:= \sum_{E \in \mathcal{T}_h} (f_h, v_h)_{0,E} + \sum_{e \subset \Gamma_N} (g_h, v_h)_{0,e}, \end{aligned} \quad (4.14)$$

and the discrete problem is:

$$\text{Find } u_h \in V_h^{\text{nc}} \text{ such that } a_h(u_h, v_h) = \ell_h(v_h) \text{ for all } v_h \in V_h^{\text{nc}}. \quad (4.15)$$

Theorem 4.4. The discrete problem (4.15) has a unique solution $u_h \in V_h^{\text{nc}}$. Moreover, under Assumption 2.1 on the mesh, we have

$$\|u - u_h\|_{1,\mathcal{T}_h} \leq Ch^k |u|_{k+1,\Omega}. \quad (4.16)$$

Proof. Since Assumption 3.1 holds (the bilinear form is k -consistent and stable), problem (4.15) has a unique solution u_h . Moreover, an abstract estimate similar to (3.12) holds: for every approximation $u_I \in V_h^{\text{nc}}$ of u and for every approximation u_π of u that is piecewise in \mathbb{P}_k , we have

$$|u - u_h|_{1,\mathcal{T}_h} \leq C(|u - u_I|_{1,\mathcal{T}_h} + |u - u_\pi|_{1,\mathcal{T}_h} + \mathfrak{F}_h + \mathfrak{N}_h), \quad (4.17)$$

where C is a constant independent of h , $|\cdot|_{1,\mathcal{T}_h}$ is the broken H^1 -norm, and, for any h , \mathfrak{F}_h and \mathfrak{N}_h , respectively, are the smallest constants such that

$$|\ell(v_h) - \ell_h(v_h)| \leq \mathfrak{F}_h |v_h|_{1,\mathcal{T}_h}, \quad |\mathcal{N}_h(u, v_h)| \leq \mathfrak{N}_h |v_h|_{1,\mathcal{T}_h} \quad \text{for all } v_h \in V_h^{\text{nc}}. \quad (4.18)$$

The proof of (4.17) goes like that of Theorem 3.2, with the addition of the non-conformity term (4.4). Setting $\delta_h = u_h - u_I$, without repeating all the steps of the

proof, and using (4.3) we obtain

$$\begin{aligned}\alpha_* |\delta_h|_{1,\mathcal{T}_h}^2 &\leq \ell_h(\delta_h) - \ell(\delta_h) - \sum_E (a_h^E(u_I - u_\pi, \delta_h) + a^E(u_\pi - u, \delta_h)) - \mathcal{N}_h(u, \delta_h) \\ &\leq C(\mathfrak{F}_h + \mathfrak{N}_h + |u_I - u_\pi|_{1,\mathcal{T}_h} + |u - u_\pi|_{1,\mathcal{T}_h}) |\delta_h|_{1,\mathcal{T}_h},\end{aligned}$$

and (4.17) follows by the triangle inequality. For the right-hand side we have, from (4.10)–(4.12),

$$\begin{aligned}\ell(v_h) - \ell_h(v_h) &= \sum_{E \in \mathcal{T}_h} (f - f_h, v_h)_{0,E} + \sum_{e \subset \Gamma_N} (g - g_h, v_h)_e \\ &\leq C h^k (\|f\|_{k,\Omega} + \|g\|_{k-1/2,\Gamma_N}) |v_h|_{1,\mathcal{T}_h} \quad \text{for all } v_h \in V_h^{\text{nc}}.\end{aligned}\tag{4.19}$$

From (4.5), (4.19) and classical approximation results (see e.g. Brenner and Scott 2008) in (4.17), we finally have the optimal estimate (4.16). \square

5. H^2 -conforming approximations

With virtual elements it is quite easy to construct high-regularity approximations. Here we shall deal with C^1 approximations, having in mind, as an example of a fourth-order problem, a plate bending problem in the Kirchhoff–Love model:

$$D\Delta^2 w = f \text{ in } \Omega, \quad w = \frac{\partial w}{\partial n} = 0 \text{ on } \partial\Omega, \tag{5.1}$$

where $D = Et^3/12(1-\mu^2)$ is the bending rigidity, E is the Young's modulus, t is the thickness, μ is the Poisson's ratio, and we assumed that the plate is clamped all over the boundary. In order to write the variational formulation of (5.1), we define

$$a(v, w) = D \left[(1-\mu) \int_{\Omega} w_{/ij} v_{/ij} dx + \mu \int_{\Omega} \Delta w \Delta v dx \right], \quad \langle f, v \rangle = \int_{\Omega} fv dx. \tag{5.2}$$

In (5.2), $v_{/i} = \partial v / \partial x_i$, $i = 1, 2$, and we used the summation convention of repeated indices. Throughout this section $w_{/n}$ will denote the normal derivative, $w_{/t}$ the tangential derivative in the anticlockwise orientation of the boundary, and so on. When no confusion occurs we might also use w_n , w_t

The variational formulation of (5.1) is then:

$$\text{Find } w \in V := H_0^2(\Omega) \text{ such that } a(w, v) = \langle f, v \rangle \text{ for all } v \in V. \tag{5.3}$$

In the following subsections we recall the discretization of (5.3) presented in Brezzi and Marini (2013) and Chinosi and Marini (2016). For other approaches we refer to Zhao, Chen and Zhang (2016) and Antonietti, Manzini and Verani (2018) for nonconforming approximations, to Antonietti, Beirão da Veiga, Scacchi and Verani (2016) for application to the Cahn–Hilliard equation, to Brenner, Sung and Tan (2021) for optimal control problems, and to Wang and Zhao (2021) for conforming and nonconforming approximations of contact problems.

5.1. The local VEM spaces

Let E be a polygon in \mathcal{T}_h . The local spaces will depend on three integer indices (r, s, m) , related to the degree of accuracy $k \geq 2$ by

$$r = \max\{3, k\}, \quad s = k - 1, \quad m = k - 4. \quad (5.4)$$

We set

$$\begin{aligned} W_{r,s,m}(E) \\ := \{w \in H^2(E) : w|_e \in \mathbb{P}_r(e), w_{n|e} \in \mathbb{P}_s(e) \text{ for any } e, \Delta^2 w \in \mathbb{P}_m(E)\}. \end{aligned} \quad (5.5)$$

The degrees of freedom in $W_{r,s,m}(E)$ are

- (D_0) the values of $w, w_{/1}$ and $w_{/2}$ at the vertices,
 - (D_1) for $r \geq 4$, the moments $\int_e w q_{r-4} \, de$, for $q_{r-4} \in \mathbb{P}_{r-4}(e)$ and any $e \subset \partial E$,
 - (D_2) for $s \geq 2$, the moments $\int_e w_{/n} q_{s-2} \, de$, for $q_{s-2} \in \mathbb{P}_{s-2}(e)$ and any $e \subset \partial E$,
 - (D_3) for $m \geq 0$, the moments $\int_E w q_m \, dE$, for $q_m \in \mathbb{P}_m(E)$.
- (5.6)

We note that the VEM space $W_{r,s,m}(E)$ will contain all polynomials \mathbb{P}_k with

$$k = \min\{r, s + 1, m + 4\} \geq 2,$$

which will be the order of precision. We point out once more that the above degrees of freedom need to be properly scaled in such a way that they all have the same dimension. For a discussion and details of this issue we refer to [Brezzi and Marini \(2013\)](#).

Lemma 5.1. The degrees of freedom (5.6) are unisolvant for $W_{r,s,m}(E)$.

Proof. The proof follows the usual path. Since the number of degrees of freedom equals the dimension of $W_{r,s,m}(E)$, it is enough to show that a function w having all the degrees of freedom vanishing is identically zero. We first observe that $(D_0) = 0$ implies that w and ∇w vanish at the vertices of E . Therefore, on each edge, w is a polynomial of degree r vanishing at the two endpoints with its tangential derivative. Hence, letting t denote the edge variable, and t_1 and t_2 the coordinates of the endpoints, w will have the expression $w = (t - t_1)^2(t - t_2)^2 q_{r-4}$. Then, from the vanishing of the degrees of freedom (D_1) , we deduce that $w \equiv 0$ on each edge. Similarly, from the vanishing of (D_0) and (D_2) , we deduce that $w_{/n}$ vanishes identically on each edge. Indeed, on each edge $w_{/n}$ is a polynomial of degree s vanishing at the two endpoints. Its expression is then $w_{/n} = (t - t_1)(t - t_2) q_{s-2}$ which, together with $(D_2) = 0$, implies $w_{/n} \equiv 0$ on each edge. Consequently

$$w \equiv 0 \quad w_{/n} \equiv 0 \quad \text{on } \partial E.$$

Finally, this together with $(D_3) = 0$ and integration by parts twice gives

$$\begin{aligned} \int_E (\Delta w)^2 \, dE &= - \int_E \nabla w \cdot \nabla \Delta w \, dE + \int_{\partial E} \frac{\partial w}{\partial n} \Delta w \, ds \\ &= \int_E w \Delta^2 w \, dE - \int_{\partial E} w \frac{\partial \Delta w}{\partial n} \, ds + \int_{\partial E} \frac{\partial w}{\partial n} \Delta w \, ds = 0 \end{aligned}$$

since $\Delta^2 w \in \mathbb{P}_m(E)$. Then it follows that $\Delta w = 0$, and since $w = 0$ on the boundary we deduce that $w \equiv 0$ in E . \square

5.2. Construction of a computable discrete bilinear form

As in Section 3 we begin by defining, for $k \geq 2$, an operator $\Pi_k^\Delta: W_{r,s,m}(E) \rightarrow \mathbb{P}_k(E) \subset W_{r,s,m}(E)$ defined as the solution of

$$\begin{cases} a^E(\Pi_k^\Delta \psi, q) = a^E(\psi, q) & \text{for all } \psi \in W_{r,s,m}(E), q \in \mathbb{P}_k(E), \\ \int_{\partial E} (\Pi_k^\Delta \psi - \psi) \, ds = 0, & \int_{\partial E} \nabla(\Pi_k^\Delta \psi - \psi) \, ds = 0. \end{cases} \quad (5.7)$$

We note that for $v \in \mathbb{P}_k(E)$ the first equation in (5.7) implies $(\Pi_k^\Delta v)_{ij} = v_{ij}$ for $i, j = 1, 2$, which joined with the second equation easily gives

$$\Pi_k^\Delta v = v \quad \text{for all } v \in \mathbb{P}_k(E). \quad (5.8)$$

Hence Π_k^Δ is a projector operator onto $\mathbb{P}_k(E)$. We also observe that Π_k^Δ is computable from the degrees of freedom (D_0) – (D_3) , as can be easily seen upon integration by parts twice of the term $a^E(\psi, q)$. Choosing $a_h^E(v, w) = a^E(\Pi_k^\Delta v, \Pi_k^\Delta w)$ would guarantee consistency but not stability. Then, as in the previous section, we add a stabilizing term, and set

$$a_h^E(v, w) := a^E(\Pi_k^\Delta v, \Pi_k^\Delta w) + \mathcal{S}^E((I - \Pi_k^\Delta)v, (I - \Pi_k^\Delta)w), \quad (5.9)$$

where \mathcal{S}^E is any symmetric bilinear form to be chosen in such a way that it scales like $a^E(\cdot, \cdot)$ and is positive on the kernel of Π_k^Δ , that is, there exist two positive constants c_1, c_2 such that

$$c_1 a^E(v, v) \leq \mathcal{S}^E(v, v) \leq c_2 a^E(v, v) \quad \text{for all } v \text{ such that } \Pi_k^\Delta v = 0.$$

Assuming, for example, that the degrees of freedom (5.6) are all scaled like the vertex values, we can take

$$\mathcal{S}^E(v, w) := h_E^{-2} \sum_{i=1}^{\#dofs} \text{dof}_i(v) \text{dof}_i(w). \quad (5.10)$$

Lemma 5.2. The discrete bilinear form (5.9) is k -consistent and stable.

Proof. The proof goes exactly like that of Lemma 3.6, and we do not repeat it. \square

5.3. Construction of the right-hand side

In order to build an approximation of the term $\langle f, v \rangle$ in a simple and easy way, it is convenient to have internal degrees of freedom in $W_{r,s,m}(E)$, and this means, according to (5.4), that $k \geq 4$ is needed. Brezzi and Marini (2013) made suitable choices for different values of k , enough to guarantee the proper order of convergence in H^2 . Here we report the choice made in Chinosi and Marini (2016), which once more makes use of the *enhancement trick* of Ahmad *et al.* (2013). For that, we modify the definition (5.5). For $k \geq 2$, and r and s related to k by (5.4), let $\tilde{W}_k(E)$ be the new local space, given by

$$\tilde{W}_k(E) := \{v \in H^2(E) : v|_e \in \mathbb{P}_r(e), v_{n|e} \in \mathbb{P}_s(e) \text{ for all } e \subset \partial E, \Delta^2 v \in \mathbb{P}_{k-2}(E)\}.$$

The degrees of freedom in $\tilde{W}_k(E)$ would be (5.6), plus the moments of degree $k-3$ and $k-2$, but for the construction of the operator Π_k^Δ only the degrees of freedom (5.6) are needed. Once Π_k^Δ has been constructed, we *copy* its moments. More precisely, we define

$$\text{for } k = 2, \quad W_2(E) = \left\{ v \in \tilde{W}_2(E), \text{ and } \int_E v \, dE = \int_E \Pi_2^\Delta v \, dE \right\}, \quad (5.11)$$

$$\begin{aligned} \text{for } k \geq 3, \quad W_k(E) = & \left\{ v \in \tilde{W}_k(E), \text{ and } \int_E v p_\alpha \, dE = \int_E \Pi_k^\Delta v p_\alpha \, dE, \right. \\ & \left. p_\alpha \in \mathbb{P}_\alpha^{\text{hom}}, \alpha = k-3, k-2 \right\}. \end{aligned} \quad (5.12)$$

It can be checked that the degrees of freedom (5.6) are the same, but the added conditions on the moments now allow us to compute the L^2 -projection of any $v \in W_k$ onto $\mathbb{P}_{k-2}(E)$, and not only onto $\mathbb{P}_{k-4}(E)$ as before. So taking, in each element, f_h as the L^2 -projection of f onto the space of polynomials of degree $k-2$, that is,

$$f_h|_E = \Pi_{k-2}^0 f \quad \text{for all } E \in \mathcal{T}_h,$$

we obtain

$$\langle f, v \rangle_E - \langle f_h, v \rangle_E = \int_E (f - \Pi_{k-2}^0 f) v \, dE \leq Ch_E^{k-1} |f|_{k-1,E} \|v\|_{2,E}. \quad (5.13)$$

We are now ready to write the discrete problem.

5.4. The global problem: error estimates

Let \mathcal{T}_h be a decomposition of Ω into polygons, satisfying Assumption 2.1. The global space W_h is defined as a patchwork of the spaces (5.11) or (5.12), depending on the value of k :

$$W_h := \{v \in H_0^2(\Omega) : v|_E \in W_k(E) \text{ for all } E \in \mathcal{T}_h\}. \quad (5.14)$$

The global bilinear form and right-hand side are defined by summing over the elements of \mathcal{T}_h :

$$a_h(v_h, w_h) := \sum_{E \in \mathcal{T}_h} a_h^E(v_h, w_h), \quad \langle f_h, v_h \rangle := \sum_{E \in \mathcal{T}_h} (\Pi_{k-2}^0 f, v_h)_{0,E}, \quad (5.15)$$

and the discrete problem is:

$$\text{Find } w_h \in W_h \text{ such that } a_h(w_h, v_h) = \langle f_h, v_h \rangle \text{ for all } v_h \in W_h. \quad (5.16)$$

We have the analogue of Theorem 3.2.

Theorem 5.3. The discrete problem (5.16) has a unique solution w_h . Moreover, for every approximation w_I of w in W_h and for every approximation w_π of w that is piecewise in \mathbb{P}_k , we have

$$|w - w_h|_{2,\Omega} \leq C(|w - w_I|_{2,\Omega} + |w - w_\pi|_{2,\mathcal{T}_h} + \|f - f_h\|_{W'_h}), \quad (5.17)$$

where C is a constant independent of h , $\|\cdot\|_{2,\mathcal{T}_h}$ is the broken H^2 -norm, and

$$\|f - f_h\|_{W'_h} := \sup_{v_h \in W_h} \frac{\langle f - f_h, v_h \rangle}{|v_h|_{2,\Omega}}. \quad (5.18)$$

Proof. Following the proof of the abstract Theorem 3.2 step by step, the result follows easily. \square

If w_I is the interpolant of w in W_h , defined through the degrees of freedom (5.6), thanks to Assumption 2.1 on the mesh we have

$$\|w - w_I\|_{2,\Omega} \leq C h^{k-1} \|w\|_{k+1,\Omega}. \quad (5.19)$$

Similarly,

$$\|w - w_\pi\|_{2,\mathcal{T}_h} \leq C h^{k-1} \|w\|_{k+1,\Omega}. \quad (5.20)$$

Finally, the following convergence theorem holds.

Theorem 5.4. Let w be the solution of problem (5.3), and let w_h be the solution of the discrete problem (5.16). The following holds true: for $k \geq 2$,

$$\|w - w_h\|_{2,\Omega} \leq C h^{k-1} |w|_{k+1,\Omega}. \quad (5.21)$$

Proof. Using (5.19), (5.20) and (5.13) in (5.17), the result (5.21) follows. \square

We conclude this section with a couple of remarks.

Remark 5.5. The lowest-order element of our family, corresponding to the choice $r = 3, s = 1, m = -2$, can be seen as the extension to polygons of the finite element composite triangle known as the *reduced Hsieh–Clough–Tocher* element. On a triangle they have the same degrees of freedom ($w, w_{/x}, w_{/y}$ at the vertices), they both contain \mathbb{P}_2 and share the same order of accuracy, $k = 2$. Similar considerations apply to the second-lowest element of the family (corresponding to $r = 3, s = 2, m = -1$), which can be seen as the extension to polygons of the well-known finite

element composite *Hsieh–Clough–Tocher* triangle. On a triangle, the degrees of freedom are the same ($w, w_{/x}, w_{/y}$ at the vertices and $w_{/n}$ at the midpoints of the edges), \mathbb{P}_3 is included in the local spaces, and thus the order of precision is $k = 3$ for both.

6. $H(\text{div})$, $H(\text{rot})$ and $H(\text{curl})$ -conforming approximations

In a number of applications, for instance electromagnetism or diffusion problems in mixed form, spaces such as L^2 , H^1 or H^2 cannot be used alone. They must be suitably coupled with other functional spaces, such as $H(\text{div})$, $H(\text{rot})$ and $H(\text{curl})$. In the present section we will show how to design VEM discretizations of such spaces.

Virtual element spaces of $H(\text{div})$ type were initially introduced in Brezzi, Falk and Marini (2014) and later improved in Beirão da Veiga, Brezzi, Marini and Russo (2016b). Within the large literature involved in the application of such spaces to advanced diffusion problems we mention Benedetto, Borio and Scialò (2017) and Benedetto *et al.* (2022).

Subsequently, $H(\text{div})$ and $H(\text{curl})$ VEM spaces in two and three dimensions were introduced in Beirão da Veiga, Brezzi, Marini and Russo (2016a) and then improved in a series of papers by Beirão da Veiga *et al.* (2017a, 2018a,b), which also dealt with the magneto-static equations as a model problem. Among the papers dealing with the application and extension of such spaces for more advanced problems, we mention Dassi, Di Barba and Russo (2020a), Beirão da Veiga, Dassi, Manzini and Mascotto (2022a,b), Cao, Chen, Guo and Lin (2022b) and Cao, Chen and Guo (2022a).

Let us begin by introducing some further notation and definitions that will be useful henceforth.

6.1. Polynomial spaces and exact sequences

In the following we let i denote the mapping that to every real *number* c associates the constant *function* (zero-degree polynomial) identically equal to c , and we let o denote the mapping that to every *function* (polynomial) associates the *number* 0.

Then we recall that we have the exactness of the following sequences.

- In two dimensions:

$$\mathbb{R} \xrightarrow{i} \mathbb{P}_r \xrightarrow{\text{grad}} [\mathbb{P}_{r-1}]^2 \xrightarrow{\text{rot}} \mathbb{P}_{r-2} \xrightarrow{o} \mathbb{R} \quad (6.1)$$

or equivalently

$$\mathbb{R} \xrightarrow{i} \mathbb{P}_r \xrightarrow{\text{rot}} [\mathbb{P}_{r-1}]^2 \xrightarrow{\text{div}} \mathbb{P}_{r-2} \xrightarrow{o} \mathbb{R} \quad (6.2)$$

are exact sequences.

- In three dimensions:

$$\mathbb{R} \xrightarrow{i} \mathbb{P}_r \xrightarrow{\mathbf{grad}} [\mathbb{P}_{r-1}]^3 \xrightarrow{\mathbf{curl}} [\mathbb{P}_{r-2}]^3 \xrightarrow{\operatorname{div}} \mathbb{P}_{r-3} \xrightarrow{o} \mathbb{R} \quad (6.3)$$

is an exact sequence.

We recall that *exact* means that the *image of every operator coincides with the kernel of the following one*. To better explain the consequences of these statements we introduce some additional notation. Given an integer s , we define the following polynomial spaces.

- In two dimensions:

$$\mathcal{G}_s := \mathbf{grad}(\mathbb{P}_{s+1}) \subseteq [\mathbb{P}_s]^2, \quad \mathcal{R}_s := \mathbf{rot}(\mathbb{P}_{s+1}) \subseteq [\mathbb{P}_s]^2. \quad (6.4)$$

- In three dimensions:

$$\mathcal{G}_s := \mathbf{grad}(\mathbb{P}_{s+1}) \subseteq [\mathbb{P}_s]^3, \quad \mathcal{R}_s := \mathbf{curl}([\mathbb{P}_{s+1}]^3) \subseteq [\mathbb{P}_s]^3. \quad (6.5)$$

We then set

$$\begin{aligned} \mathcal{G}_s^c &:= \text{a complement of } \mathcal{G}_s \text{ in } [\mathbb{P}_s]^d, \\ \mathcal{R}_s^c &:= \text{a complement of } \mathcal{R}_s \text{ in } [\mathbb{P}_s]^d. \end{aligned} \quad (6.6)$$

In the original paper, [Beirão da Veiga et al. \(2016a\)](#), we chose \mathcal{G}_s^c and \mathcal{R}_s^c as the L^2 -orthogonal complements of \mathcal{G}_s and \mathcal{R}_s , respectively. A more modern choice, described in [Beirão da Veiga et al. \(2018a\)](#), is as follows.

- In two dimensions:

$$\mathcal{G}_s^c := \{\mathbf{x}^\perp \mathbb{P}_{s-1}\}, \quad \mathcal{R}_s^c := \{\mathbf{x} \mathbb{P}_{s-1}\}. \quad (6.7)$$

- In three dimensions:

$$\mathcal{G}_s^c := \{\mathbf{x} \wedge [\mathbb{P}_{s-1}]^3\}, \quad \mathcal{R}_s^c := \{\mathbf{x} \mathbb{P}_{s-1}\}. \quad (6.8)$$

The choices (6.7), (6.8) are much easier to handle from the computational point of view. Finally we recall (see (2.1)) that \mathbb{P}_s^0 are the polynomials of \mathbb{P}_s having zero mean value.

The following properties are consequences of the exact sequences above.

- In two dimensions: (6.1) implies that, for all integer s ,

$$\mathbf{grad} \text{ is an isomorphism from } \mathbb{P}_s^0 \text{ to } \mathcal{G}_{s-1}, \quad (6.9a)$$

$$\mathbf{v} \in [\mathbb{P}_s]^2 \implies \operatorname{rot} \mathbf{v} = 0 \text{ if and only if } \mathbf{v} \in \mathcal{R}_s, \quad (6.9b)$$

$$\operatorname{rot} \text{ is an isomorphism from } \mathcal{G}_s^c \text{ to the whole } \mathbb{P}_{s-1}, \quad (6.9c)$$

and equivalently (6.2) implies that

$$\mathbf{rot} \text{ is an isomorphism from } \mathbb{P}_s^0 \text{ to } \mathcal{R}_{s-1}, \quad (6.10a)$$

$$\mathbf{v} \in [\mathbb{P}_s]^2 \implies \operatorname{div} \mathbf{v} = 0 \text{ if and only if } \mathbf{v} \in \mathcal{G}_s, \quad (6.10b)$$

$$\operatorname{div} \text{ is an isomorphism from } \mathcal{R}_s^c \text{ to the whole } \mathbb{P}_{s-1}. \quad (6.10c)$$

- In three dimensions: (6.3) implies that

$$\boldsymbol{v} \in [\mathbb{P}_s]^3 \implies \mathbf{curl} \, \boldsymbol{v} = 0 \text{ if and only if } \boldsymbol{v} \in \mathcal{G}_s, \quad (6.11a)$$

$$\boldsymbol{v} \in [\mathbb{P}_s]^3 \implies \operatorname{div} \boldsymbol{v} = 0 \text{ if and only if } \boldsymbol{v} \in \mathcal{R}_s, \quad (6.11b)$$

$$\mathbf{grad} \text{ is an isomorphism from } \mathbb{P}_s^0 \text{ to } \mathcal{G}_{s-1}, \quad (6.11c)$$

$$\mathbf{curl} \text{ is an isomorphism from } \mathcal{G}_s^c \text{ to } \mathcal{R}_{s-1}, \quad (6.11d)$$

$$\operatorname{div} \text{ is an isomorphism from } \mathcal{R}_s^c \text{ to the whole } \mathbb{P}_{s-1}. \quad (6.11e)$$

Properties (6.9b) and (6.10b), as well as properties (6.11a) and (6.11b), are just particular cases of well-known results in calculus.

From the definitions above (see also Beirão da Veiga *et al.* 2016a), we can easily deduce the following.

- In two dimensions:

$$\dim \mathcal{G}_k = \dim \mathcal{R}_k = \pi_{k+1,2} - 1, \quad \dim \mathcal{G}_k^c = \dim \mathcal{R}_k^c = \pi_{k-1,2}. \quad (6.12)$$

- In three dimensions:

$$\begin{aligned} \dim \mathcal{G}_k &= \pi_{k+1,3} - 1, & \dim \mathcal{R}_k &= 3\pi_{k+1,3} - \pi_{k+2,3} + 1, \\ \dim \mathcal{G}_k^c &= \dim \mathcal{R}_{k-1} = 3\pi_{k,3} - \pi_{k+1,3} + 1, & \dim \mathcal{R}_k^c &= \pi_{k-1,3}. \end{aligned} \quad (6.13)$$

For the sake of clarity we define $\gamma_{k,d} := \dim \mathcal{G}_k$ and $\varrho_{k,d} := \dim \mathcal{R}_k$.

6.2. Spaces $H(\operatorname{div})$, $H(\operatorname{rot})$ and $H(\mathbf{curl})$

The elements of our local virtual element spaces will be the solutions, within each element, of suitable *div-curl* systems. Consequently it will be convenient to recall the *compatibility conditions* (between the data inside the element and those at the boundary) that are required in order to have a solution. We recall the spaces defined in (2.4): for a polygon E ,

$$H(\operatorname{div}; E) := \{\boldsymbol{v} \in [L^2(E)]^2 : \operatorname{div} \boldsymbol{v} \in L^2(E)\}, \quad (6.14)$$

$$H(\operatorname{rot}; E) := \{\boldsymbol{v} \in [L^2(E)]^2 : \operatorname{rot} \boldsymbol{v} \in L^2(E)\}, \quad (6.15)$$

and for a polyhedron P ,

$$H(\operatorname{div}; P) := \{\boldsymbol{v} \in [L^2(P)]^3 : \operatorname{div} \boldsymbol{v} \in L^2(P)\}, \quad (6.16)$$

$$H(\mathbf{curl}; P) := \{\boldsymbol{v} \in [L^2(P)]^3 : \mathbf{curl} \, \boldsymbol{v} \in [L^2(P)]^3\}. \quad (6.17)$$

We now assume that we are given, on a simply connected polygon E , two smooth functions f_d and f_r , and, on the boundary ∂E , two edge-wise smooth functions g_n and g_t . We recall that the problem

$$\text{Find } \boldsymbol{v} \in H(\operatorname{div}; E) \cap H(\operatorname{rot}; E) \text{ such that } \begin{cases} \operatorname{div} \boldsymbol{v} = f_d, \operatorname{rot} \boldsymbol{v} = f_r & \text{in } E \\ \boldsymbol{v} \cdot \mathbf{n} = g_n & \text{on } \partial E \end{cases} \quad (6.18)$$

has a unique solution if and only if

$$\int_E \operatorname{div} \mathbf{v} \, dE = \int_{\partial E} g_n \, ds. \quad (6.19)$$

Similarly, the problem

$$\text{Find } \mathbf{v} \in H(\operatorname{div}; E) \cap H(\operatorname{rot}; E) \text{ such that } \begin{cases} \operatorname{div} \mathbf{v} = f_d, \operatorname{rot} \mathbf{v} = f_r & \text{in } E \\ \mathbf{v} \cdot \mathbf{t} = g_t & \text{on } \partial E \end{cases} \quad (6.20)$$

has a unique solution if and only if

$$\int_E \operatorname{rot} \mathbf{v} \, dE = \int_{\partial E} g_t \, ds. \quad (6.21)$$

In three dimensions, on a simply connected polyhedron P we assume that we are given a smooth scalar function f_d and a smooth vector-valued function f_r , with $\operatorname{div} f_r = 0$. On the boundary ∂P we assume that we are given a face-wise smooth scalar function g_n and a face-wise smooth tangent vector field \mathbf{g}_t , whose tangential components are continuous at the edges of ∂P . Then we recall that the problem

$$\text{Find } \mathbf{v} \in H(\operatorname{div}; P) \cap H(\operatorname{curl}; P) \text{ such that } \begin{cases} \operatorname{div} \mathbf{v} = f_d, \operatorname{curl} \mathbf{v} = f_r & \text{in } P \\ \mathbf{v} \cdot \mathbf{n} = g_n & \text{on } \partial P \end{cases} \quad (6.22)$$

has a unique solution if and only if

$$\int_P \operatorname{div} \mathbf{v} \, dP = \int_{\partial P} g_n \, ds, \quad (6.23)$$

and similarly the problem

$$\text{Find } \mathbf{v} \in H(\operatorname{div}; P) \cap H(\operatorname{curl}; P) \text{ such that } \begin{cases} \operatorname{div} \mathbf{v} = f_d, \operatorname{curl} \mathbf{v} = f_r & \text{in } P \\ \mathbf{v}_t = \mathbf{g}_t & \text{on } \partial P \end{cases} \quad (6.24)$$

has a unique solution if and only if

$$f_r \cdot \mathbf{n} = \operatorname{rot}_2 \mathbf{g}_t \text{ on } \partial P. \quad (6.25)$$

For more details concerning the solutions of the *div-curl* system we refer, for instance, to [Auchmuty and Alexander \(2001, 2005\)](#) and the references therein.

6.3. Two-dimensional face elements

These spaces are the same as those of [Brezzi et al. \(2014\)](#), although here we propose a different set of degrees of freedom.

On a polygon E , for k integer ≥ 1 , we set

$$\begin{aligned} V_{2,k}^{\text{face}}(E) &\coloneqq \{\mathbf{v} \in H(\operatorname{div}; E) \cap H(\operatorname{rot}; E) : \mathbf{v} \cdot \mathbf{n}|_e \in \mathbb{P}_k(e) \text{ for any edge } e \text{ of } E, \\ &\quad \operatorname{div} \mathbf{v} \in \mathbb{P}_{k-1}(E) \text{ and } \operatorname{rot} \mathbf{v} \in \mathbb{P}_{k-1}(E)\}. \end{aligned} \quad (6.26)$$

We recall from Section 6.2 that given

- a function g defined on ∂E such that $g|_e \in \mathbb{P}_k(e)$ for all $e \in \partial E$,
- a polynomial $f_d \in \mathbb{P}_{k-1}(E)$ such that

$$\int_E f_d \, dE = \int_{\partial E} g \, ds, \quad (6.27)$$

- a polynomial $f_r \in \mathbb{P}_{k-1}(E)$,

we can find a unique vector $\mathbf{v} \in V_{2,k}^{\text{face}}(E)$ such that

$$\mathbf{v} \cdot \mathbf{n} = g \text{ on } \partial E, \quad \operatorname{div} \mathbf{v} = f_d \text{ in } E, \quad \operatorname{rot} \mathbf{v} = f_r \text{ in } E. \quad (6.28)$$

The dimension of $V_{2,k}^{\text{face}}(E)$ is given by

$$\begin{aligned} \dim V_{2,k}^{\text{face}}(E) &= N_e \dim \mathbb{P}_k(e) + (\dim \mathbb{P}_{k-1}(E) - 1) + \dim \mathbb{P}_{k-1}(E) \\ &= N_e \pi_{k,1} + \pi_{k-1,2} - 1 + \pi_{k-1,2} \\ &= N_e \pi_{k,1} + 2\pi_{k-1,2} - 1. \end{aligned} \quad (6.29)$$

A convenient set of degrees of freedom for functions \mathbf{v} in $V_{2,k}^{\text{face}}(E)$ will be

$$\begin{aligned} (D_1) \quad & \int_e \mathbf{v} \cdot \mathbf{n} p_k \, de \quad \text{for any edge } e, \text{ for all } p_k \in \mathbb{P}_k(e), \\ (D_2) \quad & \int_E \mathbf{v} \cdot \mathbf{g}_{k-2} \, dE \quad \text{for all } \mathbf{g}_{k-2} \in \mathcal{G}_{k-2}, \\ (D_3) \quad & \int_E \mathbf{v} \cdot \mathbf{g}_k^c \, dE \quad \text{for all } \mathbf{g}_k^c \in \mathcal{G}_k^c. \end{aligned} \quad (6.30)$$

Recalling (6.12), we easily see that the number of degrees of freedom (6.30) equals the dimension of $V_{2,k}^{\text{face}}(E)$ as given in (6.29).

Theorem 6.1. The degrees of freedom (6.30) are unisolvant for $V_{2,k}^{\text{face}}(E)$.

Proof. Since the number of degrees of freedom (6.30) equals the dimension of $V_{2,k}^{\text{face}}(E)$, to prove unisolvence we just need to show that if, for a given \mathbf{v} in $V_{2,k}^{\text{face}}(E)$, all the degrees of freedom (6.30) are zero, that is, if

$$\int_e \mathbf{v} \cdot \mathbf{n} p_k \, de = 0 \quad \text{for any edge } e, \text{ for all } p_k \in \mathbb{P}_k(e), \quad (6.31)$$

$$\int_E \mathbf{v} \cdot \mathbf{g}_{k-2} \, dE = 0 \quad \text{for all } \mathbf{g}_{k-2} \in \mathcal{G}_{k-2}, \quad (6.32)$$

$$\int_E \mathbf{v} \cdot \mathbf{g}_k^c \, dE = 0 \quad \text{for all } \mathbf{g}_k^c \in \mathcal{G}_k^c, \quad (6.33)$$

then we must have $\mathbf{v} = 0$. Assume that for a certain $\mathbf{v} \in V_{2,k}^{\text{face}}(E)$ we have (6.31)–(6.33). Since $\mathbf{v} \cdot \mathbf{n}|_e \in \mathbb{P}_k(e)$ for any e , (6.31) implies that $\mathbf{v} \cdot \mathbf{n} \equiv 0$ on ∂E . Using

the fact that $\operatorname{div} \mathbf{v} \in \mathbb{P}_{k-1}$ and setting $q_{k-1} := \operatorname{div} \mathbf{v}$, we have from (6.31)–(6.32)

$$\begin{aligned} \int_E |\operatorname{div} \mathbf{v}|^2 dE &= \int_E \operatorname{div} \mathbf{v} q_{k-1} dE \\ &= \int_{\partial E} \mathbf{v} \cdot \mathbf{n} q_{k-1} ds - \int_E \mathbf{v} \cdot \operatorname{grad} q_{k-1} dE = 0. \end{aligned} \quad (6.34)$$

Hence we have $\operatorname{div} \mathbf{v} = 0$ which, together with $\mathbf{v} \cdot \mathbf{n} \equiv 0$ on ∂E , gives

$$\int_E \mathbf{v} \cdot \operatorname{grad} \varphi dE = 0 \quad \text{for all } \varphi \in H^1(E) \quad (6.35)$$

after integration by parts. According to the definition of (6.26), $\operatorname{rot} \mathbf{v} \in \mathbb{P}_{k-1}$. Looking at (6.9c), we then have that $\operatorname{rot} \mathbf{v} = \operatorname{rot} \mathbf{q}_k^c$ for some $\mathbf{q}_k^c \in \mathcal{G}_k^c$. Now the difference $\mathbf{v} - \mathbf{q}_k^c$ satisfies $\operatorname{rot}(\mathbf{v} - \mathbf{q}_k^c) = 0$, and as E is simply connected, it follows that $\mathbf{v} = \mathbf{q}_k^c + \operatorname{grad} \varphi$ for some $\mathbf{q}_k^c \in \mathcal{G}_k^c$ and some $\varphi \in H^1(E)$. Then

$$\int_E |\mathbf{v}|^2 dE = \int_E \mathbf{v} \cdot (\mathbf{q}_k^c + \operatorname{grad} \varphi) dE = 0, \quad (6.36)$$

since the first term is zero by (6.33) and the second term is zero by (6.35). \square

Remark 6.2. The degrees of freedom (D_1) in (6.30) are fairly natural. A possible variant would be to use, on each edge e , the values of $\mathbf{v} \cdot \mathbf{n}$ at $k+1$ suitable points on e . Moreover, the degrees of freedom (D_2) in (6.30) could be replaced, after integration by parts, by

$$\int_E \operatorname{div} \mathbf{v} q_{k-1} dE \quad \text{for all } q_{k-1} \in \mathbb{P}_{k-1}^0. \quad (6.37)$$

Finally, the degrees of freedom (D_3) in (6.30) could be replaced by

$$\int_E \operatorname{rot} \mathbf{v} q_{k-1} dE \quad \text{for all } q_{k-1} \in \mathbb{P}_{k-1} \quad (6.38)$$

as in the original paper of Brezzi *et al.* (2014).

Computing the L^2 -projection

As mentioned above, the virtual functions are not explicitly known inside the elements, and their reconstruction is not straightforward. Hence we use suitable projections onto polynomials. Here we show how to construct the L^2 -projection onto $[\mathbb{P}_k(E)]^2$, which is possibly the most convenient and surely the most commonly used. We point out that thanks to the definition of the space $V_{2,k}^{\text{face}}(E)$ and the degrees of freedom (D_3) in (6.30), the *enhancement trick* is not necessary here. Indeed, using the same integration by parts applied in (6.34), the degrees of freedom (D_1) and (D_2) in (6.30) allow us to compute $\int_E \operatorname{div} \mathbf{v} q_{k-1} dE$ for all $q_{k-1} \in \mathbb{P}_{k-1}(E)$, and since $\operatorname{div} \mathbf{v} \in \mathbb{P}_{k-1}(E)$, we can compute the divergence of any $\mathbf{v} \in V_{2,k}^{\text{face}}(E)$ exactly. In turn this implies, again by using integration by parts and (D_1) in (6.30),

that we can also compute

$$\int_E \mathbf{v} \cdot \mathbf{g}_k \, dE \quad \text{for all } \mathbf{g}_k \in \mathcal{G}_k \quad (6.39)$$

and in fact

$$\int_E \mathbf{v} \cdot \mathbf{grad} \varphi \, dE \quad \text{for all } \varphi \text{ polynomial on } E. \quad (6.40)$$

The above property, combined with (D_3) in (6.30), allows us to compute the integrals against any $\mathbf{q}_k \in [\mathbb{P}_k(E)]^2$ and thus yields the following important result.

Theorem 6.3. The $L^2(E)$ -projection operator

$$\Pi_k^0: V_{2,k}^{\text{face}}(E) \longrightarrow [\mathbb{P}_k(E)]^2 \quad (6.41)$$

is computable using the degrees of freedom (6.30).

The global two-dimensional face space

Given a polygonal domain Ω and a decomposition \mathcal{T}_h of Ω into a finite number of polygonal elements E , we can now consider the *global* space

$$V_{2,k}^{\text{face}}(\Omega) := \{\mathbf{v} \in H(\text{div}; \Omega): \mathbf{v}|_E \in V_{2,k}^{\text{face}}(E) \text{ for any element } E \in \mathcal{T}_h\}. \quad (6.42)$$

Note that in (6.42) we require that the elements \mathbf{v} of $V_{2,k}^{\text{face}}(\Omega)$ have a divergence that is *globally* (and not just element-wise) in $L^2(\Omega)$. Hence the normal component of vectors $\mathbf{v} \in V_{2,k}^{\text{face}}(\Omega)$ will have to be single-valued at the inter-element edges. The global degrees of freedom are the natural extension of the local degrees of freedom (6.30). It follows immediately that the dimension of $V_{2,k}^{\text{face}}(\Omega)$ is given by

$$\begin{aligned} \dim(V_{2,k}^{\text{face}}(\Omega)) &= \pi_{k,1} \times \{\text{number of edges in } \mathcal{T}_h\} \\ &\quad + (2\pi_{k-1,2} - 1) \times \{\text{number of elements in } \mathcal{T}_h\}. \end{aligned}$$

6.4. Two-dimensional edge elements

The edge elements in two dimensions correspond exactly to the face elements, just rotating everything by $\pi/2$. For the sake of completeness we just recall the definition of the spaces and the corresponding degrees of freedom.

On a polygon E we set

$$\begin{aligned} V_{2,k}^{\text{edge}}(E) &:= \{\mathbf{v} \in H(\text{div}; E) \cap H(\text{rot}; E): \mathbf{v} \cdot \mathbf{t}|_e \in \mathbb{P}_k(e) \text{ for any edge } e \text{ of } E, \\ &\quad \text{rot } \mathbf{v} \in \mathbb{P}_{k-1}(E) \text{ and } \text{div } \mathbf{v} \in \mathbb{P}_{k-1}(E)\}. \end{aligned} \quad (6.43)$$

A convenient set of degrees of freedom for elements $\mathbf{v} \in V_{2,k}^{\text{edge}}(E)$ is

$$\begin{aligned}(D_1) \quad & \int_e \mathbf{v} \cdot \mathbf{t} p_k \, de \quad \text{for any edge } e, \text{ for } p_k \in \mathbb{P}_k(e), \\ (D_2) \quad & \int_E \mathbf{v} \cdot \mathbf{r}_{k-2} \, dE \quad \text{for all } \mathbf{r}_{k-2} \in \mathcal{R}_{k-2}, \\ (D_3) \quad & \int_E \mathbf{v} \cdot \mathbf{r}_k^c \, dE \quad \text{for all } \mathbf{r}_k^c \in \mathcal{R}_k^c.\end{aligned}\tag{6.44}$$

Remark 6.4. Here too we could use alternative degrees of freedom, in analogy with those discussed in Remark 6.2. In particular we point out that we can uniquely identify an element \mathbf{v} of $V_{2,k}^{\text{edge}}(E)$ by prescribing its tangential component $\mathbf{v} \cdot \mathbf{t}$ (in $\mathbb{P}_k(e)$) on every edge, its rotation $\text{rot } \mathbf{v}$ (in $\mathbb{P}_{k-1}^0(E)$), and its divergence $\text{div } \mathbf{v}$ (in $\mathbb{P}_{k-1}(E)$).

Remark 6.5. Obviously, here too we can define the L^2 -projection onto \mathbb{P}_k , exactly as before, with \mathcal{R}_k^c taking the role of \mathcal{G}_k^c .

Given a polygonal domain Ω and a decomposition \mathcal{T}_h of Ω into a finite number of polygonal elements E , we can now consider the *global* space

$$V_{2,k}^{\text{edge}}(\Omega) := \{\mathbf{v} \in H(\text{rot}; \Omega) : \mathbf{v}|_E \in V_{2,k}^{\text{edge}}(E) \text{ for any element } E \in \mathcal{T}_h\}.\tag{6.45}$$

Note that the tangential component of vectors $\mathbf{v} \in V_{2,k}^{\text{edge}}(\Omega)$ will have to be single-valued at the inter-element edges. The degrees of freedom for $\mathbf{v} \in V_{2,k}^{\text{edge}}(\Omega)$ are the obvious extension of the local degrees of freedom (6.44), and the dimension of $V_{2,k}^{\text{edge}}(\Omega)$ is

$$\begin{aligned}\dim(V_{2,k}^{\text{edge}}(\Omega)) = & \pi_{k,1} \times \{\text{number of edges in } \mathcal{T}_h\} \\ & + (2\pi_{k-1,2} - 1) \times \{\text{number of elements in } \mathcal{T}_h\}.\end{aligned}$$

6.5. Three-dimensional face elements

The three-dimensional $H(\text{div})$ -conforming spaces follow in a very natural way the path of their two-dimensional companions.

On a polyhedron P we set

$$\begin{aligned}V_{3,k}^{\text{face}}(P) := & \{\mathbf{v} \in H(\text{div}; P) \cap H(\text{curl}; P) : \mathbf{v} \cdot \mathbf{n}_P^f \in \mathbb{P}_k(f) \text{ for any face } f \text{ of } P, \\ & \text{div } \mathbf{v} \in \mathbb{P}_{k-1}(P) \text{ and } \text{curl } \mathbf{v} \in \mathcal{R}_{k-1}(P)\}.\end{aligned}\tag{6.46}$$

The dimension of $V_{3,k}^{\text{face}}(P)$ is given by

$$\dim(V_{3,k}^{\text{face}}(P)) = N_f \pi_{k,2} + \dim \mathcal{G}_{k-2} + \dim \mathcal{R}_{k-1} = N_f \pi_{k,2} + \gamma_{k-2,3} + \varrho_{k-1,3}.\tag{6.47}$$

The local degrees of freedom will be

$$\begin{aligned} (D_1) \quad & \int_f \mathbf{v} \cdot \mathbf{n}_P^f p_k \, df \quad \text{for any face } f, \text{ for } p_k \in \mathbb{P}_k(f), \\ (D_2) \quad & \int_P \mathbf{v} \cdot \mathbf{g}_{k-2} \, dP \quad \text{for all } \mathbf{g}_{k-2} \in \mathcal{G}_{k-2}, \\ (D_3) \quad & \int_P \mathbf{v} \cdot \mathbf{g}_k^c \, dP \quad \text{for all } \mathbf{g}_k^c \in \mathcal{G}_k^c. \end{aligned} \quad (6.48)$$

It is not difficult to check that the number of the above degrees of freedom is given by

$$N_f \pi_{k,2} + \dim \mathcal{G}_{k-2} + \dim \mathcal{G}_k^c, \quad (6.49)$$

which equals the dimension of $V_{3,k}^{\text{face}}(P)$ as given in (6.47).

Lemma 6.6. The degrees of freedom (6.48) are unisolvant for the space $V_{3,k}^{\text{face}}(P)$.

Proof. The proof follows the same steps as in the two-dimensional case and is therefore omitted. \square

Remark 6.7. We note that also in the three-dimensional case there are alternative choices of degrees of freedom, as in Remark 6.2.

Remark 6.8. Obviously, here too we can compute the L^2 -projection onto \mathbb{P}_k , exactly as before (see Theorem 6.3).

The global three-dimensional face space

Now, having a polyhedral domain Ω and a decomposition \mathcal{T}_h of Ω into a finite number of polyhedrons P , we can consider the global space

$$V_{3,k}^{\text{face}}(\Omega) := \{ \mathbf{v} \in H(\text{div}; \Omega) : \mathbf{v}|_P \in V_{3,k}^{\text{face}}(P) \text{ for all elements } P \in \mathcal{T}_h \}. \quad (6.50)$$

As for the two-dimensional case, we note that the normal component of the elements of $V_{3,k}^{\text{face}}(\Omega)$ will be ‘continuous’ at the inter-element face. The degrees of freedom for the global space $V_{3,k}^{\text{face}}(\Omega)$ are the obvious extension of the local ones already described, and the dimension of $V_{3,k}^{\text{face}}(\Omega)$ is

$$\begin{aligned} \dim(V_{3,k}^{\text{face}}(\Omega)) = & \pi_{k,2} \times \{ \text{number of faces in } \mathcal{T}_h \} \\ & + (\gamma_{k-2,3} + \varrho_{k-1,3}) \times \{ \text{number of elements in } \mathcal{T}_h \}. \end{aligned}$$

6.6. Three-dimensional edge elements

We begin by introducing some additional notation that will be useful below. For a smooth three-dimensional field $\boldsymbol{\varphi}$ on P and for a face f with normal \mathbf{n}_P^f , we define the tangential component of $\boldsymbol{\varphi}$ as

$$\boldsymbol{\varphi}_f := \boldsymbol{\varphi} - (\boldsymbol{\varphi} \cdot \mathbf{n}_P^f) \mathbf{n}_P^f, \quad (6.51)$$

while $\boldsymbol{\varphi}_t$ denotes the vector field defined on the boundary of P whose restriction on each face f is $\boldsymbol{\varphi}_f$. Note that $\boldsymbol{\varphi}_f$ as defined in (6.51) is different from $\boldsymbol{\varphi} \wedge \mathbf{n}_P^f$; indeed, if for instance $\mathbf{n}_P^f = (0, 0, 1)$ and $\boldsymbol{\varphi} = (\varphi_1, \varphi_2, \varphi_3)$, then

$$\boldsymbol{\varphi}_f = (\varphi_1, \varphi_2, 0) \quad \text{while} \quad \boldsymbol{\varphi} \wedge \mathbf{n}_P^f = (\varphi_2, -\varphi_1, 0). \quad (6.52)$$

Both fields $\boldsymbol{\varphi}_f$ and $\boldsymbol{\varphi} \wedge \mathbf{n}_P^f$ can be considered as two-dimensional vectors in the plane of the face f .

Moreover, we introduce the following space.

Definition 6.9. We define the boundary space $\mathcal{B}(\partial P)$ as the space of \mathbf{v} in $[L^2(\partial P)]^3$ such that $\mathbf{v}_f \in H(\text{div}; f) \cap H(\text{rot}; f)$ on each face f of P , and such that on each edge e (common to the faces f_1 and f_2), $\mathbf{v}_{f_1} \cdot \mathbf{t}_e$ and $\mathbf{v}_{f_2} \cdot \mathbf{t}_e$ coincide (where \mathbf{t}_e is a unit tangential vector to e). Then we define $\mathcal{B}_t(\partial P)$ as the space of the tangential components of the elements of $\mathcal{B}(\partial P)$.

Definition 6.10. We now define the boundary VEM space $B_k^{\text{edge}}(\partial P)$ as

$$B_k^{\text{edge}}(\partial P) = \{\mathbf{v} \in \mathcal{B}_t(\partial P) : \mathbf{v}_f \in V_{2,k}^{\text{edge}}(f) \text{ on any face } f \in \partial P\}. \quad (6.53)$$

Recalling the previous discussion about the two-dimensional virtual elements $V_{2,k}^{\text{edge}}(f)$, we can easily see that for a polyhedron with N_e edges and N_f faces, the dimension β_k of $B_k^{\text{edge}}(\partial P)$ is given by

$$\beta_k = N_e \pi_{k,1} + N_f (2\pi_{k-1,2} - 1). \quad (6.54)$$

The local spaces

On a polyhedron P we set

$$V_{3,k}^{\text{edge}}(P) := \{\mathbf{v} \mid \mathbf{v}_t \in B_k^{\text{edge}}(\partial P), \text{div } \mathbf{v} \in \mathbb{P}_{k-1}(P), \text{ and } \mathbf{curl} \mathbf{curl} \mathbf{v} \in \mathcal{R}_{k-2}(P)\}. \quad (6.55)$$

In order to compute the dimension of the space $V_{3,k}^{\text{edge}}(P)$, we first observe that, given a vector \mathbf{g} in $B_k^{\text{edge}}(\partial P)$, a function f_d in \mathbb{P}_{k-1} and a vector $f_r \in \mathcal{R}_{k-2}(P)$, we can find a unique \mathbf{v} in $V_{3,k}^{\text{edge}}(P)$ such that

$$\mathbf{v}_t = \mathbf{g} \text{ on } \partial P, \quad \text{div } \mathbf{v} = f_d \text{ in } P, \quad \mathbf{curl} \mathbf{curl} \mathbf{v} = f_r \text{ in } P. \quad (6.56)$$

To prove it we consider the following auxiliary problems. The first is:

$$\text{Find } \mathbf{H} \text{ in } H(\text{div}; P) \cap H(\mathbf{curl}; P) \text{ such that } \begin{cases} \mathbf{curl} \mathbf{H} = f_r, \quad \text{div } \mathbf{H} = 0 & \text{in } P, \\ \mathbf{H} \cdot \mathbf{n} = \text{rot}_2 \mathbf{g} & \text{on } \partial P, \end{cases} \quad (6.57)$$

which is uniquely solvable since

$$\int_{\partial P} \text{rot}_2 \mathbf{g} \, dS = 0. \quad (6.58)$$

The second is:

$$\text{Find } \psi \text{ in } H(\text{div}; P) \cap H(\text{curl}; P) \text{ such that } \begin{cases} \mathbf{curl} \psi = \mathbf{H}, \text{ div } \psi = 0 & \text{in } P, \\ \psi_t = g & \text{on } \partial P, \end{cases} \quad (6.59)$$

which is also uniquely solvable since

$$\mathbf{H} \cdot \mathbf{n} = \text{rot}_2 \mathbf{g}. \quad (6.60)$$

The third problem is:

$$\text{Find } \varphi \in H_0^1(P) \text{ such that } \Delta \varphi = f_d \text{ in } P, \quad (6.61)$$

which also has a unique solution. Then it is not difficult to see that the choice

$$\mathbf{v} := \psi + \mathbf{grad} \varphi \quad (6.62)$$

solves our problem. Indeed, it is clear that $(\mathbf{grad} \varphi)_t = 0$, that $\text{div}(\mathbf{grad} \varphi) = f_d$ and that $\mathbf{curl} \mathbf{curl}(\mathbf{grad} \varphi) = 0$: added to (6.57) and (6.59), these produce the right conditions. It is also clear that the solution \mathbf{v} of (6.56) is unique.

Hence we can conclude that the dimension of $V_{3,k}^{\text{edge}}(P)$ is given by

$$\dim V_{3,k}^{\text{edge}}(P) = \beta_k + \pi_{k-1,3} + \varrho_{k-2,3}, \quad (6.63)$$

where $\beta_k = \dim B_k^{\text{edge}}(\partial P)$ is defined in (6.54).

The local degrees of freedom

A possible set of degrees of freedom for the space $V_{3,k}^{\text{edge}}(P)$ is as follows.

- For every edge e :

$$(D_1) \quad \int_e \mathbf{v} \cdot \mathbf{t} p_k \, de \quad \text{for all } p_k \in \mathbb{P}_k(e). \quad \left. \right\}$$

- For every face f :

$$(D_2) \quad \int_f \mathbf{v} \cdot \mathbf{r}_k^c \, df \quad \text{for all } \mathbf{r}_k^c \in \mathcal{R}_k^c(f), \quad \left. \right\}$$

$$(D_3) \quad \int_f \mathbf{v} \cdot \mathbf{r}_{k-2} \, df \quad \text{for all } \mathbf{r}_{k-2} \in \mathcal{R}_{k-2}(f). \quad \left. \right\}$$

- Inside P :

$$(D_4) \quad \int_P \mathbf{v} \cdot \mathbf{r}_k^c \, dP \quad \text{for all } \mathbf{r}_k^c \in \mathcal{R}_k^c, \quad \left. \right\}$$

$$(D_5) \quad \int_P \mathbf{v} \cdot \mathbf{r}_{k-2} \, dP \quad \text{for all } \mathbf{r}_{k-2} \in \mathcal{R}_{k-2}. \quad \left. \right\}$$

The total number of degrees of freedom (6.64) is clearly equal to β_k as given in (6.54), and the number of degrees of freedom (D_5) is equal to $\varrho_{k-2,3}$. On the other

hand, using (6.11e) we see that the number of degrees of freedom (D_4) is equal to $\pi_{k-1,3}$, so that the total number of degrees of freedom (6.64) equals the dimension of $V_{3,k}^{\text{edge}}(P)$ as computed in (6.63).

Lemma 6.11. The degrees of freedom (6.64) are unisolvant for the space $V_{3,k}^{\text{edge}}(P)$.

Proof. Having seen that the number of degrees of freedom (6.64) equals the dimension of $V_{3,k}^{\text{edge}}(P)$, in order to see their unisolvence we only need to check that a vector $\mathbf{v} \in V_{3,k}^{\text{edge}}(P)$ that satisfies

$$\int_e \mathbf{v} \cdot \mathbf{t} p_k \, de = 0 \quad \text{for any edge } e \text{ of } P \text{ and } p_k \in \mathbb{P}_k(e), \quad (6.65)$$

$$\int_f \mathbf{v} \cdot \mathbf{r}_k^c \, df = 0 \quad \text{for any face } f \text{ of } P \text{ and } \mathbf{r}_k^c \in \mathcal{R}_k^c(f), \quad (6.66)$$

$$\int_f \mathbf{v} \cdot \mathbf{r}_{k-2} \, df = 0 \quad \text{for any face } f \text{ of } P \text{ and } \mathbf{r}_{k-2} \in \mathcal{R}_{k-2}(f), \quad (6.67)$$

$$\int_P \mathbf{v} \cdot \mathbf{r}_k^c \, dP = 0 \quad \text{for all } \mathbf{r}_k^c \in \mathcal{R}_k^c(P), \quad (6.68)$$

$$\int_P \mathbf{v} \cdot \mathbf{r}_{k-2} \, dP = 0 \quad \text{for all } \mathbf{r}_{k-2} \in \mathcal{R}_{k-2}(P), \quad (6.69)$$

is necessarily equal to zero.

In fact, recalling the results of Section 6.4, it is fairly obvious that (6.65)–(6.67) imply that $\mathbf{v}_t = 0$ on ∂P . Moreover, since $\mathbf{curl} \mathbf{curl} \mathbf{v} \in \mathcal{R}_{k-2}(P)$, we are allowed to take $\mathbf{r}_{k-2} = \mathbf{curl} \mathbf{curl} \mathbf{v}$ as a test function in (6.69). Integration by parts (using $\mathbf{v}_t = 0$) gives

$$0 = \int_P \mathbf{v} \cdot \mathbf{curl} \mathbf{curl} \mathbf{v} \, dP = \int_P (\mathbf{curl} \mathbf{v}) \cdot (\mathbf{curl} \mathbf{v}) \, dP \quad (6.70)$$

and therefore we get $\mathbf{curl} \mathbf{v} = 0$. Using this, and again $\mathbf{v}_t = 0$, we easily check, integrating by parts, that

$$\int_P \mathbf{v} \cdot \mathbf{curl} \varphi \, dP = 0 \quad \text{for all } \varphi \in H(\mathbf{curl}; P). \quad (6.71)$$

Now we recall that from definition (6.55) of $V_{3,k}^{\text{edge}}(P)$ we have that $\text{div } \mathbf{v}$ is in \mathbb{P}_{k-1} . From (6.11e) we then deduce that there exists a $\mathbf{q}_k^c \in \mathcal{R}_k^c$ with $\text{div } \mathbf{q}_k^c = \text{div } \mathbf{v}$, so that the divergence of $\mathbf{v} - \mathbf{q}_k^c$ is zero, and then (since P is simply connected)

$$\mathbf{v} - \mathbf{q}_k^c = \mathbf{curl} \varphi \quad (6.72)$$

for some $\varphi \in H(\mathbf{curl}; P)$. At this point we can use (6.71) and (6.72) to conclude, as in (6.36), that

$$\int_P |\mathbf{v}|^2 \, dP = \int_P \mathbf{v} \cdot (\mathbf{q}_k^c + \mathbf{curl} \varphi) \, dP = \int_P \mathbf{v} \cdot \mathbf{q}_k^c \, dP + \int_P \mathbf{v} \cdot \mathbf{curl} \varphi \, dP = 0. \quad \square$$

Remark 6.12. As in the previous cases, we observe that the degrees of freedom (6.64) are not the only possible choice. To start with, we can change the degrees of freedom in each face, according to Remark 6.2. Moreover, in the spirit of (6.56) we could assign, instead of (D_4) or (D_5) in (6.64), $\mathbf{curl} \mathbf{curl} \mathbf{v}$ in $\mathcal{R}_{k-2}(P)$ or $\operatorname{div} \mathbf{v}$ in $\mathbb{P}_{k-1}(P)$, respectively.

The global three-dimensional edge space is defined as

$$V_{3,k}^{\text{edge}}(\Omega) := \left\{ \mathbf{v} \in H(\mathbf{curl}; \Omega) : \mathbf{v}|_P \in V_{3,k}^{\text{edge}}(P) \text{ for any element } P \in \mathcal{T}_h \right\}, \quad (6.73)$$

and the degrees of freedom are the natural extension of the local ones defined in (6.64). The dimension of $V_{3,k}^{\text{edge}}(\Omega)$ is

$$\begin{aligned} \dim(V_{3,k}^{\text{edge}}(\Omega)) &= \pi_{k,1} \times \{\text{number of edges in } \mathcal{T}_h\} \\ &\quad + (2\pi_{k-1,2} - 1) \times \{\text{number of faces in } \mathcal{T}_h\} \\ &\quad + (\pi_{k-1,3} + \varrho_{k-1,3}) \times \{\text{number of polyhedra in } \mathcal{T}_h\}. \end{aligned}$$

6.7. Virtual exact sequences

We now show that, for the obvious choices of the polynomial degrees, the set of virtual spaces introduced in this subsection constitutes an exact sequence. We start with the (simpler) two-dimensional case. Let $V_{2,k}^{\text{vert}}(\Omega)$ denote the same H^1 -conforming space introduced in (3.28), and

$$V_{2,k}^{\text{elem}}(\Omega) = \{v \in L^2(\Omega) : v|_E \in \mathbb{P}_k(E) \text{ for any element } E \in \mathcal{T}_h\}. \quad (6.74)$$

Then we have the following theorem.

Theorem 6.13. Let $k \geq 2$ and assume that Ω is a simply connected polygon, decomposed into a finite number of polygons E . Then the sequences

$$\mathbb{R} \xrightarrow{i} V_{2,k}^{\text{vert}}(\Omega) \xrightarrow{\mathbf{grad}} V_{2,k-1}^{\text{edge}}(\Omega) \xrightarrow{\operatorname{rot}} V_{2,k-2}^{\text{elem}}(\Omega) \xrightarrow{o} 0 \quad (6.75)$$

and

$$\mathbb{R} \xrightarrow{i} V_{2,k}^{\text{vert}}(\Omega) \xrightarrow{\operatorname{rot}} V_{2,k-1}^{\text{face}}(\Omega) \xrightarrow{\operatorname{div}} V_{2,k-2}^{\text{elem}}(\Omega) \xrightarrow{o} 0 \quad (6.76)$$

are both exact sequences.

Proof. We note first that the two sequences are practically the same, up to a rotation of $\pi/2$. Hence we will just show the exactness of the sequence (6.75). Essentially, the only non-trivial part will be to show that

a.1 for every $\mathbf{v} \in V_{2,k-1}^{\text{edge}}(\Omega)$ with $\operatorname{rot} \mathbf{v} = 0$ there exists a $\varphi \in V_{2,k}^{\text{vert}}(\Omega)$ such that $\mathbf{grad} \varphi = \mathbf{v}$,

a.2 for every $q \in V_{2,k-2}^{\text{elem}}(\Omega)$ there exists a $\mathbf{v} \in V_{2,k-1}^{\text{edge}}(\Omega)$ such that $\operatorname{rot} \mathbf{v} = q$.

We start with **a.1**. As Ω is simply connected, the condition $\operatorname{rot} \mathbf{v} = 0$ implies that there exists a function $\varphi \in H^1(\Omega)$ such that $\operatorname{grad} \varphi = \mathbf{v}$ in Ω . On every edge e of \mathcal{T}_h such φ will obviously also satisfy

$$\frac{\partial \varphi}{\partial \mathbf{t}_e} = \mathbf{v} \cdot \mathbf{t}_e \in \mathbb{P}_{k-1}(e). \quad (6.77)$$

Then the restriction of φ to each $E \in \mathcal{T}_h$ satisfies

$$\varphi|_e \in \mathbb{P}_k(e) \text{ for any } e \in \partial E, \quad \Delta \varphi \equiv \operatorname{div} \mathbf{v} \in \mathbb{P}_{k-2}(E), \quad (6.78)$$

so that clearly $\varphi \in V_{2,k}^{\text{vert}}(\Omega)$.

To deal with **a.2**, we first construct a $\boldsymbol{\varphi}$ in $[H^1(\Omega)]^2$ such that $\operatorname{rot} \boldsymbol{\varphi} = q$ and

$$\boldsymbol{\varphi} \cdot \mathbf{t} = \frac{\int_{\Omega} q \, d\Omega}{|\partial\Omega|} \quad \text{on } \partial\Omega, \quad (6.79)$$

where \mathbf{t} is the unit anticlockwise tangent vector to $\partial\Omega$, and $|\partial\Omega|$ is the length of $\partial\Omega$. Then we consider the element $\mathbf{v} \in V_{2,k-1}^{\text{edge}}(\Omega)$ such that

$$\mathbf{v} \cdot \mathbf{t}_e := \Pi_{k-1}^0(\boldsymbol{\varphi} \cdot \mathbf{t}_e) \quad \text{for any edge } e \in \mathcal{T}_h \quad (6.80)$$

and, within each element E ,

$$\operatorname{rot} \mathbf{v} = \operatorname{rot} \boldsymbol{\varphi} = q, \quad \operatorname{div} \mathbf{v} = 0. \quad (6.81)$$

Clearly such a \mathbf{v} solves the problem. \square

Remark 6.14. The construction in the proof of **a.2** could also be done if the two-dimensional domain Ω is a *closed surface*, obtained as union of polygons. To fix the ideas, assume that we deal with the boundary ∂P of a polyhedron P , and that on every face f of P we are given a polynomial q_f of degree $k - 2$, in such a way that

$$\sum_{f \in \partial P} \int_f q_f \, df = 0. \quad (6.82)$$

Then there exists an element $\mathbf{v} \in B_{k-1}^{\text{edge}}(\partial P)$ such that on each face f we have $\operatorname{rot}_2(\mathbf{v}|_f) = q_f$. To see that this is true, we define first, for each face f , the number

$$\tau_f := \int_f q_f \, df.$$

Then we fix, on each edge e , an orientation \mathbf{t}_e , we orient each face f with the outward normal, and we define, for each edge e of f , the anticlockwise tangent unit vector \mathbf{t}_c^e . Then we consider the *combinatorial problem* (defined on the topological decomposition \mathcal{T}_h) of finding for each edge e a real number σ_e , such that for each face f

$$\sum_{e \subset \partial f} \sigma_e \mathbf{t}_e \cdot \mathbf{t}_c^f = \tau_f. \quad (6.83)$$

This could be solved using the same approach used in the above proof, applied to a flat polygonal decomposition that is topologically equivalent to the decomposition of ∂P with one face removed. The last face will fit automatically, due to (6.82). Then we take \mathbf{v} such that on each edge $\mathbf{v} \cdot \mathbf{t} \in \mathbb{P}_{k-1}$ with $\int_e \mathbf{v} \cdot \mathbf{t}_e \, de = \sigma_e$, and for each face, $\operatorname{div} \mathbf{v}_f = 0$, $\operatorname{rot} \mathbf{v}_f = q_f$.

We are now ready to consider the three-dimensional case. Let $V_{3,k}^{\text{vert}}(\Omega)$ denote the H^1 -conforming space obtained by gluing together the local spaces introduced in (3.45), and let

$$V_{3,k}^{\text{elem}}(\Omega) := \{v \in L^2(\Omega) : v|_P \in \mathbb{P}_k(P) \text{ for any element } P \in \mathcal{T}_h\}. \quad (6.84)$$

Then we have the following theorem.

Theorem 6.15. Let $k \geq 3$, and assume that Ω is a simply connected polyhedron, decomposed into a finite number of polyhedra P . Then the sequence

$$\mathbb{R} \xrightarrow{i} V_{3,k}^{\text{vert}}(\Omega) \xrightarrow{\mathbf{grad}} V_{3,k-1}^{\text{edge}}(\Omega) \xrightarrow{\mathbf{curl}} V_{3,k-2}^{\text{face}}(\Omega) \xrightarrow{\operatorname{div}} V_{3,k-3}^{\text{elem}}(\Omega) \xrightarrow{o} 0 \quad (6.85)$$

is exact.

Proof. It is quite obvious, looking at the definitions of the spaces, that

- a constant function is in $V_{3,k}^{\text{vert}}(\Omega)$ and has zero gradient,
- the gradient of a function of $V_{3,k}^{\text{vert}}(\Omega)$ is in $V_{3,k-1}^{\text{edge}}(\Omega)$ and has zero **curl**,
- the **curl** of a vector in $V_{3,k-1}^{\text{edge}}(\Omega)$ is in $V_{3,k-2}^{\text{face}}(\Omega)$ and has zero divergence,
- the divergence of a vector of $V_{3,k-2}^{\text{face}}(\Omega)$ is in $V_{3,k-3}^{\text{elem}}(\Omega)$.

Hence, essentially, we have to prove that

- b.1** for every $\mathbf{v} \in V_{3,k-1}^{\text{edge}}(\Omega)$ with $\mathbf{curl} \mathbf{v} = 0$ there exists a $\varphi \in V_{3,k}^{\text{vert}}(\Omega)$ such that $\mathbf{grad} \varphi = \mathbf{v}$,
- b.2** for every $\boldsymbol{\tau} \in V_{3,k-2}^{\text{face}}(\Omega)$ with $\operatorname{div} \boldsymbol{\tau} = 0$ there exists a $\boldsymbol{\varphi} \in V_{3,k-1}^{\text{edge}}(\Omega)$ such that $\mathbf{curl} \boldsymbol{\varphi} = \boldsymbol{\tau}$,
- b.3** for every $q \in V_{3,k-3}^{\text{elem}}(\Omega)$ there exists a $\boldsymbol{\sigma} \in V_{3,k-2}^{\text{face}}(\Omega)$ such that $\operatorname{div} \boldsymbol{\sigma} = q$.

The proof of **b.1** is immediate, as in the two-dimensional case **a.1**: the function (unique up to a constant) φ such that $\mathbf{grad} \varphi = \mathbf{v}$ will satisfy (6.77) on each edge. Moreover, its restriction φ_f to each face f will satisfy $\mathbf{grad}_2 \varphi_f = \mathbf{v}_f$, and so on.

Let us therefore look at **b.2**. Given $\boldsymbol{\tau} \in V_{3,k-2}^{\text{face}}(\Omega)$ with $\operatorname{div} \boldsymbol{\tau} = 0$, we first consider (as in Remark 6.14) the element $\mathbf{g} \in B_{k-1}^{\text{edge}}(\partial\Omega)$ such that, on each face $f \subset \partial\Omega$,

$$\operatorname{rot}_2(\mathbf{g}|_f) = \boldsymbol{\tau} \cdot \mathbf{n} \ (\in \mathbb{P}_{k-2}(f)). \quad (6.86)$$

Note that

$$\sum_{f \subset \partial\Omega} \int_f \boldsymbol{\tau} \cdot \mathbf{n}_\Omega^f df = \int_\Omega \operatorname{div} \boldsymbol{\tau} d\Omega = 0, \quad (6.87)$$

so that the compatibility condition (6.82) is satisfied. Then we solve in Ω the *div-curl* problem

$$\operatorname{div} \boldsymbol{\psi} = 0 \text{ and } \operatorname{curl} \boldsymbol{\psi} = \boldsymbol{\tau} \text{ in } \Omega, \quad \text{with } \boldsymbol{\psi}_t = \mathbf{g} \text{ on } \partial\Omega. \quad (6.88)$$

The (unique) solution of (6.88) has enough regularity to take the trace of its tangential component on each edge e , and therefore, after deciding an orientation t_e for every edge e in \mathcal{T}_h , we can take

$$\eta_e := \Pi_{k-1}^0(\boldsymbol{\psi} \cdot t_e) \quad \text{on each edge } e \text{ in } \mathcal{T}_h. \quad (6.89)$$

At this point, for each element P we construct $\boldsymbol{\varphi} \in B_{k-1}^{\text{edge}}(\partial P)$ by requiring that

$$\begin{aligned} \boldsymbol{\varphi} \cdot t_e &= \eta_e \text{ on each edge } e, \\ \operatorname{rot}_2 \boldsymbol{\varphi}_f &= \boldsymbol{\tau} \cdot \mathbf{n}_P^f \text{ and } \operatorname{div} \boldsymbol{\varphi}_f = 0 \text{ in each face } f \subset \partial P. \end{aligned} \quad (6.90)$$

Then we can define $\boldsymbol{\varphi}$ inside each element by choosing, together with (6.90),

$$\operatorname{curl} \boldsymbol{\varphi} = \boldsymbol{\tau} \text{ and } \operatorname{div} \boldsymbol{\varphi} = 0 \text{ in each element } P. \quad (6.91)$$

It is easy to see that the boundary conditions given in (6.90) are *compatible* with the requirement $\operatorname{curl} \boldsymbol{\varphi} = \boldsymbol{\tau}$, so that the solution of (6.91) exists. Moreover, it is easy to see that all the necessary orientations fit, in such a way that $\operatorname{curl} \boldsymbol{\varphi}$ is globally in $[L^2(\Omega)]^3$, so that in fact $\boldsymbol{\varphi} \in V_{3,k-1}^{\text{edge}}(\Omega)$.

Finally we have to prove b.3. The proof follows the two-dimensional case very closely: given $q \in V_{3,k-3}^{\text{elem}}(\Omega)$, we first choose $\boldsymbol{\beta} \in [H^1(\Omega)]^3$ such that

$$\operatorname{div} \boldsymbol{\beta} = q \text{ in } \Omega \quad \text{and} \quad \boldsymbol{\beta} \cdot \mathbf{n}_\Omega = \frac{\int_\Omega q d\Omega}{|\partial\Omega|}, \quad (6.92)$$

where now $|\partial\Omega|$ is obviously the *area* of $\partial\Omega$. Then on each face f of \mathcal{T}_h we take

$$\boldsymbol{\sigma} \cdot \mathbf{n}_\Omega^f = \Pi_{k-2}^0(\boldsymbol{\beta} \cdot \mathbf{n}_\Omega^f) \quad (6.93)$$

and inside each element P we take $\operatorname{div} \boldsymbol{\sigma} = q$ and $\operatorname{curl} \boldsymbol{\sigma} = 0$. Note again that condition $\operatorname{div} \boldsymbol{\sigma} = q$ is *compatible* with the boundary conditions (6.93) and the orientations will fit in such a way that actually $\operatorname{div} \boldsymbol{\sigma} \in L^2(\Omega)$, so that $\boldsymbol{\sigma} \in V_{3,k-2}^{\text{face}}(\Omega)$. \square

Remark 6.16. Although here we are not dealing with applications, we point out that, as is well known (see e.g. Bossavit 1988, Mattiussi 1997, Hiptmair 2001, Arnold, Falk and Winther 2006b), the exactness of the above sequences is of paramount importance in proving several properties (e.g. the various forms of *inf-sup*, the ellipticity in the kernel, etc.) that are crucial in the study of convergence of mixed formulations (see e.g. Boffi, Brezzi and Fortin 2013).

6.8. A hint on more general cases

As already pointed out in the final part of Brezzi *et al.* (2014) for the particular case of two-dimensional face elements, we observe here that in all four cases considered in this paper (face elements and edge elements in two and three dimensions), we have at least three parameters to play with in order to create variants of our elements.

For instance, considering the case of three-dimensional face elements, we could choose three different integers k_b , k_r and k_d (all ≥ -1) and consider instead of (6.46) the spaces

$$\begin{aligned} V_{3,\mathbf{k}}^{\text{face}}(P) := \{ \mathbf{v} \in H(\text{div}; P) \cap H(\mathbf{curl}; P) : \mathbf{v} \cdot \mathbf{n}_P^f \in \mathbb{P}_{k_b}(f) \text{ for any face } f \text{ of } P, \\ \text{div } \mathbf{v} \in \mathbb{P}_{k_d}(P), \mathbf{curl } \mathbf{v} \in \mathcal{R}_{k_r}(P) \}, \end{aligned} \quad (6.94)$$

where obviously \mathbf{k} is given by $\mathbf{k} := (k_b, k_d, k_r)$. Taking, for a given integer k , the three indices as $k_b = k$, $k_d = k - 1$, $k_r = k - 1$, we again obtain the elements in (6.46), which in turn are the natural extension of the Brezzi–Douglas–Marini $H(\text{div})$ -conforming elements. If we had taken $k_b = k$, $k_d = k$, $k_r = k - 1$, for $k \geq 0$, we would instead mimic the Raviart–Thomas elements. In particular, on simplices and for $k = 0$ we recover the RT₀ element exactly.

We also point out that if we know *a priori* that (say, in a mixed formulation) the *vector part* of the solution of our problem will be a gradient, we could consider the choice $k_b = k$, $k_d = k - 1$, $k_r = -1$, obtaining a space that contains all polynomial vectors in \mathcal{G}_k (i.e. vectors that are gradients of some scalar polynomial of degree $\leq k + 1$), a space that is rich enough to provide an optimal approximation of our unknown.

Similarly, for the spaces in (6.55) one can consider the variants

$$V_{3,\mathbf{k}}^{\text{edge}}(P) := \{ \mathbf{v} \mid v_t \in B_{k_b}^{\text{edge}}(\partial P), \text{div } \mathbf{v} \in \mathbb{P}_{k_d}(P) \text{ and } \mathbf{curl } \mathbf{curl } \mathbf{v} \in \mathcal{R}_{k_r-1}(P) \}. \quad (6.95)$$

On the other hand, for nodal VEMs we can play with two indices, say k_b and k_Δ , to have

$$V_{3,\mathbf{k}}^{\text{vert}}(P) := \{ v \mid v|_{\partial P} \in B_{k_b}^{\text{vert}}(\partial P) \text{ and } \Delta v \in \mathbb{P}_{k_\Delta-2}(P) \}, \quad (6.96)$$

and needless to say, in the definition of $B_{k_b}^{\text{vert}}(\partial P)$, the degree of Δ_2 in each face could be different from k_b .

6.9. Serendipity elements

Some of the discrete spaces appearing in the diagram (6.75) are not suitable for practical computations. Indeed, as discussed in Section 3.8 for the space $V_{3,\mathbf{k}}^{\text{vert}}(\Omega)$, the chosen set of degrees of freedom only allows us to compute projections of sub-optimal order. A simple way out would be to enlarge the spaces and add degrees of freedom, in the spirit of (3.37), but this would result in high computational costs. The best choice is instead to make use of serendipity variants of the above spaces, which allow us to reduce the number of degrees of freedom while still being able

to compute projections of the required order. An example of this strategy was shown in Section 3.6, but here we have the additional difficulty that the involved serendipity projections need to be compatible with the exact sequence structure. Such serendipity sequences constitute the current state of the art of virtual element discrete complexes, and we refer the reader to [Beirão da Veiga et al. \(2017a, 2018a,b\)](#) for a detailed description. Here we limit ourselves to showing a brief example in the two-dimensional case, where the aim is to build the serendipity exact sequence (6.76).

In the following we will focus on a single sample element E , the global version following trivially. Furthermore, for simplicity of exposition we assume that $\eta > k$, so that no polynomial bubbles exist on the polygon E (see Section 3.6).

For k integer, $k \geq 1$, we begin by enlarging the original scalar VEM space (3.15) as in (3.37), which we recall here (with a different notation):

$$W_k^{\text{node}}(E) := \{v \in C^0(\bar{E}) : v|_e \in P_k(e) \text{ for each } e \subset \partial E, \Delta v \in P_k(E)\}, \quad (6.97)$$

with the degrees of freedom

- (D₁) the values of v at the vertices of E ,
- (D₂) for any edge e , the moments $\int_e v p_{k-2} \, de$, for all $p_{k-2} \in \mathbb{P}_{k-2}(e)$,
- (D₃) $\int_E (\nabla v \cdot \mathbf{x}) p_k \, dE$, for all $p_k \in \mathbb{P}_k(E)$.

Note that, using integration by parts, it is easy to check that the set of degrees of freedom (6.98) is equivalent to the set (3.38), where the moments $\int_E v p_k \, dE$ are assigned instead of (D₃). We associate with the above space the enlarged edge space

$$W_{k-1}^{\text{edge}}(E) := \left\{ \mathbf{v} \in [L^2(E)]^2 : \operatorname{div} \mathbf{v} \in P_k(E), \operatorname{rot} \mathbf{v} \in P_{k-1}(E), \mathbf{v}|_e \cdot \mathbf{t}_e \in P_{k-1}(e) \text{ for all } e \subset \partial E \right\}, \quad (6.99)$$

with the degrees of freedom

- (D₁) the moments $\int_e (\mathbf{v} \cdot \mathbf{t}_e) p_{k-1} \, de$, for all $p_{k-1} \in \mathbb{P}_{k-1}(e)$ and any edge e ,
- (D₂) the moments $\int_E \mathbf{v} \cdot \mathbf{x} p_k \, dE$, for all $p_k \in \mathbb{P}_k(E)$,
- (D₃) $\int_E \operatorname{rot} \mathbf{v} p_{k-1}^0 \, dE$, for all $p_{k-1}^0 \in \mathbb{P}_{k-1}^0(E)$.

It can be easily checked that such spaces form an exact sequence:

$$\mathbb{R} \xrightarrow{i} W_k^{\text{node}}(E) \xrightarrow{\nabla} W_{k-1}^{\text{edge}}(E) \xrightarrow{\operatorname{rot}} \mathbb{P}_{k-1}(E) \xrightarrow{o} 0. \quad (6.101)$$

On the other hand, $W_k^{\text{node}}(E)$ and $W_{k-1}^{\text{edge}}(E)$ have a large number of internal degrees of freedom, a particularly cumbersome situation when planning to use such spaces on the faces of a polyhedron (in order to design their three-dimensional counterparts). We therefore introduce the following serendipity variants. Let us introduce the projection operator $\Pi_S^{\text{node}} : W_k^{\text{node}}(E) \rightarrow \mathbb{P}_k(E)$, defined by

$$\begin{cases} \int_{\partial E} \partial_t (q - \Pi_S^{\text{node}} q) \partial_t p \, ds = 0 & \text{for all } p \in \mathbb{P}_k(E), \\ \int_{\partial E} (\mathbf{x} \cdot \mathbf{n})(q - \Pi_S^{\text{node}} q) \, ds = 0. \end{cases} \quad (6.102)$$

It can be proved (see [Beirão da Veiga et al. 2017a](#)) that the above operator is well-defined. We can then introduce the serendipity nodal space as

$$SV_k^{\text{node}}(E) := \left\{ q \in W_k^{\text{node}}(E) : \int_E \nabla(q - \Pi_S^{\text{node}} q) \cdot \mathbf{x} \, p_k \, dE = 0 \text{ for all } p_k \in \mathbb{P}_k \right\}. \quad (6.103)$$

Clearly, a set of degree of freedom for $SV_k^{\text{node}}(E)$ is given by (D_1) – (D_2) in [\(6.98\)](#); the set (D_3) is no longer needed. Analogously, after defining the space

$$S_{k-1}^{\text{edge}} := \mathbf{grad} \mathbb{P}_k \oplus \mathbf{x}^\perp \mathbb{P}_{k-1}, \quad (6.104)$$

we introduce the well-defined operator $\Pi_S^{\text{edge}} : W_{k-1}^{\text{edge}}(E) \rightarrow S_{k-1}^{\text{edge}}$:

$$\int_{\partial E} [(\mathbf{v} - \Pi_S^{\text{edge}} \mathbf{v}) \cdot \mathbf{t}] [\nabla p \cdot \mathbf{t}] \, ds = 0 \quad \text{for all } p \in \mathbb{P}_k(E), \quad (6.105)$$

$$\int_{\partial E} (\mathbf{v} - \Pi_S^{\text{edge}} \mathbf{v}) \cdot \mathbf{t} \, ds = 0, \quad (6.106)$$

$$\int_E \text{rot}(\mathbf{v} - \Pi_S^{\text{edge}} \mathbf{v}) p_{k-1}^0 \, dE = 0 \quad \text{for all } p_{k-1}^0 \in \mathbb{P}_{k-1}^0(E). \quad (6.107)$$

We can now define the *serendipity edge space* as

$$SV_{k-1}^{\text{edge}}(E) = \left\{ \mathbf{v} \in W_{k-1}^{\text{edge}}(E) : \int_E (\mathbf{v} - \Pi_S^{\text{edge}} \mathbf{v}) \cdot \mathbf{x} \, p_k \, dE = 0 \text{ for all } p_k \in \mathbb{P}_k \right\}. \quad (6.108)$$

A set of degrees of freedom for $SV_{k-1}^{\text{edge}}(E)$ is given by (D_1) and (D_3) in [\(6.100\)](#). The above projections have been carefully chosen so that the serendipity spaces still form an exact sequence:

$$\mathbb{R} \xrightarrow{i} SV_k^{\text{node}}(E) \xrightarrow{\nabla} SV_{k-1}^{\text{edge}}(E) \xrightarrow{\text{rot}} \mathbb{P}_{k-1}(E) \xrightarrow{o} 0. \quad (6.109)$$

When compared with their counterparts in [\(6.101\)](#), the above spaces are smaller, but allow the same computability in terms of projection operators and have the same approximation properties. We finally observe that interpolation and stability estimates for serendipity edge and face VEM spaces can be found in [Beirão da Veiga, Mascotto and Meng \(2022c\)](#) and [Beirão da Veiga and Mascotto \(2022\)](#).

7. The elasticity problem

In the present section we introduce the virtual element method for linear and nonlinear elasticity, paying particular attention to almost incompressible materials. After the development of the H^1 -conforming VEM of order k (Beirão da Veiga *et al.* 2013*b*), it was immediately recognized that (for $k \geq 2$) this discrete space was also suitable for building a simple and effective displacement or pressure inf-sup stable pair for incompressible elasticity. This observation led to the contribution by Beirão da Veiga, Brezzi and Marini (2013*a*), who introduced a virtual element family for linear elasticity in primal form, robust in the incompressible limit.

The main part of this section is indeed based on Beirão da Veiga *et al.* (2013*a*), but with a more modern viewpoint on many details, such as the construction used in the bilinear forms and the adoption of enhanced VE spaces. In particular, we also present a different viewpoint on the same method, which sets the basic background for generalization to nonlinear problems. In the final part of this section (mainly inspired by Beirão da Veiga, Lovadina and Mora 2015; see also Artioli, Beirão da Veiga, Lovadina and Sacco 2017*b*) we describe the VE discretization of nonlinear elasticity problems in small deformations and comment briefly on more complex problems such as inelasticity and large deformations (Chi, Beirão da Veiga and Paulino 2017).

The present section constitutes only a brief introduction to the very wide research area of VEMs for solid mechanics. The main motivations of the success of VEMs in the solid mechanics engineering community were (1) the ease of combining the method with (or embedding the method in) existing FEM codes, (2) the robustness to large mesh distortions, (3) the possibility of automatically handling hanging nodes, (4) the simplicity and efficiency of the formulation for the lowest-order case (one Gauss node per element). Among the many advances in the literature, we mention (in addition to the above) only a few sample papers regarding topology optimization (Gain *et al.* 2015, Chi *et al.* 2020), contact problems (Wriggers *et al.* 2016), Hellinger–Reissner elasticity (Artioli, de Miranda, Lovadina and Patruno 2018, Dassi, Lovadina and Visinoni 2020*b*), fracture and crack propagation (Hussein *et al.* 2019, Artioli, Marfia and Sacco 2020), elastodynamics (Park, Chi and Paulino 2020) and elasticity and plasticity for finite deformations (Wriggers, Reddy, Rust and Hudobivnik 2017, Wriggers and Hudobivnik 2017).

7.1. The linear elasticity problem

We consider the deformation problem of a linearly elastic body subjected to a volume load and with given boundary conditions, under the hypothesis of small deformations. In the main part of this section we will focus on the two-dimensional case, while hints on the three-dimensional case (which is essentially analogous) will be given at the end. Let Ω be a polygonal domain and let Γ be its boundary. Let λ and μ be positive coefficients (Lamé coefficients) and let f be a vector-valued function belonging to $[L^2(\Omega)]^2$. For the sake of simplicity we will use

(homogeneous) Dirichlet boundary conditions. The strong form of the equations reads

$$A_{\lambda,\mu} \mathbf{u} = \mathbf{f} \text{ in } \Omega \quad \text{and} \quad \mathbf{u} = 0 \text{ on } \Gamma,$$

where the linear elliptic operator $A_{\lambda,\mu}$ is given by

$$A_{\lambda,\mu} \mathbf{u} := - \begin{pmatrix} 2\mu(u_{1,xx} + \frac{1}{2}(u_{1,yy} + u_{2,xy})) + \lambda(u_{1,xx} + u_{2,yx}) \\ 2\mu(\frac{1}{2}(u_{1,yx} + u_{2,xx}) + u_{2,yy}) + \lambda(u_{1,xy} + u_{2,yy}) \end{pmatrix}.$$

In order to introduce the corresponding variational formulation, we consider the space

$$\mathbf{V} := [H_0^1(\Omega)]^2 \tag{7.1}$$

and the bilinear form

$$a(\mathbf{u}, \mathbf{v}) := 2\mu \int_{\Omega} \boldsymbol{\epsilon}(\mathbf{u}) : \boldsymbol{\epsilon}(\mathbf{v}) \, d\Omega + \lambda \int_{\Omega} \operatorname{div} \mathbf{u} \operatorname{div} \mathbf{v} \, d\Omega \equiv 2\mu a_{\mu}(\mathbf{u}, \mathbf{v}) + \lambda a_{\lambda}(\mathbf{u}, \mathbf{v}), \tag{7.2}$$

where $\boldsymbol{\epsilon}(\mathbf{u}) = (\nabla \mathbf{u} + \nabla^T \mathbf{u})/2$ as usual represents the *symmetric gradient operator*.

It is easy to see (possibly using Korn inequality in the presence of more general boundary conditions) that there exist two constants, $M > 0$ and $\alpha > 0$, depending only on Ω , λ and μ , such that

$$\alpha \|\mathbf{v}\|_{\mathbf{V}}^2 \leq a(\mathbf{v}, \mathbf{v}) \leq M \|\mathbf{v}\|_{\mathbf{V}}^2 \quad \text{for all } \mathbf{v} \in \mathbf{V}. \tag{7.3}$$

We note that $\mathbf{f} \in \mathbf{V}'$, and we let $\langle \mathbf{f}, \mathbf{v} \rangle$ denote the corresponding duality pairing (which here coincides with the usual L^2 inner product). Then the variational form of the problem reads:

$$\text{Find } \mathbf{u} \in \mathbf{V} \text{ such that } a(\mathbf{u}, \mathbf{v}) = \langle \mathbf{f}, \mathbf{v} \rangle \text{ for all } \mathbf{v} \in \mathbf{V}, \tag{7.4}$$

which clearly has a unique solution that belongs at least to $[H^s(\Omega)]^2$ for some $s > 3/2$ depending on the maximum angle in Γ .

Remark 7.1. As is well known, when the parameter $\lambda \gg \mu$, we fall into the range of the so-called ‘almost incompressible’ materials. In such a case the coercivity and continuity constants in (7.3) diverge. Unless specific care is taken in the discretization, the accuracy of numerical methods will degenerate in such situations; there is a large FEM literature in this respect (see e.g. [Boffi et al. 2013](#) and the references therein). The VEM scheme proposed here will be robust in the almost incompressible limit as well.

7.2. The discrete spaces and problem

The method described here is taken from [Beirão da Veiga et al. \(2013a\)](#) but with a more modern viewpoint on some aspects. We also refer to [Artoli, Beirão da Veiga, Lovadina and Sacco \(2017a\)](#) for a more engineering-oriented introduction. In order to introduce the discrete VEM space for the displacement field, we start

with the same scalar ‘enhanced’ spaces introduced in Section 3.6, which we recall here. For $k \geq 1$ we set

$$V_k(E) := \left\{ v \in C^0(\overline{E}) : v|_e \in \mathbb{P}_k(e) \text{ for all } e \in \partial E, \Delta v \in \mathbb{P}_k(E), \right. \\ \left. \text{and } \int_E (v - \Pi_k^{\nabla, E} v) p_s \, dE = 0 \text{ for all } p_s \in \mathbb{P}_s^{\text{hom}}(E), s = k-1, k \right\}, \quad (7.5)$$

where the operator $\Pi_k^{\nabla, E}$ was defined in (2.6). Note that the simpler space (3.15) could also be chosen, but at the price of a less accurate load approximation. The local VEM displacement space is then simply

$$V_k(E) = [V_k(E)]^2, \quad (7.6)$$

with the corresponding degrees of freedom

- (D₁) the values of v at the vertices of the polygon E ,
- (D₂) for $k \geq 2$, the moments $\int_e v \cdot p \, de$, for all $p \in [\mathbb{P}_{k-2}(e)]^2$, $e \subset \partial E$,
- (D₃) for $k \geq 2$, the moments $\int_E v \cdot p \, dE$, for all $p \in [\mathbb{P}_{k-2}(E)]^2$.

It is easy to check that $[\mathbb{P}_k(E)]^2 \subseteq V_k(E)$. Furthermore, by arguments similar to those in Section 3, we have that the following projection operators are computable in terms of the degrees of freedom (7.7):

$$\begin{aligned} \Pi_k^{\nabla, E} &: V_k(E) \rightarrow [\mathbb{P}_k(E)]^2, \\ \Pi_k^{0, E} &: V_k(E) \rightarrow [\mathbb{P}_k(E)]^2, \\ \Pi_{k-1}^{0, E} &: \nabla V_k(E) \rightarrow [\mathbb{P}_{k-1}(E)]^{2 \times 2}, \\ \Pi_{k-1}^{0, E} &: \operatorname{div} V_k(E) \rightarrow \mathbb{P}_{k-1}(E). \end{aligned} \quad (7.8)$$

The global discrete displacement space is given by

$$V_h = \{v \in V : v|_E \in V_k(E) \text{ for all } E \in \mathcal{T}_h\}$$

and the associated global degrees of freedom are trivially deduced from the local ones in the standard FEM fashion.

We now define the local bilinear forms approximating the forms $a_\mu(\cdot, \cdot)$ and $a_\lambda(\cdot, \cdot)$ in (7.2) at the element level. We will introduce such bilinear forms written in the most explicit way, which makes it easier to understand the particular treatment for the volumetric term and the ensuing robustness in the incompressible limit. Later we will show a different description of the same forms that is better suited for generalization to nonlinear problems and for implementation in an engineering perspective.

For all $E \in \mathcal{T}_h$ and all $\mathbf{v}_h, \mathbf{w}_h \in \mathbf{V}_k(E)$, we define

$$\begin{aligned} a_{\mu,h}^E(\mathbf{v}_h, \mathbf{w}_h) &:= 2\mu \int_E \boldsymbol{\Pi}_{k-1}^{0,E} \boldsymbol{\epsilon}(\mathbf{v}_h) : \boldsymbol{\Pi}_{k-1}^{0,E} \boldsymbol{\epsilon}(\mathbf{w}_h) \, dE \\ &\quad + \mu \mathcal{S}^E((I - \Pi_k^{\nabla,E})\mathbf{v}_h, (I - \Pi_k^{\nabla,E})\mathbf{w}_h), \\ a_{\lambda,h}^E(\mathbf{v}_h, \mathbf{w}_h) &:= \lambda \int_E \Pi_{k-1}^{0,E}(\operatorname{div} \mathbf{v}_h) \Pi_{k-1}^{0,E}(\operatorname{div} \mathbf{w}_h) \, dE, \end{aligned} \quad (7.9)$$

where the stabilizing form $\mathcal{S}^E(\cdot, \cdot)$ is any symmetric and computable bilinear form on $\mathbf{V}_k(E)$ that satisfies (see (3.20))

$$c_1 |\mathbf{v}_h|_{1,E}^2 \leq \mathcal{S}^E(\mathbf{v}_h, \mathbf{v}_h) \leq c_2 |\mathbf{v}_h|_{1,E}^2 \quad \text{for all } \mathbf{v}_h \in \mathbf{V}_k(E) \text{ with } \Pi_k^{\nabla,E} \mathbf{v}_h = 0 \quad (7.10)$$

uniformly in the mesh elements. The form $\mathcal{S}^E(\cdot, \cdot)$ can be taken equal to (the vector version of) the choices already discussed in Section 3 (see (3.21)–(3.23)) directly on the (properly scaled) degrees of freedom or on some boundary integrals. We note that the absence of a stabilizing term for the volumetric form $a_{\lambda,h}^E(\cdot, \cdot)$ is aimed at obtaining a scheme that is robust in the incompressible limit as well. Indeed, such a choice corresponds to a relaxation of the volumetric constraint when $\lambda \gg \mu$, as happens in PSRI finite elements or mixed approaches to elasticity (Boffi *et al.* 2013). The global versions of the above forms are obtained as usual: for all $\mathbf{v}_h, \mathbf{w}_h$ in \mathbf{V}_h ,

$$\begin{aligned} a_{\mu,h}(\mathbf{v}_h, \mathbf{w}_h) &:= \sum_{E \in \mathcal{T}_h} a_{\mu,h}^E(\mathbf{v}_h, \mathbf{w}_h), \\ a_{\lambda,h}(\mathbf{v}_h, \mathbf{w}_h) &:= \sum_{E \in \mathcal{T}_h} a_{\lambda,h}^E(\mathbf{v}_h, \mathbf{w}_h), \\ a_h(\mathbf{v}_h, \mathbf{w}_h) &:= a_{\mu,h}(\mathbf{v}_h, \mathbf{w}_h) + a_{\lambda,h}(\mathbf{v}_h, \mathbf{w}_h). \end{aligned}$$

Finally, the discrete loading term is defined by

$$\langle \mathbf{f}_h, \mathbf{v}_h \rangle := \sum_{E \in \mathcal{T}_h} \int_E \Pi_k^{0,E}(\mathbf{f}) \cdot \mathbf{v}_h \, dE = \sum_{E \in \mathcal{T}_h} \int_E \mathbf{f} \cdot \Pi_k^{0,E}(\mathbf{v}_h) \, dE. \quad (7.11)$$

We are now able to present the VEM for the linear elasticity problem

$$\text{Find } \mathbf{u}_h \in \mathbf{V}_h \text{ such that } a_h(\mathbf{u}_h, \mathbf{v}_h) = \langle \mathbf{f}_h, \mathbf{v}_h \rangle \text{ for all } \mathbf{v}_h \in \mathbf{V}_h. \quad (7.12)$$

It is easy to check that the form $a_h(\cdot, \cdot)$ is coercive on \mathbf{V}_h , so that the above problem has a unique solution.

Remark 7.2. An alternative form found in the literature for $a_{\mu,h}^E(\cdot, \cdot)$ (see e.g. Beirão da Veiga *et al.* 2013a) is

$$\begin{aligned} a_{\mu,h}^E(\mathbf{v}_h, \mathbf{w}_h) \\ := 2\mu \int_E \boldsymbol{\epsilon}(\Pi_k^{\nabla,E} \mathbf{v}_h) : \boldsymbol{\epsilon}(\Pi_k^{\nabla,E} \mathbf{w}_h) \, dE + \mu \mathcal{S}^E((I - \Pi_k^{\nabla,E})\mathbf{v}_h, (I - \Pi_k^{\nabla,E})\mathbf{w}_h). \end{aligned}$$

The more modern choice (7.9) is more appropriate for generalizations (such as variable coefficients or, as we will see below, nonlinear problems).

An equivalent form of the same scheme

As already anticipated, we introduce a different description of the same bilinear form $a_h(\cdot, \cdot)$ which is better suited for generalization to nonlinear problems and for implementation in an engineering perspective. In the following we will denote the Cauchy stress (associated to the present linearly elastic constitutive law)

$$\boldsymbol{\sigma}(\boldsymbol{\varepsilon}(\mathbf{v})) := 2\mu\boldsymbol{\varepsilon}(\mathbf{v}) + \lambda \operatorname{tr} \boldsymbol{\varepsilon}(\mathbf{v}) I \quad \text{for all } \mathbf{v} \in H^1(\Omega),$$

and recall that the continuous bilinear form (7.2) can be written as

$$a(\mathbf{v}, \mathbf{w}) = \int_{\Omega} \boldsymbol{\sigma}(\boldsymbol{\varepsilon}(\mathbf{v})) : \boldsymbol{\varepsilon}(\mathbf{w}) \, d\Omega. \quad (7.13)$$

We consider the local elastic form ($E \in \mathcal{T}_h$)

$$a_h^E(\mathbf{v}_h, \mathbf{w}_h) := a_{\mu,h}^E(\mathbf{v}_h, \mathbf{w}_h) + a_{\lambda,h}^E(\mathbf{v}_h, \mathbf{w}_h) \quad (7.14)$$

(see (7.9)). By trivial calculations and definition of the L^2 -projection, for any $\mathbf{v}_h \in \mathbf{V}_k(E)$,

$$\lambda \Pi_{k-1}^{0,E}(\operatorname{div} \mathbf{v}_h) = \lambda \Pi_{k-1}^{0,E}(\operatorname{tr} \boldsymbol{\varepsilon}(\mathbf{v}_h)) = \lambda \operatorname{tr} \boldsymbol{\Pi}_{k-1}^{0,E}(\boldsymbol{\varepsilon}(\mathbf{v}_h)),$$

where tr denotes the trace operator. Furthermore, by identical arguments, for all $\mathbf{v}_h \in \mathbf{V}_k(E)$,

$$\Pi_{k-1}^{0,E}(\operatorname{div} \mathbf{v}_h) = \operatorname{tr} \boldsymbol{\Pi}_{k-1}^{0,E}(\boldsymbol{\varepsilon}(\mathbf{v}_h)) = \boldsymbol{\Pi}_{k-1}^{0,E}(\boldsymbol{\varepsilon}(\mathbf{v}_h)) : I,$$

with I denoting the 2×2 identity tensor and $A : B = \sum_{i,j} A_{ij} B_{ij}$ for all square matrices A, B . We now combine the two above identities in the definition of $a_{\lambda,h}^E(\mathbf{v}_h, \mathbf{w}_h)$ (see (7.9)). With some simple manipulation we obtain

$$\begin{aligned} a_{\lambda,h}^E(\mathbf{v}_h, \mathbf{w}_h) &= \int_E \lambda \Pi_{k-1}^{0,E}(\operatorname{div} \mathbf{v}_h) \Pi_{k-1}^{0,E}(\operatorname{div} \mathbf{w}_h) \, dE \\ &= \int_E \lambda \operatorname{tr} \boldsymbol{\Pi}_{k-1}^{0,E}(\boldsymbol{\varepsilon}(\mathbf{v}_h)) I : \boldsymbol{\Pi}_{k-1}^{0,E}(\boldsymbol{\varepsilon}(\mathbf{w}_h)) \, dE. \end{aligned} \quad (7.15)$$

Therefore the form (7.14) can be written as

$$\begin{aligned} a_h^E(\mathbf{v}_h, \mathbf{w}_h) &= \int_E (2\mu \boldsymbol{\Pi}_{k-1}^{0,E}(\boldsymbol{\varepsilon}(\mathbf{v}_h)) + \lambda \operatorname{tr} \boldsymbol{\Pi}_{k-1}^{0,E}(\boldsymbol{\varepsilon}(\mathbf{v}_h)) I) : \boldsymbol{\Pi}_{k-1}^{0,E}(\boldsymbol{\varepsilon}(\mathbf{w}_h)) \, dE \\ &\quad + \mu \mathcal{S}^E((I - \boldsymbol{\Pi}_k^{\nabla,E}) \mathbf{v}_h, (I - \boldsymbol{\Pi}_k^{\nabla,E}) \mathbf{w}_h) \\ &= \int_E \boldsymbol{\sigma}(\boldsymbol{\Pi}_{k-1}^{0,E}(\boldsymbol{\varepsilon}(\mathbf{v}_h))) : \boldsymbol{\Pi}_{k-1}^{0,E}(\boldsymbol{\varepsilon}(\mathbf{w}_h)) \, dE \\ &\quad + \mu \mathcal{S}^E((I - \boldsymbol{\Pi}_k^{\nabla,E}) \mathbf{v}_h, (I - \boldsymbol{\Pi}_k^{\nabla,E}) \mathbf{w}_h). \end{aligned} \quad (7.16)$$

The above form is to be compared with the local version of (7.13). The expression (7.16) is equivalent to the original discrete form of the previous section, but emphasizes that the VEM discretization is obtained simply by projecting the strains onto a local polynomial space and then applying the constitutive law. The expression (7.16) is therefore suitable to easily generalize the present construction to small and large deformation nonlinear problems, as it suggests the following systematic approach: project the strains onto a polynomial space and then apply the (nonlinear) constitutive law before integrating on the element. More details will be given in Section 7.4.

Finally, it is important to stress that the stabilization depends only on the parameter μ (and is therefore unaffected by large values of λ), which is what makes the scheme robust in the incompressible limit. Also, this idea is easily extended to more complex problems, by making the stabilizing form dependent on the deviatoric part of the stresses. See also Park, Chi and Paulino (2021), for instance.

Extension to the three-dimensional case

Here we comment briefly on the three-dimensional case. The extension of the method here presented to three-dimensional problems is quite straightforward, in light of the previous developments for the scalar case. We simply replace the two-dimensional scalar space (7.5) with the scalar space described in Section 3.8, and then set

$$V_k(P) = [V_k(P)]^3 \quad (7.17)$$

for each polyhedron P in the mesh \mathcal{T}_h . The local degrees of freedom are the trivial vector-valued versions of those in (3.46). By the same arguments, it can be checked that the three-dimensional analogues of the projections appearing in (7.8) are still computable. The rest of the construction (global space and related degrees of freedom, discrete bilinear form, load approximation) is essentially identical. Although many results of the next sections apply also to the three-dimensional case with minor modifications, in the following we will continue to work in the two-dimensional framework for ease of presentation.

7.3. Convergence and robustness in the incompressible limit

The interpolation estimates for the scalar space discussed in Section 3 (formulas (3.34) and (3.36)) immediately apply to the vector-valued version (7.6). Since (7.12) is also a classical linear elliptic problem, deriving error estimates for the method would, in principle, follow exactly the same steps (and obtain analogous results) as for the Laplace problem. On the other hand such an approach would not lead to error estimates that are robust in the incompressible limit, i.e. in which the constant involved in the error does not depend on the parameter λ . In order to obtain such estimates, we need to resort to a mixed interpretation of (7.12), in which an important role is played by the pressure variable $p = \lambda \operatorname{div} \mathbf{u}$.

Here we show the main intermediate results leading to the final convergence Corollary 7.7, and refer to [Beirão da Veiga et al. \(2013a\)](#) for the proofs. In the rest of the section we assume the same Assumption 2.1 on the mesh already stated in Section 2, which could be relaxed following the ideas in [Beirão da Veiga et al. \(2017b\)](#) and [Brenner and Sung \(2018\)](#).

We define the (piecewise polynomial) auxiliary space

$$Q_h := \{q_h \in L_0^2(\Omega) : q_h \in \mathbb{P}_{k-1}(E) \text{ for all } E \in \mathcal{T}_h\}.$$

Then we have the following inf-sup lemma.

Lemma 7.3. Let $k \geq 2$ and let Assumption 2.1 hold. Then there exists a strictly positive constant β , independent of h , such that

$$\sup_{v_h \in V_h} \frac{\int_{\Omega} (\operatorname{div} v_h) q_h \, d\Omega}{\|v_h\|_{1,\Omega}} \geq \beta \|q_h\|_{0,\Omega} \quad \text{for all } q_h \in Q_h.$$

Remark 7.4. For the particular case $k = 1$, the validity of the above inf-sup condition is not assured and depends on the mesh family considered (e.g. for $k = 1$ on a triangular mesh we obtain the famous pair $\mathbb{P}_1/\mathbb{P}_0$, which is well known to fail in such a respect). Positive results for a class of polygonal meshes can be obtained by extending the ideas in [Beirão da Veiga and Lipnikov \(2010\)](#). In order to obtain inf-sup stability for any class of (shape-regular) meshes one would need to add edge-bubbles, which would imply a simple modification of the space with the addition of one degree of freedom per edge to the displacement space. We will not dwell on these variants, and assume in the following that $k \geq 2$.

By classical arguments borrowed from mixed FEMs (see [Boffi et al. 2013](#)), Lemma (7.3) implies the existence of a Fortin-like operator, that is (in particular) an optimal approximant in H^1 which ‘preserves’ the projected divergence.

Lemma 7.5. Let $k \geq 2$ and let Assumption 2.1 hold. Then there exists a positive constant C , independent of h , such that the following holds. For all v in the broken Sobolev space $[H^s(\mathcal{T}_h)]^2$, $1 \leq s \leq k + 1$, there exists $v_I \in V_h$ that satisfies

$$\begin{aligned} \|v - v_I\|_1 &\leq Ch^{s-1}|v|_{s,\mathcal{T}_h}, \\ \int_{\Omega} (\operatorname{div} v_I) q_h \, d\Omega &= \int_{\Omega} (\operatorname{div} v) q_h \, d\Omega \quad \text{for all } q_h \in Q_h, \end{aligned}$$

where by $|\cdot|_{s,\mathcal{T}_h}$ we denote the corresponding H^s broken Sobolev seminorm.

The following convergence result bounds the error $u - u_h$ in terms of the interpolation error $u - u_I$. There is also a load approximation term (which is typically neglected in FEM analysis by assuming exact integration of the right-hand side), a polynomial approximation term (stemming from the VEM approximation of the involved bilinear forms) and an explicit volumetric term.

Theorem 7.6. Let $k \geq 2$ and let Assumption 2.1 hold. Let \mathbf{u} be the solution of problem (7.4) and \mathbf{u}_h the solution of problem (7.12). Let $p = \lambda \operatorname{div} \mathbf{u}$ and p_I be its L^2 -projection in Q_h . Let \mathbf{u}_I be as defined in Lemma 7.5, and let u_π be any approximant of \mathbf{u} piecewise in $[\mathbb{P}_k]^2$. Then there exists a positive constant C , independent of h and λ , such that

$$\|\mathbf{u} - \mathbf{u}_h\|_1 \leq C(\|\mathbf{u} - \mathbf{u}_I\|_1 + \|\mathbf{u} - u_\pi\|_{1,\mathcal{T}_h} + \|p - p_I\|_0 + h\|\mathbf{f} - \mathbf{f}_h\|_0).$$

By combining the above theorem with Lemma 7.5 and standard polynomial approximation estimates, we obtain the following convergence result.

Corollary 7.7. Let the same assumptions as in Theorem 7.6 hold. Further, let \mathbf{u}, \mathbf{f} be in the broken Sobolev space $[H^s(\mathcal{T}_h)]^2$ and let p be in the the broken Sobolev space $H^{s-1}(\mathcal{T}_h)$, $1 \leq s \leq k+1$. Then there exists a constant C , independent of h and λ , such that

$$\|\mathbf{u} - \mathbf{u}_h\|_1 \leq C h^{s-1}(|\mathbf{u}|_{s,\mathcal{T}_h} + h^2 |\mathbf{f}|_{s,\mathcal{T}_h} + |p|_{s-1,\mathcal{T}_h}).$$

It is important to observe that the auxiliary variable p is also uniformly bounded independently of λ (see e.g. Remark 3.1 in Beirão da Veiga *et al.* 2013a), so the above result is indeed robust in the volumetric limit. We refer to Lemma 2.4 in Beirão da Veiga *et al.* (2013a) for the corresponding error estimate $\|\mathbf{u} - \mathbf{u}_h\|_0$.

7.4. Nonlinear elasticity

In the present section we briefly present the extension of the previous ideas to the nonlinear case, focusing on small deformation elasticity and providing references on further extensions. The main results of this section are based on Beirão da Veiga *et al.* (2015); see also Artioli *et al.* (2017b) for a more engineering-oriented approach. As in the previous part of this section we assume homogeneous Dirichlet boundary conditions for simplicity of exposition, the extension to more general kinds of boundary conditions (and loading types) being trivial.

Assuming a regime of small deformations and an elastic material, we are now given a (general) constitutive law for the material at every point $x \in \Omega$, relating strains to stresses $\boldsymbol{\sigma}$, through the function

$$\boldsymbol{\sigma} = \boldsymbol{\sigma}(x, \nabla \mathbf{u}(x)) \in \mathbb{R}_{\text{symm}}^{d \times d}. \quad (7.18)$$

Given the law (7.18), the deformation problem reads

$$\begin{cases} -\operatorname{div} \boldsymbol{\sigma} = \mathbf{f} & \text{in } \Omega, \\ \mathbf{u} = 0 & \text{on } \partial\Omega. \end{cases} \quad (7.19)$$

Now let \mathbf{V} denote the space of admissible displacements, which will, in particular, satisfy homogeneous Dirichlet boundary conditions on $\partial\Omega$ and be equal to the space of its variations. The variational formulation of the elastic deformation problem

reads:

$$\text{Find } \mathbf{u} \in \mathbf{V} \text{ such that } \int_{\Omega} \boldsymbol{\sigma}(\mathbf{x}, \nabla \mathbf{u}(\mathbf{x})) : \nabla \mathbf{v}(\mathbf{x}) \, d\Omega = \int_{\Omega} \mathbf{f}(\mathbf{x}) \cdot \mathbf{v}(\mathbf{x}) \, d\Omega \text{ for all } \mathbf{v} \in \mathbf{V}. \quad (7.20)$$

The VEM discretization of problem (7.20) follows the same approach discussed previously for obtaining (7.16). We refer, for instance, to the book by [Simo and Hughes \(2006\)](#) for a review of standard tools and terms in computational (small deformation) solid mechanics. Here we limit ourselves to recalling that typical computational codes combine a finite element construction with a constitutive algorithm, which is applied pointwise and, given the strains, computes the ensuing stresses. Such algorithm also gives the constitutive tangent, which is the algorithmically consistent tangent $\partial \boldsymbol{\sigma} / \partial \nabla \mathbf{u}$ and is needed in the Newton iterations.

We consider the same space \mathbf{V}_h in (7.6) of discrete displacements (or its three-dimensional variant) and write the discrete (nonlinear) problem

$$\text{Find } \mathbf{u}_h \in \mathbf{V}_h \text{ such that } a_{\boldsymbol{\sigma}, h}(\mathbf{u}_h; \mathbf{u}_h, \mathbf{v}_h) = \int_{\Omega} \mathbf{f}_h \cdot \mathbf{v}_h \, d\Omega \text{ for all } \mathbf{v}_h \in \mathbf{V}_h. \quad (7.21)$$

where the loading term is approximated as in (7.11), and the form is given by

$$\begin{aligned} a_{\boldsymbol{\sigma}, h}(\mathbf{w}_h; \mathbf{u}_h, \mathbf{v}_h) := & \sum_{E \in \mathcal{T}_h} \int_E \boldsymbol{\sigma}(\mathbf{x}, \boldsymbol{\Pi}_{k-1}^{0,E} \nabla \mathbf{u}_h(\mathbf{x})) : \boldsymbol{\Pi}_{k-1}^{0,E} \nabla \mathbf{v}(\mathbf{x}) \, dE \\ & + \alpha_E(\mathbf{w}_h) \mathcal{S}^E((I - \boldsymbol{\Pi}_k^{\nabla, E}) \mathbf{u}_h, (I - \boldsymbol{\Pi}_k^{\nabla, E}) \mathbf{v}_h) \end{aligned}$$

for all $\mathbf{w}_h, \mathbf{u}_h, \mathbf{v}_h \in \mathbf{V}_h$, where $\mathcal{S}^E(\cdot, \cdot)$ is the same stabilization form used for the linear case (7.10).

The scalar $\alpha_E(\mathbf{w}_h) > 0$ is also needed in order to introduce a scaling based on the constitutive law in the stabilization, and takes the role of the μ parameter in (7.16). Here, since the problem is nonlinear and the constitutive tangent depends on the displacement \mathbf{u}_h , this parameter needs to depend on the displacements (but as usual is not required to be accurate, the only purpose being a stabilizing effect). Different choices can be taken for $\alpha_E(\mathbf{w}_h)$, for instance

$$\alpha_E(\mathbf{w}_h) = \left\| \frac{\partial \boldsymbol{\sigma}}{\partial \nabla \mathbf{u}} (\mathbf{x}_E, \boldsymbol{\Pi}_0^{0,E} \nabla \mathbf{w}_h) \right\|,$$

with \mathbf{x}_E denoting the barycentre of E and $\|\cdot\|$ representing any norm on the fourth-order tensor space. We refer to the literature mentioned above and below for other possible choices of $\alpha_E(\mathbf{w}_h)$.

In order to solve the nonlinear problem (7.21), a typical approach in the engineering literature is to use an incremental loading procedure combined with Newton iterations. Such approach can also be applied here: we refer to equation (24) of [Beirão da Veiga et al. \(2015\)](#) for the details. Note moreover that the parameter

α_E can be made dependent on \mathbf{u}_h at the *previous* loading step, thus avoiding the calculation of the derivatives of α_E in the Newton iterations.

It is important to observe that the methodology described here couples very well with existing solid mechanics codes. For instance, given any ‘black-box’ constitutive algorithm for the constitutive law σ and the associated tangent matrix, this can be embedded directly into the above method. This inherent simplicity is one of the reasons for the wide success enjoyed by VEMs in the solid mechanics community. We conclude this section by mentioning some important generalizations, and recall that a wider overview of the VEM literature in solid mechanics can be found in the introduction to this section.

Almost incompressible materials. As already anticipated, simply by rendering the coefficient $\alpha_E(\mathbf{w}_h)$ dependent on the deviatoric part of the strains, the scheme acquires robustness in the incompressible limit. Since this property is also related to the inf-sup condition in Lemma 7.3, either $k \geq 2$ or certain restrictions on the mesh are required (see the discussion in Section 7.3).

Inelastic materials. The extension to inelastic materials is trivial following the same approach as for standard finite elements. One needs to keep track of the history variables on each integration point during the incremental loading procedure and apply the inelastic constitutive law as a black-box algorithm. See for instance Beirão da Veiga *et al.* (2015) and Artioli *et al.* (2017b) for more details.

Large deformations. The approach for the large deformation case follows the same pattern, and is based on a projection of the displacement gradients followed by application of the constitutive law. Nevertheless the more complex geometric setting and the potential large variation of the involved variables requires some additional care. This may call for *ad hoc* approximations of the determinant J of the displacement mapping and for suitable rules for calculating the stability parameter α_E . What makes VEMs particularly valuable in large deformation analysis is the robustness of the method to mesh deformations, which is a critical aspect for such problems. We refer the reader to Chi *et al.* (2017) for an introduction to VEMs for large deformation problems.

8. The Stokes and Navier–Stokes problems

In the present section we review some core results on divergence-free VEMs for incompressible fluid dynamics. The starting point is the construction introduced in Beirão da Veiga, Lovadina and Vacca (2017c) (see also Antonietti, Beirão da Veiga, Mora and Verani 2014) for the discretization of the Stokes problem.

Beirão da Veiga *et al.* (2017c) proposed a family of VEM velocity–pressure pairs of general ‘polynomial’ order which, in addition to being inf-sup stable, has the important property that the discrete velocity space is contained in the discrete pressure space. As a consequence the family leads to a stable scheme that guarantees a truly divergence-free velocity solution, as opposed to a relaxed divergence-free

condition as happens in standard FEMs. There are many advantages of divergence-free schemes when compared to standard inf-sup stable ones, an example being that the discrete velocity error is not polluted by the pressure. Although the above VEM scheme is not pressure-robust (in the sense of John *et al.* 2017), it still retains many advantages when compared with standard FEMs (Boffi *et al.* 2013), in addition to the possibility of using general meshes.

Later, in Vacca (2018) and Beirão da Veiga, Lovadina and Vacca (2018d), the method was extended to the Navier–Stokes and Brinkman equations. Beirão da Veiga, Mora and Vacca (2019b) and Beirão da Veiga, Dassi and Vacca (2018c) investigated the discrete Stokes complex structure underlying the VEM spaces, in both two and three dimensions, also leading to alternative schemes; for a glimpse of the related FEM literature we refer to Arnold, Falk and Winther (2006a) and Falk and Neilan (2013). Computational and implementation aspects were further detailed and developed in Dassi and Vacca (2020) and Dassi and Scacchi (2020), while Chernov *et al.* (2021) studied the hp version of the method. Liu, Li and Nie (2020) and Frerichs and Merdon (2022) proposed some right-hand side modifications to build a VEM scheme that is also pressure-robust for the Stokes problem. Beirão da Veiga, Canuto, Nochetto and Vacca (2021) analysed a model fluid interaction problem using mesh cutting techniques in combination with the above VEM approach. There have also been other developments of the VEM for fluid mechanics problems outside the divergence-free framework, some examples being nonconforming methods (Cangiani, Gyrya and Manzini 2016, Liu, Li and Chen 2017, Zhao, Zhang, Mao and Chen 2020, Liu and Chen 2019, Liu, Li and Chen 2019), non-standard mixed formulations (Cáceres, Gatica and Sequeira 2017, Gatica, Munar and Sequeira 2018b, Cáceres and Gatica 2016, Munar and Sequeira 2020, Gatica, Munar and Sequeira 2018a, Cáceres, Gatica and Sequeira 2018) and other derivations (Chen and Wang 2019, Wang, Wang and He 2020). Finally, a few references about the application of other polytopal technologies – such as polygonal FEMs, polygonal discontinuous Galerkin (DG), hybrid high-order (HHO) and hybridizable discontinuous Galerkin (HDG) – to fluid mechanic problems are those of Natarajan (2020), Botti, Di Pietro and Droniou (2018), Di Pietro and Krell (2018), Aghili and Di Pietro (2018), Castañón Quiroz and Di Pietro (2020), Lipnikov, Vassilev and Yotov (2014), Cockburn, Fu and Qiu (2017), Antonietti, Verani, Vergara and Zonca (2019) and Antonietti, Mascotto, Verani and Zonca (2022), while some references (among the many) on FEM divergence-free and pressure-robust methods are Guzmán and Scott (2019) and Guzmán and Neilan (2014, 2018), and Gauger, Linke and Schroeder (2019), Linke and Merdon (2016b), John *et al.* (2017) and Linke and Merdon (2016a).

8.1. The Navier–Stokes equations

Here we briefly review the steady Navier–Stokes equation on a polygonal simply connected domain $\Omega \subseteq \mathbb{R}^d$ with $d = 2, 3$; for more details see e.g. Girault and

Raviart (1979). We search a velocity field \mathbf{u} and a pressure field p that satisfy

$$\begin{cases} -\nu \operatorname{div}(\boldsymbol{\varepsilon}(\mathbf{u})) + (\nabla \mathbf{u}) \mathbf{u} - \nabla p = \mathbf{f} & \text{in } \Omega, \\ \operatorname{div} \mathbf{u} = 0 & \text{in } \Omega, \\ \mathbf{u} = 0 & \text{on } \partial\Omega, \end{cases} \quad (8.1)$$

where $\nu \in \mathbb{R}$, $\nu > 0$ is the viscosity of the fluid and $\mathbf{f} \in [L^2(\Omega)]^d$ represents the volume source term. Here we consider Dirichlet homogeneous boundary conditions only for simplicity, the extension to different boundary conditions being trivial. Let us define the continuous spaces

$$V := [H_0^1(\Omega)]^d, \quad Q := L_0^2(\Omega) = \left\{ q \in L^2(\Omega) : \int_{\Omega} q \, d\Omega = 0 \right\}.$$

The variational formulation of problem (8.1) reads:

Find $(\mathbf{u}, p) \in V \times Q$ such that

$$\begin{cases} \nu a(\mathbf{u}, \mathbf{v}) + c(\mathbf{u}; \mathbf{u}, \mathbf{v}) + b(\mathbf{v}, p) = (\mathbf{f}, \mathbf{v}) & \text{for all } \mathbf{v} \in V, \\ b(\mathbf{u}, q) = 0 & \text{for all } q \in Q, \end{cases} \quad (8.2)$$

where the continuous forms are

$$\begin{aligned} a(\mathbf{u}, \mathbf{v}) &:= \int_{\Omega} \boldsymbol{\varepsilon}(\mathbf{u}) : \boldsymbol{\varepsilon}(\mathbf{v}) \, d\Omega, \quad b(\mathbf{v}, q) := \int_{\Omega} q \operatorname{div} \mathbf{v} \, d\Omega, \\ c(\mathbf{w}; \mathbf{u}, \mathbf{v}) &:= \int_{\Omega} (\nabla \mathbf{u}) \mathbf{w} \cdot \mathbf{v} \, d\Omega \quad \text{for all } \mathbf{u}, \mathbf{v}, \mathbf{w} \in V, q \in Q. \end{aligned} \quad (8.3)$$

By definition, the velocity solution \mathbf{u} lies in the kernel of the bilinear form $b(\cdot, \cdot)$, which corresponds to the functions in V with vanishing divergence

$$Z := \{\mathbf{v} \in V : \operatorname{div} \mathbf{v} = 0\}. \quad (8.4)$$

We can observe by a direct computation that, for a fixed $\mathbf{w} \in Z$, the trilinear form $c(\mathbf{w}; \cdot, \cdot)$ is skew-symmetric, that is,

$$c(\mathbf{w}; \mathbf{u}, \mathbf{v}) = -c(\mathbf{w}; \mathbf{v}, \mathbf{u}) \quad \text{for all } \mathbf{u}, \mathbf{v} \in V.$$

Therefore the trilinear form $c(\cdot; \cdot, \cdot)$, for $\mathbf{w} \in Z$, is equal to its skew-symmetric part, defined by

$$c^{\text{skew}}(\mathbf{w}; \mathbf{u}, \mathbf{v}) := \frac{1}{2}(c(\mathbf{w}; \mathbf{u}, \mathbf{v}) - c(\mathbf{w}; \mathbf{v}, \mathbf{u})) \quad \text{for all } \mathbf{u}, \mathbf{v}, \mathbf{w} \in V. \quad (8.5)$$

It is well known (see e.g. Girault and Raviart 1979, Boffi *et al.* 2013) that the problem (8.2) is well-posed assuming suitable bounds on the external load \mathbf{f} and the viscosity ν . Such a ‘diffusion-dominated’ assumption requires

$$\gamma := \frac{C \| \mathbf{f} \|_{Z^*}}{\nu^2} < 1, \quad (8.6)$$

where C denotes the continuity constant of $c(\cdot; \cdot, \cdot)$ on Z with respect to the H^1 -norm. Note that the above assumption can also be stated by introducing the concept of a Helmholtz–Hodge projector (see e.g. John *et al.* 2017, Lemma 2.6 and Gauger *et al.* 2019, Theorem 3.3).

Remark 8.1 (Stokes problem). The Stokes model is simply obtained by neglecting the nonlinear convective term in (8.1).

We conclude this subsection by recalling the following useful polynomial decompositions (see also Section 6.1):

$$\begin{aligned} [\mathbb{P}_n(\mathcal{O})]^2 &= \nabla \mathbb{P}_{n+1}(\mathcal{O}) \oplus (\mathbf{x}^\perp \mathbb{P}_{n-1}(\mathcal{O})) && \text{if } \dim(\mathcal{O}) = 2, \\ [\mathbb{P}_n(\mathcal{O})]^3 &= \nabla \mathbb{P}_{n+1}(\mathcal{O}) \oplus (\mathbf{x} \wedge [\mathbb{P}_{n-1}(\mathcal{O})]^3) && \text{if } \dim(\mathcal{O}) = 3, \end{aligned} \quad (8.7)$$

where $\mathbf{x}^\perp = (x_2, -x_1)$.

8.2. Virtual element spaces in two dimensions

In the present subsection we outline an overview of the ‘divergence-free’ virtual element spaces in the two-dimensional case. In order to help the reader, we will start with the simpler spaces introduced in Beirão da Veiga *et al.* (2017c), which are sufficient to treat the Stokes problem, and afterwards review the enhanced spaces of Vacca (2018) and Beirão da Veiga *et al.* (2018d), which are also suitable for more complex problems such as Navier–Stokes and Brinkman. Here we work at the local level, i.e. by defining the local spaces and the associated degrees of freedom at the element level.

Note that we focus here only on the *velocity* space; the simpler pressure space will be introduced later, directly at the global level.

Basic virtual elements

Let $k \in \mathbb{N}$, $k \geq 2$ represent the degree of the method (for the ‘lowest-order’ case $k = 1$, which is not part of the current family, we refer to Antonietti *et al.* 2014). On each polygon $E \in \mathcal{T}_h$ we consider the (local) discrete velocity virtual space

$$\begin{aligned} \mathbf{V}_k^S(E) := \left\{ \mathbf{v} \in [C^0(\bar{E})]^2 : \right. &\left. \operatorname{rot} \Delta \mathbf{v} \in \mathbb{P}_{k-3}(E), \operatorname{div} \mathbf{v} \in \mathbb{P}_{k-1}(E), \right. \\ &\left. \mathbf{v}|_e \in [\mathbb{P}_k(e)]^2 \text{ for all } e \subset \partial E \right\} \end{aligned} \quad (8.8)$$

where as usual the operators above are to be interpreted in the distributional sense. We note that in standard VEM fashion, the definition of $\mathbf{V}_k^S(E)$ is associated with a PDE within the element, in this case a Stokes-like variational problem on E . Indeed, using (8.7) it is easy to check that the condition $\operatorname{rot} \Delta \mathbf{v} \in \mathbb{P}_{k-3}$ is equivalent to the existence of $q \in \mathbb{P}_{k-3}(E)$ such that $\Delta \mathbf{v} + \nabla s = \mathbf{x}^\perp q$ for some $s \in L_0^2(E)$; such an equation, combined with the remaining conditions in (8.8), represents a Stokes problem on the element.

It is immediate to check that $[\mathbb{P}_k(E)]^2 \subseteq \mathbf{V}_h^S(E)$, which is important for the approximation properties of the space, and that the dimension of $\mathbf{V}_h^S(E)$ is (recalling that N_e denotes the number of edges of E)

$$\dim(\mathbf{V}_h^S(E)) = 2k N_e + (k-1)(k-2)/2 + k(k+1)/2 - 1 = 2k N_e + k(k-1),$$

where the correction by minus one is related to the data compatibility condition ensuing from the Stokes theorem.

In $\mathbf{V}_k^S(E)$ we set the following degrees of freedom:

- (D₁) the values of \mathbf{v} at the vertices of the polygon E ,
 - (D₂) the edge moments $\int_e \mathbf{v} \cdot \mathbf{p} \, de$, for all $\mathbf{p} \in [\mathbb{P}_{k-2}(e)]^2$, $e \in \partial E$,
 - (D₃) the moments of $\operatorname{div} \mathbf{v}$, $\int_E (\operatorname{div} \mathbf{v}) p \, dE$, for all $p \in \mathbb{P}_{k-1}^0(E)$,
 - (D₄) for $k \geq 3$, the moments of $\int_E \mathbf{v} \cdot \mathbf{x}^\perp p \, dE$, for all $p \in \mathbb{P}_{k-3}(E)$.
- (8.9)

Lemma 8.2. The degrees of freedom (8.9) are unisolvant for $\mathbf{V}_k^S(E)$.

Proof. It is trivial to check that the number of the operators (8.9) is equal to the dimension of $\mathbf{V}_k^S(E)$. Therefore we only need to check that if $\mathbf{v} \in \mathbf{V}_h^S(E)$ vanishes on all (8.9) then $\mathbf{v} = 0$. Recalling (8.8) and since (D₁) and (D₂) in (8.9) vanish, it follows immediately that $\mathbf{v}|_{\partial E} = 0$. Due to the Stokes theorem, such a boundary condition also implies $\int_E \operatorname{div} \mathbf{v} \, dE = 0$, which combined with $\operatorname{div} \mathbf{v} \in \mathbb{P}_{k-1}(E)$ (see (8.8)) and the fact that the moments (D₃) vanish implies $\operatorname{div} \mathbf{v} = 0$. As a consequence we can write $\mathbf{v} = \operatorname{rot} \psi$ for some $\psi \in H_0^1(E)$. As a final preliminary result, we note that since $\operatorname{rot} \Delta \mathbf{v} \in \mathbb{P}_{k-3}$ and due to (8.7), we can write

$$\operatorname{rot} \Delta \mathbf{v} = \operatorname{rot}(\mathbf{x}^\perp q), \quad q \in \mathbb{P}_{k-3}(E). \quad (8.10)$$

Integration by parts, $\mathbf{v}|_{\partial E} = 0$ and $\mathbf{v} = \operatorname{rot} \psi$ now yield

$$\int_E \nabla \mathbf{v} : \nabla \mathbf{v} \, dE = - \int_E \mathbf{v} \cdot \Delta \mathbf{v} \, dE = - \int_E \operatorname{rot} \psi \cdot \Delta \mathbf{v} \, dE,$$

which, combined with integration by parts, $\psi|_{\partial E} = 0$ and (8.10), yields

$$\begin{aligned} \int_E \nabla \mathbf{v} : \nabla \mathbf{v} \, dE &= \int_E \psi \cdot \operatorname{rot} \Delta \mathbf{v} \, dE = \int_E \psi \cdot \operatorname{rot}(\mathbf{x}^\perp q) \, dE \\ &= - \int_E \operatorname{rot} \psi \cdot (\mathbf{x}^\perp q) \, dE = - \int_E \mathbf{v} \cdot (\mathbf{x}^\perp q) \, dE = 0, \end{aligned}$$

where the last identity follows from the vanishing degrees of freedom (D₄). The above identity clearly implies $\psi = 0$ and the result follows recalling $\mathbf{v} = \operatorname{rot} \psi$. \square

Remark 8.3. We observe that the degrees of freedom (D₁)–(D₂) in (8.9) allow us to compute \mathbf{v} on the boundary of the element. Furthermore, the combination of

the Stokes theorem and (D_3) allows us to compute the polynomial $\operatorname{div} \mathbf{v} \in \mathbb{P}_{k-1}(E)$. Therefore these two quantities are fully computable.

We next make an important observation. The degrees of freedom (8.9) allow us to compute (see (2.6) and (2.5) and Definition 2.2) the following projection operators exactly:

$$\begin{aligned}\Pi_k^{\nabla,E} &: \mathbf{V}_k^S(E) \rightarrow [\mathbb{P}_k(E)]^2, \\ \Pi_{k-2}^{0,E} &: \mathbf{V}_k^S(E) \rightarrow [\mathbb{P}_{k-2}(E)]^2, \\ \boldsymbol{\Pi}_{k-1}^{0,E} &: \boldsymbol{\nabla} \mathbf{V}_k^S(E) \rightarrow [\mathbb{P}_{k-1}(E)]^{2 \times 2}.\end{aligned}\quad (8.11)$$

Here we show only a proof for the first item, as the last two follow by analogous arguments. Looking at the definition of the H_0^1 -projection (2.6), we see that in order to determine the polynomial $\Pi_k^{\nabla,E} \mathbf{v}$, for any $\mathbf{v} \in \mathbf{V}_k^S(E)$, we need to compute

$$\int_E \boldsymbol{\nabla} \mathbf{v} : \boldsymbol{\nabla} \mathbf{p} \, dE \quad \text{for all } \mathbf{p} \in [\mathbb{P}_k(E)]^2. \quad (8.12)$$

Employing the polynomial decomposition (8.7) for $\Delta \mathbf{p} \in [\mathbb{P}_{k-2}(E)]^2$, we can write $\Delta \mathbf{p} = \nabla q_{k-1} + \mathbf{x}^\perp q_{k-3}$ for some $q_{k-1} \in \mathbb{P}_{k-1}(E)$ and $q_{k-3} \in \mathbb{P}_{k-3}(E)$. Therefore, integrating by parts, we deduce

$$\begin{aligned}& \int_E \boldsymbol{\nabla} \mathbf{v} : \boldsymbol{\nabla} \mathbf{p} \, dE \\&= \int_{\partial E} \mathbf{v} \cdot (\boldsymbol{\nabla} \mathbf{p}) \mathbf{n} \, ds - \int_E \mathbf{v} \cdot \Delta \mathbf{p} \, dE \\&= \int_{\partial E} \mathbf{v} \cdot (\boldsymbol{\nabla} \mathbf{p}) \mathbf{n} \, ds - \int_E \mathbf{v} \cdot (\nabla q_{k-1} + \mathbf{x}^\perp q_{k-3}) \, dE \\&= \int_{\partial E} \mathbf{v} \cdot ((\boldsymbol{\nabla} \mathbf{p}) \mathbf{n} - q_{k-1} \mathbf{n}) \, ds + \int_E \operatorname{div} \mathbf{v} q_{k-1} \, dE - \int_E \mathbf{v} \cdot \mathbf{x}^\perp q_{k-3} \, dE.\end{aligned}$$

Recalling Remark 8.3 and (D_4) in (8.9), the above identity yields that (8.12) is a computable expression.

We conclude this subsection by mentioning a drawback of the above space. The properties above show that the degrees of freedom (8.9) allow exact computation of the L^2 -projection $\Pi_{k-2}^{0,E}$ onto \mathbb{P}_{k-2} but not onto \mathbb{P}_k .

Enhanced virtual elements

In this section we will apply the *enhancement approach* to define a new (velocity) virtual space $\mathbf{V}_k(E)$, to be used in place of the space $\mathbf{V}_k^S(E)$, in such a way that the full projection $\boldsymbol{\Pi}_k^{0,E} : \mathbf{V}_k(E) \rightarrow [\mathbb{P}_k(E)]^2$ is computable from the degrees of freedom (8.9), without increasing the dimension of the space or spoiling other critical properties such as $[\mathbb{P}_k(E)]^2 \subseteq \mathbf{V}_k^S(E)$. Such an ‘enhancement approach’ was introduced in Vacca (2018) and Beirão da Veiga *et al.* (2018d), taking inspiration from Ahmad *et al.* (2013).

We first observe that in order to compute $\Pi_k^{0,E} \mathbf{v}$ we obviously need to compute

$$\int_E \mathbf{v} \cdot \mathbf{p}_k \, dE \quad \text{for any } \mathbf{p}_k \in [\mathbb{P}_k(E)]^2.$$

Using the polynomial decomposition (8.7), let $q_{k+1} \in \mathbb{P}_{k+1}(E)$ and $q_{k-1} \in \mathbb{P}_{k-1}(E)$ be such that $\mathbf{p}_k = \nabla q_{k+1} + \mathbf{x}^\perp q_{k-1}$. Then, using this and integrating by parts, we have

$$\begin{aligned} \int_E \mathbf{v} \cdot \mathbf{p}_k \, dE &= \int_E \mathbf{v} \cdot (\nabla q_{k+1} + \mathbf{x}^\perp q_{k-1}) \, dE \\ &= \int_{\partial E} \mathbf{v} \cdot \mathbf{n} q_{k+1} \, ds - \int_E \operatorname{div} \mathbf{v} q_{k+1} \, dE + \int_E \mathbf{v} \cdot \mathbf{x}^\perp q_{k-1} \, dE. \end{aligned} \quad (8.13)$$

The last integral is not computable, since the degrees of freedom (D_4) in (8.9) allow us to compute $\int_E \mathbf{v} \cdot \mathbf{x}^\perp q$ only for polynomials $q \in \mathbb{P}_{k-3}(E)$ and not for $q \in \mathbb{P}_{k-1}(E)$.

Therefore, in order to construct $V_k(E)$ we proceed as in the previous sections for the simpler Laplace problem: we first enlarge the space in order to have the computability of the missing moments, and then we introduce the so-called ‘enhanced constraints’ to recover the correct dimension of the space.

We then first introduce, on each element $E \in \mathcal{T}_h$, the augmented space

$$\begin{aligned} W_k(E) := \{ \mathbf{v} \in [C^0(\bar{E})]^2 : \operatorname{rot} \Delta \mathbf{v} \in \mathbb{P}_{k-1}(E), \operatorname{div} \mathbf{v} \in \mathbb{P}_{k-1}(E), \\ \mathbf{v}|_e \in [\mathbb{P}_k(e)]^2 \text{ for all } e \subset \partial E \}. \end{aligned} \quad (8.14)$$

The degrees of freedom in $W_k(E)$, referring to (8.9), will be

$$\begin{aligned} (D_1)-(D_2)-(D_3) \quad \text{plus} \\ (D_5) \quad \int_E \mathbf{v} \cdot \mathbf{x}^\perp p \, dE, \text{ for all } p \in \mathbb{P}_{k-1}(E). \end{aligned} \quad (8.15)$$

Although the space $W_k(E)$ has the right computability and approximation properties, it has too many degrees of freedom. We therefore reduce it and introduce the ‘enhanced’ VEM velocity space. We recall that for any non-negative integers $m \leq n$, we let $\mathbb{P}_{n/m}$ denote any subspace (fixed once and for all) of \mathbb{P}_n such that

$$\mathbb{P}_n = \mathbb{P}_m \oplus \mathbb{P}_{n/m}.$$

We define

$$\begin{aligned} V_k(E) \quad (8.16) \\ := \{ \mathbf{v} \in [C^0(\bar{E})]^2 : \mathbf{v}|_e \in [\mathbb{P}_k(e)]^2 \text{ for all } e \subset \partial E, \operatorname{rot} \Delta \mathbf{v} \in \mathbb{P}_{k-1}(E), \\ \operatorname{div} \mathbf{v} \in \mathbb{P}_{k-1}(E), \int_E (\mathbf{v} - \Pi_k^{\nabla, E} \mathbf{v}) \cdot \mathbf{x}^\perp p \, dE = 0 \text{ for all } p \in \mathbb{P}_{k-1/k-3}(E) \}. \end{aligned}$$

We point out that the important property

$$[\mathbb{P}_k(E)]^2 \subseteq V_k(E)$$

still holds.

Furthermore, we show that, as degrees of freedom in $\mathbf{V}_k(E)$, we can take the same set of degrees of freedom (8.9) introduced for $\mathbf{V}_k^S(E)$.

Property 8.4. The degrees of freedom (8.9) are unisolvant for $\mathbf{V}_k(E)$.

Proof. A simple computation, following the same argument as in the previous section, easily shows that

$$\dim(\mathbf{W}_k(E)) = 2k N_e + \frac{k(k+1)}{2} + \frac{k(k+1)}{2} - 1 = \dim(\mathbf{V}_k^S(E)) + \dim(\mathbb{P}_{k-1/k-3}(E)).$$

Since $\mathbf{V}_k(E)$ is obtained from $\mathbf{W}_k(E)$ by enforcing $\dim(\mathbb{P}_{k-1/k-3}(E))$ linear constraints, from the above identity we immediately obtain

$$\dim(\mathbf{V}_h(E)) \geq \dim(\mathbf{V}_k^S(E)).$$

Therefore, since the number of degrees of freedom in (8.9) is equal to $\dim(\mathbf{V}_k^S(E))$, the proof is concluded if we show that any $v \in \mathbf{V}_k(E)$ that vanishes on all degrees of freedom (8.9) must satisfy $v = 0$. A key observation is the fact that the operator

$$\Pi_k^{\nabla,E} : \mathbf{W}_k(E) \rightarrow [\mathbb{P}_k(E)]^2$$

depends only on (8.9); the proof is identical to that shown for $\mathbf{V}_k^S(E)$ at the end of the previous section. As a consequence, since v vanishes on all linear operators (8.9), we have $\Pi_k^{\nabla,E}(v) = 0$. Therefore, from the definition of $\mathbf{V}_k(E)$, we also have

$$\int_E v \cdot \mathbf{x}^\perp p \, dE = 0 \quad \text{for all } p \in \mathbb{P}_{k-1/k-3}(E).$$

The combination of the above equation and the fact that the moments (D_4) in (8.9) vanish for v implies that the full enlarged operator set (8.15) vanishes for v . The proof is concluded by recalling that $v \in \mathbf{V}_h(E) \subseteq \mathbf{W}_k(E)$ and that (8.15) is a set of unisolvant degrees of freedom for $\mathbf{W}_k(E)$. \square

Finally, we have the following important result.

Property 8.5. The degrees of freedom (8.9) allow us to compute exactly (see (2.5))

$$\Pi_k^{0,E} : \mathbf{V}_k(E) \rightarrow [\mathbb{P}_k(E)]^2.$$

Proof. We start from equation (8.13) and observe that the first two terms on the right-hand side are computable thanks to Remark 8.3, which clearly holds also for the new space $\mathbf{V}_k(E)$. We are therefore left with the third term $\int_E v \cdot \mathbf{x}^\perp q_{k-1}$, which we split into

$$\int_E v \cdot \mathbf{x}^\perp q_{k-1} \, dE = \int_E v \cdot \mathbf{x}^\perp p_{k-3} \, dE + \int_E v \cdot \mathbf{x}^\perp \tilde{p} \, dE,$$

with $p_{k-3} \in \mathbb{P}_{k-3}(E)$ and $\tilde{p} \in \mathbb{P}_{k-1/k-3}$. The first term above is computable from

(D_4) and the second one follows from the property built in the definition of the space (8.16):

$$\int_E \mathbf{v} \cdot \mathbf{x}^\perp \tilde{p} \, dE = \int_E \Pi_k^{\nabla, E}(\mathbf{v}) \cdot \mathbf{x}^\perp \tilde{p} \, dE. \quad \square$$

8.3. Virtual element spaces in three dimensions

The aim of this section is to present the divergence-free virtual element spaces in three dimensions. This is a natural extension of the two-dimensional VEM of Section 3 combined with the ideas introduced for the three-dimensional Laplace operators in Section 3.8. We will keep our exposition rather brief and refer the reader to [Beirão da Veiga et al. \(2018c\)](#) for further details. As in the previous section, we focus on the *velocity* space and work locally on the element.

As in Section 3.8, in order to define the *velocity* VEM space in three dimensions, we proceed in two steps: we first introduce suitable VEM spaces related to the faces of the element, and we then define the local spaces defined on the polyhedron.

As before, let $k \in \mathbb{N}$, $k \geq 2$ (for the lowest-order case $k = 1$, which falls outside the current family, we refer for instance to the velocity space introduced in [Beirão da Veiga et al. 2022a](#)). On each face f of an element $P \in \mathcal{T}_h$, we define the (scalar) face space

$$V_k(f) := \left\{ v \in C^0(\bar{f}): \Delta_2 v \in \mathbb{P}_{k+1}(f), v|_e \in \mathbb{P}_k(e) \text{ for all } e \subset \partial f, \right. \\ \left. \int_f (v - \Pi_k^{\nabla, f} v) p \, df = 0 \text{ for all } p \in \mathbb{P}_{k+1/k-2}(f) \right\}. \quad (8.17)$$

Note that the space $V_k(f)$ is slightly different from that introduced in Section 3.8 for the Laplace problem, since the ‘enhancement’ here is even more extreme; the reason for this choice will be clear in what follows. One can easily see that $V_k(f)$ satisfies $\mathbb{P}_k(f) \subseteq V_k(f)$ and that a set of degrees of freedom for $V_k(F)$ is

- (D_1) the values of v at the vertices of the face f ,
- (D_2) the edge moments $\int_e vp \, de$, for all $p \in \mathbb{P}_{k-2}(e)$, $e \subset \partial f$,
- (D_3) the moments $\int_f vp \, df$, for all $p \in \mathbb{P}_{k-2}(f)$.

Furthermore, with arguments similar to those used in Section 3, one can check that the L^2 -projection operator

$$\Pi_{k+1}^{0,f}: V_k(f) \rightarrow \mathbb{P}_{k+1}(f) \quad (8.19)$$

is computable on the basis of the degrees of freedom (8.18). Note that thanks to the particular definition of $V_k(F)$, we are able to compute the projection in the richer space $\mathbb{P}_{k+1}(F)$.

We are now able to present the three-dimensional VEM ‘divergence-free’ space for velocities; here we present the more advanced space, suitable for both the Stokes and the Navier–Stokes problems:

$$V_k(P) := \left\{ \boldsymbol{v} \in [C^0(P)]^3 : \operatorname{curl}\Delta\boldsymbol{v} \in [\mathbb{P}_{k-1}(P)]^3, \operatorname{div}\boldsymbol{v} \in \mathbb{P}_{k-1}(P), \right. \\ \left. \boldsymbol{v}|_f \subset [V_k(f)]^3 \text{ for all } f \in \partial P, \right. \\ \left. \int_P (\boldsymbol{v} - \Pi_k^{\nabla, P} \boldsymbol{v}) \cdot (\boldsymbol{x} \wedge \boldsymbol{p}) dP = 0 \text{ for all } \boldsymbol{p} \in [\mathbb{P}_{k-1/k-3}(P)]^3 \right\}. \quad (8.20)$$

The second line of (8.20) defines the space $V_k(P)$ on the boundary of the element. The first line states that the virtual functions are obtained by solving a Stokes-like problem in the element. Indeed, recalling (8.7), it can be checked that the condition $\operatorname{curl}\Delta\boldsymbol{v} \in \mathbb{P}_{k-1}$ is equivalent to the existence of $\boldsymbol{q} \in \mathbb{P}_{k-1}(P)$ such that $\Delta\boldsymbol{v} + \nabla s = \boldsymbol{x} \wedge \boldsymbol{q}$ for some $s \in L_0^2(P)$; such an equation, combined with the condition $\operatorname{div}\boldsymbol{v} \in \mathbb{P}_{k-1}(P)$ in (8.8), represents a Stokes-like problem on the element. Finally, the last condition represents an ‘enhancement’ constraint.

It is easy to check that $[\mathbb{P}_k(P)]^3 \subseteq V_k(P)$. Furthermore, with arguments similar to the previous sections, one can show that the following linear operators constitute a set of unisolvant degrees of freedom for the space $V_k(P)$:

- (D₁) the values of \boldsymbol{v} at the vertices of the polyhedron P ,
 - (D₂) the moments $\int_e \boldsymbol{v} \cdot \boldsymbol{p} de$, for all $\boldsymbol{p} \in [\mathbb{P}_{k-2}(e)]^3$, $e \subset \partial P$,
 - (D₃) the face moments $\int_f \boldsymbol{v} \cdot \boldsymbol{p} df$, for all $\boldsymbol{p} \in [\mathbb{P}_{k-2}(f)]^3$,
 - (D₄) the moments of $\operatorname{div}\boldsymbol{v}$: $\int_P (\operatorname{div}\boldsymbol{v}) p dP$, for all $p \in \mathbb{P}_{k-1}^0(P)$,
 - (D₅) for $k \geq 3$, the ‘moments’ of $\int_P \boldsymbol{v} \cdot (\boldsymbol{x} \wedge \boldsymbol{p}) dP$, for all $\boldsymbol{p} \in [\mathbb{P}_{k-3}(P)]^3$.
- (8.21)

Another critical property is that the three-dimensional versions of the projections in (8.11) are computable on the space $V_k(P)$. Here we show only the proof for

$$\Pi_k^{0,P} : V_k(P) \rightarrow [\mathbb{P}_k(P)]^3,$$

and observe that in order to compute $\Pi_k^{0,E} \boldsymbol{v}$ we need to compute

$$\int_P \boldsymbol{v} \cdot \boldsymbol{p} dP \quad \text{for any } \boldsymbol{p} \in [\mathbb{P}_k(P)]^3.$$

Using (8.7), let $q_{k+1} \in \mathbb{P}_{k+1}(P)$ and $\boldsymbol{q}_{k-1} \in [\mathbb{P}_{k-1}(P)]^3$ be such that $\boldsymbol{p} = \nabla q_{k+1} + \boldsymbol{x} \wedge \boldsymbol{q}_{k-1}$. In turn, the polynomial \boldsymbol{q}_{k-1} can be split into $\boldsymbol{q}_{k-1} = \boldsymbol{q}_{k-3} + \tilde{\boldsymbol{q}}_{k-1}$, with $\boldsymbol{q}_{k-3} \in [\mathbb{P}_{k-3}(P)]^3$ and $\tilde{\boldsymbol{q}}_{k-1} \in [\mathbb{P}_{k-1/k-3}(P)]^3$. By an argument analogous to that used in the two-dimensional case, it is easy to check that $\operatorname{div}\boldsymbol{v} \in \mathbb{P}_{k-1}(P)$

is computable using the above degrees of freedom. Then integration by parts and trivial steps yield

$$\begin{aligned}
\int_P \mathbf{v} \cdot \mathbf{p}_k \, dP &= \int_P \mathbf{v} \cdot (\nabla q_{k+1} + \mathbf{x} \wedge \mathbf{q}_{k-1}) \, dP \\
&= \sum_{f \subset \partial P} \int_f \mathbf{v} \cdot \mathbf{n} q_{k+1} \, df - \int_P \operatorname{div} \mathbf{v} q_{k+1} \, dP + \int_P \mathbf{v} \cdot (\mathbf{x} \wedge \mathbf{q}_{k-1}) \, dP \\
&= \sum_{f \subset \partial P} \int_f \Pi_{k+1}^{0,f} \mathbf{v} \cdot \mathbf{n} q_{k+1} \, df - \int_P \operatorname{div} \mathbf{v} q_{k+1} \, dP \\
&\quad + \int_P \mathbf{v} \cdot (\mathbf{x} \wedge \mathbf{q}_{k-1}) \, dP + \int_P \Pi_k^{\nabla,P} \mathbf{v} \cdot (\mathbf{x} \wedge \tilde{\mathbf{q}}_{k-1}) \, dP. \tag{8.22}
\end{aligned}$$

All the above terms are computable: the first one since $\Pi_{k+1}^{0,f} \mathbf{v}$ is computable on each face (see (8.19)), the second one since $\operatorname{div} \mathbf{v}$ is known and computable, the third one using (D_5) in (8.21) and the fourth one since $\Pi_k^{\nabla,P} \mathbf{v}$ is computable. Note that the first term motivates the need for the particular definition used in (8.17).

8.4. The discrete VEM problem

Let \mathcal{T}_h be a decomposition of the domain $\Omega \subset \mathbb{R}^d$ with $d = 2, 3$ into general polytopal elements. In order to keep the same exposition in two and three dimensions, we will indicate the generic element with the letter E (thus representing a polygon if $d = 2$ and a polyhedron if $d = 3$).

For any $E \in \mathcal{T}_h$, let $V_k(E)$ denote one of the enhanced velocity VEM spaces introduced in the previous sections ((8.16) in two dimensions and (8.20) in three dimensions, respectively). The global velocity VEM space is defined by

$$V_h := \{\mathbf{v} \in V : \mathbf{v}|_E \in V_k(E) \text{ for all } E \in \mathcal{T}_h\}, \tag{8.23}$$

and the global degrees of freedom are given by the standard degree of freedom assembly as in the FEM. The discrete pressure space is given by the piecewise polynomial functions of degree $k - 1$, that is, the local and global pressure spaces are simply given by

$$\begin{aligned}
Q_h(E) &:= \mathbb{P}_{k-1}(E) \text{ for all } E \in \mathcal{T}_h, \\
Q_h &:= \{q \in Q : q|_E \in Q_h(E) \text{ for all } E \in \mathcal{T}_h\}. \tag{8.24}
\end{aligned}$$

We recall the following results stating some interpolation properties of the velocity space (see Proposition 4.2 in Beirão da Veiga *et al.* 2017c and Theorem 4.1 in Beirão da Veiga *et al.* 2018d) and the inf-sup stability of the pair (V_h, Q_h) (see Proposition 4.3 in Beirão da Veiga *et al.* 2017c).

Proposition 8.6. Under Assumption 2.1, let $\mathbf{v} \in [H^s(\mathcal{T}_h)]^d$ with $1 < s \leq k + 1$. Then there exists $\mathbf{v}_h \in V_h$ such that

$$\|\mathbf{v} - \mathbf{v}_h\|_0 + h\|\nabla \mathbf{v} - \nabla \mathbf{v}_h\|_0 \lesssim h^s |\mathbf{v}|_{s, \mathcal{T}_h},$$

where the hidden constant depends only on k and the shape regularity constant ϱ .

Proposition 8.7. Given the discrete spaces V_h and Q_h defined in (8.23) and (8.24) respectively, there exists a positive constant $\widehat{\beta}$, independent of h , such that

$$\sup_{v_h \in V_h, v_h \neq 0} \frac{b(v_h, q_h)}{\|\nabla v_h\|_0} \geq \widehat{\beta} \|q_h\|_0 \quad \text{for all } q_h \in Q_h.$$

We now define computable discrete local forms, following a construction similar to that shown in Section 3.7:

$$a_h^E(u, v) := \int_E (\Pi_{k-1}^{0,E} \boldsymbol{\epsilon}(u)) : (\Pi_{k-1}^{0,E} \boldsymbol{\epsilon}(v)) \, dE + \mathcal{S}^E((I - \Pi_k^{0,E})u, (I - \Pi_k^{0,E})v), \quad (8.25)$$

$$c_h^{o,E}(w; u, v) := \int_E [(\Pi_{k-1}^{0,E} \nabla u) \Pi_k^{0,P} w] \cdot \Pi_k^{0,E} v \, dE, \quad (8.26)$$

$$c_h^{\text{skew},E}(w; u, v) := \frac{1}{2} (c_h^{o,E}(w; u, v) - c_h^{o,E}(w; v, u)), \quad (8.27)$$

for all $w, u, v \in V_h(E)$, where clearly

$$\Pi_k^{0,E} \boldsymbol{\epsilon}(v) = \frac{\Pi_k^{0,E} \nabla v + (\Pi_k^{0,E} \nabla v)^T}{2}$$

and the symmetric stabilizing form $\mathcal{S}^E: V_h(E) \times V_h(E) \rightarrow \mathbb{R}$ satisfies

$$\|\nabla v\|_{0,E}^2 \lesssim \mathcal{S}^E(v, v) \lesssim \|\nabla v\|_{0,E}^2 \quad \text{for all } v \in V_h(E) \cap \text{Ker}(\Pi_k^{0,E}). \quad (8.28)$$

The condition above essentially requires the stabilizing term $\mathcal{S}^E(v, v)$ to scale as $\|\nabla v\|_{0,E}^2$. Possible choices for the stabilization are the same ones already discussed in Section 3.3.

The global virtual forms are defined by simply summing the local contributions:

$$a_h(u, v) := \sum_{E \in \mathcal{T}_h} a_h^E(u, v), \quad c_h(w; u, v) := \sum_{E \in \mathcal{T}_h} c_h^{\text{skew},E}(w; u, v) \quad (8.29)$$

for all $w, u, v \in V_h$. We point out that

- the symmetry of $a_h(\cdot, \cdot)$ together with (8.28) easily implies that $a_h(\cdot, \cdot)$ is continuous and coercive with respect to the H^1 -norm,
- the discrete trilinear form $c_h(\cdot; \cdot, \cdot)$ is skew-symmetric and is continuous with respect to the H^1 -norm.

Finally, the discrete right-hand side is defined by the computable quantity

$$(f_h, v) := \sum_{E \in \mathcal{T}_h} \int_E \Pi_k^{0,E} f \cdot v \, dE = \sum_{E \in \mathcal{T}_h} \int_E f \cdot \Pi_k^{0,E} v \, dE \quad \text{for all } v \in V_h. \quad (8.30)$$

Referring to the discrete spaces (8.23), (8.24), the discrete forms (8.29), the $b(\cdot, \cdot)$ form in (8.3) and the approximated load term (8.30), the virtual element approximation of the Navier–Stokes equation is given by:

Find $(\mathbf{u}_h, p_h) \in \mathbf{V}_h \times Q_h$ such that (8.31)

$$\begin{cases} v a_h(\mathbf{u}_h, \mathbf{v}_h) + c_h(\mathbf{u}_h; \mathbf{u}_h, \mathbf{v}_h) + b(\mathbf{v}_h, p_h) = (\mathbf{f}_h, \mathbf{v}_h) & \text{for all } \mathbf{v}_h \in \mathbf{V}_h, \\ b(\mathbf{u}_h, q_h) = 0 & \text{for all } q_h \in Q_h. \end{cases}$$

A crucial observation is that definitions (8.23) and (8.24), along with Proposition 8.7, imply that $\operatorname{div} \mathbf{V}_h = Q_h$. Therefore the discrete kernel is a subspace of the continuous kernel \mathbf{Z} (see (8.4)):

$$\mathbf{Z}_h := \{\mathbf{v}_h \in \mathbf{V}_h : b(\mathbf{v}_h, q_h) = 0 \text{ for all } q_h \in Q_h\} \subseteq \mathbf{Z}. \quad (8.32)$$

Consequently, the second equation of (8.31) implies that the discrete velocity $\mathbf{u}_h \in \mathbf{V}_h$ is *exactly divergence-free*.

The well-posedness of the discrete problems is stated in the following theorem.

Theorem 8.8. Let \widehat{C} represent the continuity constant of the form $c_h(\cdot, \cdot, \cdot)$ in Z_h . Under the data assumption

$$\widehat{\gamma} := \frac{\widehat{C} \| \mathbf{f}_h \|_{\mathbf{Z}'_h}}{\widehat{\alpha}^2 v^2} < 1, \quad (8.33)$$

with the usual definition of dual norm, problem (8.31) is well-posed.

8.5. Convergence results and exploring the divergence-free property

Here we briefly emphasize the main benefits of the proposed VEM scheme, in addition to the capability (shared by any VEM scheme) of using general polytopal meshes. The divergence-free property and the kernel inclusion (8.32) entail a range of advantages.

- The error components partly decouple, as shown in the converge results below. Namely, the influence of the pressure in the velocity error is weaker with respect to standard inf-sup stable elements (see Beirão da Veiga *et al.* 2018d).
- The scheme in (8.31) is equivalent to a suitable reduced problem. The internal divergence-moment degrees of freedom (\mathbf{D}_3) in (8.18) for $d = 2$, (\mathbf{D}_4) in (8.21) for $d = 3$) and the associated pressure degrees of freedom can be automatically ignored in the final linear system (see Beirão da Veiga *et al.* 2017c).
- The proposed virtual element enjoys an underlying discrete Stokes complex structure (see Beirão da Veiga *et al.* 2019b, Beirão da Veiga *et al.* 2018c).
- The space \mathbf{V}_h is uniformly stable also for the Darcy equation (see Vacca 2018).

We finally state a convergence result for the proposed virtual element scheme (8.31). We refer to Theorem 4.6 in [Beirão da Veiga et al. \(2018d\)](#) for the proof.

Proposition 8.9. Under the assumptions (8.6), (8.33) and Assumption 2.1, let $(\mathbf{u}, p) \in V \times Q$ be the solution of problem (8.2) and let $(\mathbf{u}_h, p_h) \in V_h \times Q_h$ be the solution of problem (8.31). Assuming that \mathbf{u} and \mathbf{f} belong to $[H^{k+1}(\mathcal{T}_h)]^d$ and $p \in H^k(\mathcal{T}_h)$, we have

$$\|\mathbf{u} - \mathbf{u}_h\|_1 \leq h^k \chi_1(\mathbf{u}) + h^{k+2} \chi_2(\mathbf{f}), \quad (8.34)$$

$$\|p - p_h\|_0 \leq h^k \chi_3(p) + h^k \chi_4(\mathbf{u}) + h^{k+2} \chi_5(\mathbf{f}), \quad (8.35)$$

where the χ_i , $i = 1, \dots, 5$ are suitable functions independent of h (but which may depend on the material parameters, k and ϱ).

Note that the velocity error does not depend directly on the discrete pressures, but only indirectly through the presence of the *higher-order* loading term in (8.34). Indeed, the velocity error of classical mixed FE methods would have an additional term, of order $O(h^k)$, depending on the exact pressure p . In some situations the partial decoupling of the errors stated in (8.34) induces a positive effect on the velocity approximation.

Remark 8.10. In the context of the approximation of the Navier–Stokes equation, a numerical method is said to be pressure-robust (see e.g. [John et al. 2017](#)) if the discrete velocity solution depends only on the Helmholtz–Hodge projector of the load \mathbf{f} (as happens for the exact velocity field). For instance, if the load is a gradient field then the continuous velocity vanishes, and the discrete velocity computed with a pressure-robust method vanishes as well. Thus method (8.31) is not pressure-robust, as it does not guarantee such a property. On the other hand the dependence on the full load is much weaker with respect to standard mixed schemes, thus leading, for instance, to a higher rate of convergence whenever the load is a gradient. Modified schemes have been proposed in [Liu et al. \(2020\)](#) and [Frerichs and Merdon \(2022\)](#) in order to get a fully pressure-robust VEM scheme. Such approaches have the drawback of requiring a suitable Raviart–Thomas interpolation of the test functions with respect to a sub-triangulation of the mesh \mathcal{T}_h .

References

- R. A. Adams (1975), *Sobolev Spaces*, Vol. 65 of Pure and Applied Mathematics, Academic Press.
- J. Aghili and D. A. Di Pietro (2018), An advection-robust hybrid high-order method for the Oseen problem, *J. Sci. Comput.* **77**, 1310–1338.
- B. Ahmad, A. Alsaedi, F. Brezzi, L. D. Marini and A. Russo (2013), Equivalent projectors for virtual element methods, *Comput. Math. Appl.* **66**, 376–391.

- P. F. Antonietti, L. Beirão da Veiga, D. Mora and M. Verani (2014), A stream virtual element formulation of the Stokes problem on polygonal meshes, *SIAM J. Numer. Anal.* **52**, 386–404.
- P. F. Antonietti, L. Beirão da Veiga, S. Scacchi and M. Verani (2016), A C^1 virtual element method for the Cahn–Hilliard equation with polygonal meshes, *SIAM J. Numer. Anal.* **54**, 34–57.
- P. F. Antonietti, G. Manzini and M. Verani (2018), The fully nonconforming virtual element method for biharmonic problems, *Math. Models Methods Appl. Sci.* **28**, 387–407.
- P. F. Antonietti, L. Mascotto, M. Verani and S. Zonca (2022), Stability analysis of polytopic discontinuous Galerkin approximations of the Stokes problem with applications to fluid–structure interaction problems, *J. Sci. Comput.* **90**, 23.
- P. F. Antonietti, M. Verani, C. Vergara and S. Zonca (2019), Numerical solution of fluid–structure interaction problems by means of a high order discontinuous Galerkin method on polygonal grids, *Finite Elem. Anal. Des.* **159**, 1–14.
- D. N. Arnold and G. Awanou (2011), The serendipity family of finite elements, *Found. Comput. Math.* **11**, 337–344.
- D. N. Arnold, D. Boffi and R. S. Falk (2002), Approximation by quadrilateral finite elements, *Math. Comp.* **71**, 909–922.
- D. N. Arnold, F. Brezzi, B. Cockburn and L. D. Marini (2001), Unified analysis of discontinuous Galerkin methods for elliptic problems, *SIAM J. Numer. Anal.* **39**, 1749–1779.
- D. N. Arnold, R. S. Falk and R. Winther (2006a), Differential complexes and stability of finite element methods, I: The de Rham complex, in *Compatible Spatial Discretizations*, Vol. 142 of IMA Volumes in Mathematics and its Applications, Springer, pp. 24–46.
- D. N. Arnold, R. S. Falk and R. Winther (2006b), Finite element exterior calculus, homological techniques, and applications, *Acta Numer.* **15**, 1–155.
- E. Artioli, L. Beirão da Veiga, C. Lovadina and E. Sacco (2017a), Arbitrary order 2D virtual elements for polygonal meshes, I: Elastic problem, *Comput. Mech.* **60**, 355–377.
- E. Artioli, L. Beirão da Veiga, C. Lovadina and E. Sacco (2017b), Arbitrary order 2D virtual elements for polygonal meshes, II: Inelastic problem, *Comput. Mech.* **60**, 643–657.
- E. Artioli, S. de Miranda, C. Lovadina and L. Patruno (2018), A family of virtual element methods for plane elasticity problems based on the Hellinger–Reissner principle, *Comput. Methods Appl. Mech. Engrg.* **340**, 978–999.
- E. Artioli, S. Marfia and E. Sacco (2020), VEM-based tracking algorithm for cohesive/frictional 2D fracture, *Comp. Meth. Appl. Mech. Engrg.* **365**, 112956.
- G. Auchmuty and J. C. Alexander (2001), L^2 well-posedness of planar div-curl systems, *Arch. Ration. Mech. Anal.* **160**, 91–134.
- G. Auchmuty and J. C. Alexander (2005), L^2 -well-posedness of 3D div-curl boundary value problems, *Quart. Appl. Math.* **63**, 479–508.
- B. Ayuso de Dios, K. Lipnikov and G. Manzini (2016), The nonconforming virtual element method, *ESAIM Math. Model. Numer. Anal.* **50**, 879–904.
- L. Beirão da Veiga and K. Lipnikov (2010), A mimetic discretization of the Stokes problem with selected edge bubbles, *SIAM J. Sci. Comput.* **32**, 875–893.
- L. Beirão da Veiga and L. Mascotto (2022), Interpolation and stability properties of low-order face and edge virtual element spaces, *IMA J. Numer. Anal.* **2022**, drac008.
- L. Beirão da Veiga, F. Brezzi and L. D. Marini (2013a), Virtual elements for linear elasticity problems, *SIAM J. Numer. Anal.* **51**, 794–812.

- L. Beirão da Veiga, F. Brezzi, A. Cangiani, G. Manzini, L. D. Marini and A. Russo (2013b), Basic principles of virtual element methods, *Math. Models Methods Appl. Sci.* **23**, 199–214.
- L. Beirão da Veiga, F. Brezzi, F. Dassi, L. D. Marini and A. Russo (2017a), Virtual element approximation of 2D magnetostatic problems, *Comput. Methods Appl. Mech. Engrg* **327**, 173–195.
- L. Beirão da Veiga, F. Brezzi, F. Dassi, L. D. Marini and A. Russo (2018a), A family of three-dimensional virtual elements with applications to magnetostatics, *SIAM J. Numer. Anal.* **56**, 2940–2962.
- L. Beirão da Veiga, F. Brezzi, F. Dassi, L. D. Marini and A. Russo (2018b), Lowest order virtual element approximation of magnetostatic problems, *Comput. Methods Appl. Mech. Engrg* **332**, 343–362.
- L. Beirão da Veiga, F. Brezzi, L. D. Marini and A. Russo (2014), The hitchhiker’s guide to the virtual element method, *Math. Models Methods Appl. Sci.* **24**, 1541–1573.
- L. Beirão da Veiga, F. Brezzi, L. D. Marini and A. Russo (2016a), $H(\text{div})$ and $H(\text{curl})$ -conforming VEM, *Numer. Math.* **133**, 303–332.
- L. Beirão da Veiga, F. Brezzi, L. D. Marini and A. Russo (2016b), Mixed virtual element methods for general second order elliptic problems on polygonal meshes, *ESAIM Math. Model. Numer. Anal.* **50**, 727–747.
- L. Beirão da Veiga, F. Brezzi, L. D. Marini and A. Russo (2016c), Serendipity nodal VEM spaces, *Comp. Fluids* **141**, 2–12.
- L. Beirão da Veiga, F. Brezzi, L. D. Marini and A. Russo (2016d), Virtual element methods for general second order elliptic problems on polygonal meshes, *Math. Models Methods Appl. Sci.* **26**, 729–750.
- L. Beirão da Veiga, F. Brezzi, L. D. Marini and A. Russo (2020), Polynomial preserving virtual elements with curved edges, *Math. Models Methods Appl. Sci.* **30**, 1555–1590.
- L. Beirão da Veiga, C. Canuto, R. H. Nochetto and G. Vacca (2021), Equilibrium analysis of an immersed rigid leaflet by the virtual element method, *Math. Models Methods Appl. Sci.* **31**, 1323–1372.
- L. Beirão da Veiga, A. Chernov, L. Mascotto and A. Russo (2016e), Basic principles of hp virtual elements on quasiuniform meshes, *Math. Models Methods Appl. Sci.* **26**, 1567–1598.
- L. Beirão da Veiga, F. Dassi and G. Vacca (2018c), The Stokes complex for virtual elements in three dimensions, *Math. Models Methods Appl. Sci.* **30**, 477–512.
- L. Beirão da Veiga, F. Dassi, G. Manzini and L. Mascotto (2022a), The virtual element method for the 3D resistive magnetohydrodynamic model. Submitted for publication. Available at [arXiv:2201.04417v1](https://arxiv.org/abs/2201.04417v1).
- L. Beirão da Veiga, F. Dassi, G. Manzini and L. Mascotto (2022b), Virtual elements for Maxwell’s equations, *Comput. Math. Appl.* **116**, 82–99.
- L. Beirão da Veiga, C. Lovadina and D. Mora (2015), A virtual element method for elastic and inelastic problems on polytope meshes, *Comput. Methods Appl. Mech. Engrg* **295**, 327–346.
- L. Beirão da Veiga, C. Lovadina and A. Russo (2017b), Stability analysis for the virtual element method, *Math. Models Methods Appl. Sci.* **27**, 2557–2594.
- L. Beirão da Veiga, C. Lovadina and G. Vacca (2017c), Divergence free virtual elements for the Stokes problem on polygonal meshes, *ESAIM Math. Model. Numer. Anal.* **51**, 509–535.

- L. Beirão da Veiga, C. Lovadina and G. Vacca (2018d), Virtual elements for the Navier–Stokes problem on polygonal meshes, *SIAM J. Numer. Anal.* **56**, 1210–1242.
- L. Beirão da Veiga, G. Manzini and L. Mascotto (2019a), A posteriori error estimation and adaptivity in hp virtual elements, *Numer. Math.* **143**, 139–175.
- L. Beirão da Veiga, L. Mascotto and J. Meng (2022c), Interpolation and stability estimates for edge and face virtual elements of general order, *Math. Models Methods Appl. Sci.* **32**, 1589–1631.
- L. Beirão da Veiga, D. Mora and G. Vacca (2019b), The Stokes complex for virtual elements with application to Navier–Stokes flows, *J. Sci. Comput.* **81**, 990–1018.
- L. Beirão da Veiga, A. Russo and G. Vacca (2019c), The virtual element method with curved edges, *ESAIM Math. Model. Numer. Anal.* **53**, 375–404.
- M. F. Benedetto, S. Berrone, A. Borio, S. Pieraccini and S. Scialò (2016), A hybrid mortar virtual element method for discrete fracture network simulations, *J. Comput. Phys.* **306**, 148–166.
- M. F. Benedetto, A. Borio and S. Scialò (2017), Mixed virtual elements for discrete fracture network simulations, *Finite Elem. Anal. Des.* **134**, 55–67.
- M. F. Benedetto, A. Borio, F. Kyburg, J. Mollica and S. Scialò (2022), An arbitrary order mixed virtual element formulation for coupled multi-dimensional flow problems, *Comput. Methods Appl. Mech. Engrg* **391**, 114204.
- S. Berrone and A. Raeli (2022), Efficient partitioning of conforming virtual element discretizations for large scale discrete fracture network flow parallel solvers, *Eng. Geol.* **306**, 106747.
- S. Bertoluzza, M. Pennacchio and D. Prada (2019), High order VEMs on curved domains, *Rend. Lincei Mat. Appl.* **30**, 391–412.
- D. Boffi, F. Brezzi and M. Fortin (2013), *Mixed Finite Element Methods and Applications*, Vol. 44 of Springer Series in Computational Mathematics, Springer.
- A. Bossavit (1988), Mixed finite elements and the complex of Whitney forms, in *The Mathematics of Finite Elements and Applications, VI (Uxbridge, 1987)*, Academic Press, pp. 137–144.
- L. Botti, D. A. Di Pietro and J. Droniou (2018), A hybrid high-order discretisation of the Brinkman problem robust in the Darcy and Stokes limits, *Comput. Methods Appl. Mech. Engrg* **341**, 278–310.
- S. C. Brenner and L. R. Scott (2008), *The Mathematical Theory of Finite Element Methods*, Vol. 15 of Texts in Applied Mathematics, third edition, Springer.
- S. C. Brenner and L.-Y. Sung (2018), Virtual element methods on meshes with small edges or faces, *Math. Models Methods Appl. Sci.* **28**, 1291–1336.
- S. C. Brenner, Q. Guan and L.-Y. Sung (2017), Some estimates for virtual element methods, *Comput. Methods Appl. Math.* **17**, 553–574.
- S. C. Brenner, L.-Y. Sung and Z. Tan (2021), A C^1 virtual element method for an elliptic distributed optimal control problem with pointwise state constraints, *Math. Models Methods Appl. Sci.* **31**, 2887–2906.
- F. Brezzi and L. D. Marini (2013), Virtual element methods for plate bending problems, *Comput. Methods Appl. Mech. Engrg* **253**, 455–462.
- F. Brezzi and L. D. Marini (2021), Finite elements and virtual elements on classical meshes, *Vietnam J. Math.* **49**, 871–899.
- F. Brezzi, R. S. Falk and L. D. Marini (2014), Basic principles of mixed virtual element methods, *ESAIM Math. Model. Numer. Anal.* **48**, 1227–1240.

- E. Cáceres and G. N. Gatica (2016), A mixed Virtual Element Method for the pseudostress-velocity formulation of the Stokes problem, *IMA J. Numer. Anal.* **37**, 296–331.
- E. Cáceres, G. N. Gatica and F. A. Sequeira (2017), A mixed virtual element method for the Brinkman problem, *Math. Models Methods Appl. Sci.* **27**, 707–743.
- E. Cáceres, G. N. Gatica and F. A. Sequeira (2018), A mixed virtual element method for quasi-Newtonian Stokes flows, *SIAM J. Numer. Anal.* **56**, 317–343.
- A. Cangiani, E. H. Georgoulis, T. Pryer and O. J. Sutton (2017), A posteriori error estimates for the virtual element method, *Numer. Math.* **137**, 857–893.
- A. Cangiani, V. Gyrya and G. Manzini (2016), The nonconforming virtual element method for the Stokes equations, *SIAM J. Numer. Anal.* **54**, 3411–3435.
- S. Cao and L. Chen (2018), Anisotropic error estimates of the linear virtual element method on polygonal meshes, *SIAM J. Numer. Anal.* **56**, 2913–2939.
- S. Cao, L. Chen and R. Guo (2022a), Immersed virtual element methods for Maxwell interface problems in three dimensions. Available at [arXiv:2202.09987](https://arxiv.org/abs/2202.09987).
- S. Cao, L. Chen, R. Guo and F. Lin (2022b), Immersed virtual element methods for elliptic interface problems in two dimensions, *J. Sci. Comput.* **93**, 12.
- D. Castañón Quiroz and D. A. Di Pietro (2020), A hybrid high-order method for the incompressible Navier–Stokes problem robust for large irrotational body forces, *Comput. Math. Appl.* **79**, 2655–2677.
- L. Chen and J. Huang (2018), Some error analysis on virtual element methods, *Calcolo* **55**, 5.
- L. Chen and F. Wang (2019), A divergence free weak virtual element method for the Stokes problem on polytopal meshes, *J. Sci. Comput.* **78**, 864–886.
- A. Chernov, C. Marcati and L. Mascotto (2021), p - and hp - virtual elements for the Stokes problem, *Adv. Comput. Math.* **47**, 24.
- H. Chi, L. Beirão da Veiga and G. Paulino (2017), Some basic formulations of the virtual element method (VEM) for finite deformations, *Comput. Methods Appl. Mech. Engrg* **318**, 148–192.
- H. Chi, A. Pereira, I. F. M. Menezes and G. H. Paulino (2020), Virtual element method (VEM)-based topology optimization: An integrated framework, *Struct. Mult. Optim.* **62**, 1089–1114.
- E. B. Chin and N. Sukumar (2021), Scaled boundary cubature scheme for numerical integration over planar regions with affine and curved boundaries, *Comput. Methods Appl. Mech. Engrg* **380**, 113796.
- E. B. Chin, J. B. Lasserre and N. Sukumar (2015), Numerical integration of homogeneous functions on convex and nonconvex polygons and polyhedra, *Comput. Mech.* **56**, 967–981.
- C. Chinosi and L. D. Marini (2016), Virtual element method for fourth order problems: L^2 -estimates, *Comput. Math. Appl.* **72**, 1959–1967.
- P. G. Ciarlet (1978), *The Finite Element Method for Elliptic Problems*, Vol. 4 of Studies in Mathematics and its Applications, North-Holland.
- M. Cihan, B. Hudobivnik, J. Korelc and P. Wriggers (2022), A virtual element method for 3D contact problems with non-conforming meshes, *Comput. Methods Appl. Mech. Engrg* **402**, 115385.
- B. Cockburn, G. Fu and W. Qiu (2017), A note on the devising of superconvergent HDG methods for Stokes flow by M -decompositions, *IMA J. Numer. Anal.* **37**, 730–749.

- F. Dassi and S. Scacchi (2020), Parallel block preconditioners for three-dimensional virtual element discretizations of saddle-point problems, *Comput. Methods Appl. Mech. Engrg.* **372**, 113424.
- F. Dassi and G. Vacca (2020), Bricks for mixed high-order virtual element method: Projectors and differential operators, *Appl. Numer. Math.* **155**, 140–159.
- F. Dassi, P. Di Barba and A. Russo (2020a), Virtual element method and permanent magnet simulations: Potential and mixed formulations, *IET Sci. Meas. Technol.* **14**, 1098–1104.
- F. Dassi, A. Fumagalli, A. Scotti and G. Vacca (2022), Bend 3d mixed virtual element method for Darcy problems, *Comput. Math. Appl.* **119**, 1–12.
- F. Dassi, C. Lovadina and M. Visinoni (2020b), A three-dimensional Hellinger–Reissner virtual element method for linear elasticity problems, *Comput. Methods Appl. Mech. Engrg.* **364**, 112910.
- D. A. Di Pietro and S. Krell (2018), A hybrid high-order method for the steady incompressible Navier–Stokes problem, *J. Sci. Comput.* **74**, 1677–1705.
- R. S. Falk and M. Neilan (2013), Stokes complexes and the construction of stable finite elements with pointwise mass conservation, *SIAM J. Numer. Anal.* **51**, 1308–1326.
- D. Frerichs and C. Merdon (2022), Divergence-preserving reconstructions on polygons and a really pressure-robust virtual element method for the Stokes problem, *IMA J. Numer. Anal.* **42**, 597–619.
- A. L. Gain, G. H. Paulino, L. S. Duarte and I. F. M. Menezes (2015), Topology optimization using polytopes, *Comput. Methods Appl. Mech. Engrg.* **293**, 411–430.
- F. Gardini, G. Manzini and G. Vacca (2019), The nonconforming virtual element method for eigenvalue problems, *ESAIM Math. Model. Numer. Anal.* **53**, 749–774.
- G. N. Gatica, M. Munar and F. A. Sequeira (2018a), A mixed virtual element method for a nonlinear Brinkman model of porous media flow, *Calcolo* **55**, 21.
- G. N. Gatica, M. Munar and F. A. Sequeira (2018b), A mixed virtual element method for the Navier–Stokes equations, *Math. Models Methods Appl. Sci.* **28**, 2719–2762.
- N. Gauger, A. Linke and P. Schroeder (2019), On high-order pressure-robust space discretisations, their advantages for incompressible high Reynolds number generalised Beltrami flows and beyond, *SMAI J. Comput. Math.* **5**, 88–129.
- V. Girault and P.-A. Raviart (1979), *Finite Element Approximation of the Navier–Stokes Equations*, Vol. 749 of Lecture Notes in Mathematics, Springer.
- J. Guzmán and M. Neilan (2014), Conforming and divergence-free Stokes elements on general triangular meshes, *Math. Comp.* **83**, 15–36.
- J. Guzmán and M. Neilan (2018), Inf-sup stable finite elements on barycentric refinements producing divergence-free approximations in arbitrary dimensions, *SIAM J. Numer. Anal.* **56**, 2826–2844.
- J. Guzmán and L. R. Scott (2019), The Scott–Vogelius finite elements revisited, *Math. Comp.* **88**, 515–529.
- R. Hiptmair (2001), Discrete Hodge operators, *Numer. Math.* **90**, 265–289.
- A. Hussein, F. Aldakheel, B. Hudobivnik, P. Wriggers, P.-A. Guidault and O. Allix (2019), A computational framework for brittle crack-propagation based on efficient virtual element method, *Finite Elem. Anal. Des.* **159**, 15–32.
- V. John, A. Linke, C. Merdon, M. Neilan and L. G. Rebholz (2017), On the divergence constraint in mixed finite element methods for incompressible flows, *SIAM Rev.* **59**, 492–544.

- A. Linke and C. Merdon (2016a), On velocity errors due to irrotational forces in the Navier–Stokes momentum balance, *J. Comput. Phys.* **313**, 654–661.
- A. Linke and C. Merdon (2016b), Pressure-robustness and discrete Helmholtz projectors in mixed finite element methods for the incompressible Navier–Stokes equations, *Comput. Methods Appl. Mech. Engrg* **311**, 304–326.
- K. Lipnikov, D. Vassilev and I. Yotov (2014), Discontinuous Galerkin and mimetic finite difference methods for coupled Stokes–Darcy flows on polygonal and polyhedral grids, *Numer. Math.* **126**, 321–360.
- X. Liu and Z. Chen (2019), The nonconforming virtual element method for the Navier–Stokes equations, *Adv. Comput. Math.* **45**, 51–74.
- X. Liu, J. Li and Z. Chen (2017), A nonconforming virtual element method for the Stokes problem on general meshes, *Comput. Methods Appl. Mech. Engrg* **320**, 694–711.
- X. Liu, R. Li and Z. Chen (2019), A virtual element method for the coupled Stokes–Darcy problem with the Beaver–Joseph–Saffman interface condition, *Calcolo* **56**, 48.
- X. Liu, R. Li and Y. Nie (2020), A divergence-free reconstruction of the nonconforming virtual element method for the Stokes problem, *Comput. Methods Appl. Mech. Engrg* **372**, 113351.
- L. Mascotto, I. Perugia and A. Pichler (2019), A nonconforming Trefftz virtual element method for the Helmholtz problem, *Math. Models Methods Appl. Sci.* **29**, 1619–1656.
- C. Mattiussi (1997), An analysis of finite volume, finite element, and finite difference methods using some concepts from algebraic topology, *J. Comput. Phys.* **133**, 289–309.
- D. Mora, G. Rivera and R. Rodríguez (2015), A virtual element method for the Steklov eigenvalue problem, *Math. Models Methods Appl. Sci.* **25**, 1421–1445.
- D. Mora, G. Rivera and R. Rodriguez (2017), A posteriori error estimates for a virtual element method for the Steklov eigenvalue problem, *Comput. Math. Appl.* **74**, 2172–2190.
- M. Munar and F. A. Sequeira (2020), A posteriori error analysis of a mixed virtual element method for a nonlinear Brinkman model of porous media flow, *Comput. Math. Appl.* **80**, 1240–1259.
- S. Natarajan (2020), On the application of polygonal finite element method for Stokes flow: A comparison between equal order and different order approximation, *Comput. Aided Geom. Design* **77**, 101813.
- K. Park, H. Chi and G. H. Paulino (2020), Numerical recipes for elastodynamic virtual element methods with explicit time integration, *Int. J. Num. Meth. Engrg* **121**, 1–31.
- K. Park, H. Chi and G. H. Paulino (2021), B-bar virtual element method for nearly incompressible and compressible materials, *Meccanica* **56**, 1423–1439.
- J. C. Simo and T. J. R. Hughes (2006), *Computational Inelasticity*, Vol. 7, Springer Science & Business Media.
- G. Vacca (2018), An H^1 -conforming virtual element for Darcy and Brinkman equations, *Math. Models Methods Appl. Sci.* **28**, 159–194.
- F. Wang and J. Zhao (2021), Conforming and nonconforming virtual element methods for a Kirchhoff plate contact problem, *IMA J. Numer. Anal.* **41**, 1496–1521.
- G. Wang, Y. Wang and Y. He (2020), A posteriori error estimates for the virtual element method for the Stokes problem, *J. Sci. Comput.* **84**, 37.
- P. Wriggers and B. Hudobivnik (2017), A low order virtual element formulation for finite elasto-plastic deformations, *Comput. Methods Appl. Mech. Engrg* **327**, 459–477.

- P. Wriggers, B. D. Reddy, W. Rust and B. Hudobivnik (2017), Efficient virtual element formulations for compressible and incompressible finite deformations, *Comput. Mech.* **60**, 253–268.
- P. Wriggers, W. T. Rust and B. D. Reddy (2016), A virtual element method for contact, *Comput. Mech.* **58**, 1039–1050.
- J. Zhao, S. Chen and B. Zhang (2016), The nonconforming virtual element method for plate bending problems, *Math. Models Methods Appl. Sci.* **26**, 1671–1687.
- J. Zhao, B. Zhang, S. Mao and S. Chen (2020), The nonconforming virtual element method for the Darcy–Stokes problem, *Comput. Methods Appl. Mech. Engrg* **370**, 113251.